Lawrence Berkeley National Laboratory
Recent Work

Title

PHOSPHORUS-31 NMR MAGNETIZATION TRANSFER MEASUREMENTS OF METABOLIC REACTION RATES IN THE RAT HEART AND KIDNEY in vivo

Permalink

https://escholarship.org/uc/item/75v4s382

Author

Koretsky, A.P.

Publication Date

1984-08-01

eScholarship.org Powered by the California Digital Library
University of California

LBL-18376

Lawrence Berkeley Laboratory
UNIVERSITY OF CALIFORNIA

CHEMICAL BIODYNAMICS DIVISION

RECEIVED
LAWRENCE
BERKELEY LABORATORY
NOV 1 1984
LIBRARY AND
DOCUMENTS SECTION

PHOSPHORUS-31 NMR MAGNETIZATION TRANSFER MEASUREMENTS OF METABOLIC REACTION RATES IN THE RAT HEART AND KIDNEY *in vivo*

A.P. Koretsky
(Ph.D. Thesis)

August 1984

TWO-WEEK LOAN COPY
This is a Library Circulating Copy which may be borrowed for two weeks.

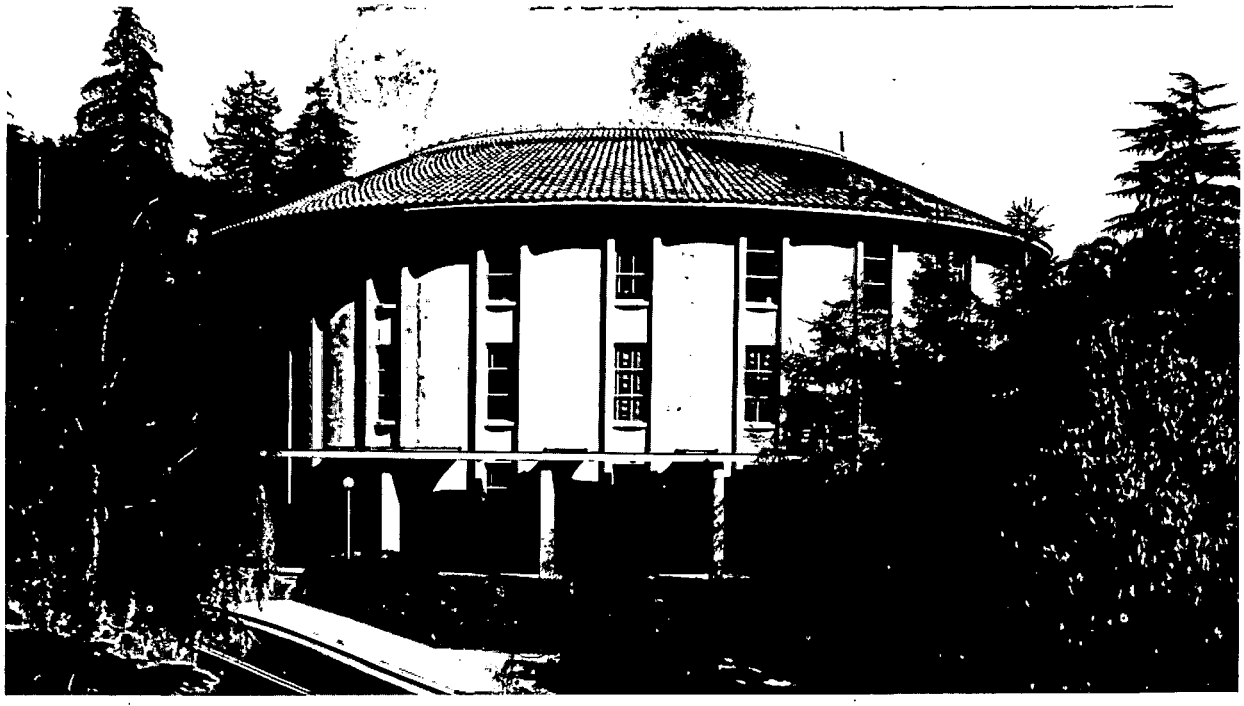

Prepared for the U.S. Department of Energy under Contract DE-AC03-76SF00098

LBL-18376

DISCLAIMER

This document was prepared as an account of work sponsored by the United States Government. While this document is believed to contain correct information, neither the United States Government nor any agency thereof, nor the Regents of the University of California, nor any of their employees, makes any warranty, express or implied, or assumes any legal responsibility for the accuracy, completeness, or usefulness of any information, apparatus, product, or process disclosed, or represents that its use would not infringe privately owned rights. Reference herein to any specific commercial product, process, or service by its trade name, trademark, manufacturer, or otherwise, does not necessarily constitute or imply its endorsement, recommendation, or favoring by the United States Government or any agency thereof, or the Regents of the University of California. The views and opinions of authors expressed herein do not necessarily state or reflect those of the United States Government or any agency thereof or the Regents of the University of California.

LBL-18376

PHOSPHORUS-31 NMR MAGNETIZATION TRANSFER MEASUREMENTS OF METABOLIC REACTION RATES IN THE RAT HEART AND KIDNEY *in vivo*

Alan Paul Koretsky

Ph.D. Thesis

Lawrence Berkeley Laboratory
University of California
Berkeley, California 94720

August 1984

Phosphorus-31 NMR Magnetization Transfer Measurements of Metabolic Reaction Rates in the Rat Heart and Kidney *in vivo*

Alan Paul Koretsky

Abstract

^{31}P NMR is a unique tool to study bioenergetics in living cells. The application of magnetization transfer techniques to the measurement of steady-state enzyme reaction rates provides a new approach to understanding the regulation of high energy phosphate metabolism. This dissertation is concerned with the measurement of the rates of ATP synthesis in the rat kidney and of the creatine kinase catalyzed reaction in the rat heart *in situ*.

Chronically implanted detection coils, employing a balanced matching configuration of capacitors in the tuned circuit, were used to obtain ^{31}P NMR spectra from heart, kidney, and liver *in situ*. Gated spectra of heart obtained at systole and diastole and the effects of fructose on kidney and liver were studied. The ability to observe other nuclei using implanted coils is illustrated with ^{39}K NMR spectra from kidney and muscle.

The theoretical considerations of applying magnetization transfer techniques to intact organs are discussed with emphasis on the problems associated with multiple exchange reactions and compartmentation of reactants. Experimental measurements of the ATP synthesis rate (13 μmol/min/gm tissue) were compared to whole kidney oxygen consumption and Na^+ reabsorption rates to derive ATP/O (0.8-1.7)and Na^+/ATP (4-10)

values. The problems associated with ATP synthesis rate measurements in kidney, e.g. the heterogeneity of the inorganic phosphate resonance, are discussed and experiments to overcome these problems proposed.

In heart, the forward (phosphocreatine to ATP) rate (10 mM/sec) through creatine kinase was measured to be larger than the reverse rate (7 mM/sec). Using a double saturation technique the effect of the competing exchange between the γ and β phosphates of ATP on the measured reverse rate was shown to be insignificant. To account for the difference in forward and reverse rates a model is proposed based on the compartmentation of a small (below the sensitivity of NMR) pool of ATP. It is shown that saturation transfer can detect exchange between small and large pools of metabolites, whereas inversion transfer or two-dimensional NMR exchange techniques cannot. This difference between magnetization transfer techniques affords a test for the involvement of small metabolite pools in exchange reactions.

Kenneth Sauer

PREFACE

Man stands before Nature, reaching out in an attempt to understand. The scientific age is distinctive in that this reaching out has been an aggressive reaching for descriptions that work. A reaching which has, as its most important ingredient, an active interplay between thought and experiment, technology and intuition. It is this aggressive reaching which is at the root of the successes of our scientific sensibiltiy.

It is currently fashionable in the study of the history of science to lay great weight on the importance of intuition in guiding the development of science. The heroes have become those individuals responsible for the insights which are thought to have led to the important paradigm shifts. However perception and introspection are only meaningful in their proper contexts; contexts which owe to our technical abilities. Without computer technology to act as an allegory, theories of perception might be formulated in a very different way. Indeed it is often our technical ability which tempers where we turn for the insights which change our lives.

This has been particularly true in biology and medicine. The ability which x-ray crystallography has given us to solve molecular structures has led to the notion that structure defines function. An elegant example of this is the Watson-Crick conception of the molecular basis of genetics, a field wich today stands primed to change the face of human kind. T.H. Huxley in 1885 recognized the importance of technique in biology when he stated, "What an enormous revolution would be in biology, if physics or chemistry could supply the physiologist

with a means of making out the molecular structure of living tissues comparable to that which the spectroscope affords to the inquirer into the nature of the heavenly bodies."

Man's desire to develop technologies which allow a non-invasive telescopic view of the body's functioning dates at least to the Vedic Scriptures of India. Mental techniques were described which gave impressions of the workings of the various organ systems; impressions which were to aid in guiding the diagnosis and treatment of disease. More recently the use of ultra-sound and x-ray imaging has allowed detailed visualization of anatomical structures. In parallel to these advances, the biochemist has followed Huxley's intuition and borrowed spectroscopic techniques from the physicist and chemist to get information concerning biochemical reactions in isolated cells and organ systems. One of the richest of these tools, nuclear magnetic resonance (NMR) spectroscopy has in the past decade developed to the point where Huxley's wish has become a reality.

First performed in molecular beams by I. Rabi in the 1930's and extended to condensed phases in 1946 by E. Purcell and F. Bloch, NMR gives us the ability to detect specific nuclei in molecules in a manner which appears, at this stage, to be harmless to living things. The development of NMR imaging techniques by P. Lauterbur and R. Damadian has given us a tool which can visualize anatomical structure as well as look at the underlying level of biochemical processing which occurs. This opens up the potential for understanding the normal biochemical functioning of tissue in human beings, as well as the possibility of detecting abnormalities in the metabolism of a specific tissue before pathologic changes begin. The implications for medicine and biology

are immense.

This dissertation attempts to make a contribution to both the technical development of in vivo NMR as well as the types of information that can be learned by the application of NMR to living tissue. A light is shining in a new direction to help us stand and reach out. I feel fortunate to have participated in what will be thought of as the early stumblings along this new direction. It is my hope, however naïve, that along with the fuller description of life that NMR offers comes an increased wisdom to improve the relationship we stand in with Nature and our fellow inhabitants on this planet.

Alan Koretsky

Berkeley, California

September, 1984

ACKNOWLEDGEMENTS

Communication is an art at which I'm not very accomplished. The words which have been used to describe the experiments which constitute this thesis have, for the most part, been adequate. However my words seem impotent as I set out to thank the people who were essential to this work and my fulfilling the requirements necessary to receive a Ph.D.

The work described here is interdisciplinary in nature, utilizing a physical technique to study a physiological problem. This undertaking was successful because I was given the freedom to move about in two laboratories. The Melvin Calvin Laboratory of Chemical Biodynamics at the University of California at Berkeley (UCB) and the Department of Pharmaceutical Chemistry's NMR laboratory at the University of California at San Francisco (UCSF) have provided very enriching environments in which to learn how to do science.

That this cross-bay project worked out is testimony to the flexibility of the two men who were my major advisors; Mel Klein at UCB and Michael Weiner at UCSF. Mel got me started in NMR and Michael introduced me to the problems which seem suited for NMR to solve. Their individual marks are clearly stamped on this work. My respect for them as scientists takes second place only to my respect for them as human beings. They have, with patience and consideration, guided and helped me to grow and mature. I remain forever in their debt and hope that someday I can be half as good an advisor. The Hindu student expresses his love, gratitude, and respect for his teachers by saying Jai Guru Dev (All Hail Dear Teacher), a phrase I shout out for Michael

and Mel.

Everyday represents at least one new problem and there were many, many people over the last three years at UCSF who have helped me to overcome these hurdles. Tom James, the director of the UCSF NMR lab generously gave me free run of his resources and was a source of insightful criticism throughout the course of this work.

On a day to day basis I learned more about NMR and its quirks from Vladimir (or Vlady, as his wife, Vivian affectionately refers to him) Basus and Joseph Murphy-Boesch. Appendix 2 represents a collaboration between Joe and myself. Both Joe and Vladimir are exceptionally talented people whose abilities and experience were greatly appreciated. Peter Bendel aided the early efforts of this project with his considerable expertise. The surgical techniques necessary to accomplish this work were developed with Sandy Pomeranz, Bill Strauss, Sam Wang, and most recently, Xian Ai. Sam desrves all the credit for successfully implanting coils around the heart. Drs. Floyd Rector, Willaim Parmley, and R. Curtis Morris lent support to this project with either space, supplies, or encouragement. In particular Dr. Rector and the people associated with his lab, Marty Cogan, Bob Alpern, and Ken Wong were helpful in innumerable ways.

Being a man without a desk at UCSF meant I often needed a spare NMR tube, pippette, a place to lay my sleeping bag, or a friendly hello during particularly frustrating times. Especially helpful in these matters were: Nancy Shine, Bob Tilton, Steve Brown, Tak Kuntz, Tom Marshner, Michael (I want my MTV) Moseley, and Greg Young.

Recently, I've had the pleasure of collaborating with some of the growing numbers of people interested in <u>in vivo</u> NMR at UCSF. In

particular, Bill Adam stimulated our obtaining ^{39}K NMR spectra, Jackie James instigated the liver work, and Ricardo Gonzalez-Mendez with Larry Litt got me involved in some spectroscopy of the brain.

The Laboratory of Chemical Biodynamics is a very special place which not only takes the name of Melvin Calvin but also reflects his unbounded enthusiasm for science. Consequently there are many people who have made the lab a great place to be associated with and have taught me a great deal over the years. It is said that the microcosm reflects the macrocosm; such is the case with Mel's group which embodies the spirit of this great lab. Tom Pratum (whom I owe a special thanks to for doling out some much needed verbal abuse), Connie O'Shiro, Willy Shih, and Sun Un have all been sources of NMR information. Dave Britt, Dave Goodin, Stan Sorscher, Tim Walker, and Beverly Packard have taught me things in a number of different fields.

The lab has many full time support staff who have impinged upon my work. As every one knows, it is the administrative assistants who keep things running, thus an extra special thanks go to Beth Klingel (especially for Chapter 5), Lois Soule, and Gloria Goldberg. Gary Smith and Everett Harvey kept the computer functioning, Mike Press helped with some electronic difficulties, Brad Peconom kept the supplies roling in, Ethel Lefall kept the glassware clean and the coffee hot, and Vangie and Bonita answered the phone; thank you all.

Many others helped in ways to numerous to mention; Mary Blackwell, Stephen Treon, Ti-Sheng Young, David Pearlman (thanks for the plotting program), and Kerry Karukstis all deserve special mention.

Professors Ken Sauer and John Forte read this thesis critically and thus eliminated a number of errors. Though he's probably not

aware, Ken has, by his example, taught me a great deal about organizing a research group.

My parents, Shirley and Len, besides bringing me into the world, have instilled in me a respect for myself and my fellow human beings which makes me the person I am today. My sisters, Arlene, Gene, and Marcia, and their growing families have always made me feel that no matter what happened they'd be there if I needed them.

Finally, there are the two people whom I have felt the closest to over the past six years. The only words which express my feelings about Greg Karczmar and Julie Montanari are that I love them both very much. What they've meant to me and this work can never be adequately stated or repaid, but as a token of my appreciation I dedicate this work to them.

Financial support for this work came from the Veterns Administration Research Service, the Northern California Heart Association, and the Office of Energy Research, Office of Health and Environmental Research, Health Effects Research Division of the Department of Energy under contract DE-AC03-76SF00098.

I'd like to finish this section by acknowledging that for a great many people in the world life is not a blessing but a nightmare. Starvation and disease are a way of life for millions and it is really at their expense that this work was funded.

TABLE OF CONTENTS

Page

CHAPTER 1: THE PROBLEM AND THE APPROACH

1.1 Introduction..... 1

1.2 The Question of Stoichiometry: The Neccessity of Measuring ATP Turnover Rates..... 8

1.3 Other Enzymatic Reactions Important to ATP Metabolism..... 14

1.4 The Approach: *in Vivo* ^{31}P NMR..... 15

1.5 References..... 21

CHAPTER 2: *IN VIVO* MAGNETIZATION TRANSFER: THEORY AND PREVIOUS WORK

2.1 Introduction and Historical Background..... 24

2.2 Principles of Magnetization Transfer..... 25

2.3 Saturation Transfer..... 28

2.4 Inversion Transfer and 2D NMR..... 31

2.5 Unidirectional Rate Constants and the Order of a Reaction..... 33

2.6 Limitations and Complications of Magnetization Transfer Measurements of Reaction Rates..... 35

2.7 Review of Magnetization Transfer Studies to Investigate High Energy Phosphate Metabolism..... 41

2.8 Conclusions..... 52

2.9 References..... 54

CHAPTER 3: THE ART AND SCIENCE OF IMPLANTED RF COILS

3.1 Introduction..... 57

3.2 Materials and Methods..... 58

3.3 Results and Discussion..... 64

3.4 Conclusions..... 82

3.5 References..... 84

CHAPTER 4: SATURATION TRANSFER STUDIES OF RAT HEART AND KIDNEY *IN SITU*

4.1 Introduction..... 87

4.2 Materials and Methods..... 88

4.3 Results..... 91

4.4 Discussion..... 106

4.5 Conclusions..... 110

4.6 References..... 112

CHAPTER 5: DETECTION OF EXCHANGE REACTIONS INVOLVING SMALL METABOLITE POOLS USING NMR MAGNETIZATION TRANSFER TECHNIQUES: RELEVANCE TO SUBCELLULAR COMPARTMENTATION OF CREATINE KINASE

5.1 Introduction..... 115

5.2 Theory..... 117

5.3 Results..... 119

5.4 Implications for Creatine Kinase Reaction Rate Measurements *in Vivo*..... 126

5.5 Conclusions..... 132

5.6 References..... 133

APPENDIX 1: SATURATION OF A NMR SIGNAL..... 135

APPENDIX 2: AN *IN VIVO* PROBE CIRCUIT FOR IMPROVED SENSITIVITY

A2.1 Introduction..... 137

A2.2 Background..... 137

A2.3 The New Circuit..... 141

A2.4 Experimental Verification of the New Tuning Scheme.. 143

A2.5 Conclusions..... 148

A2.6 References..... 151

CHAPTER 1: THE PROBLEM AND THE APPROACH

1.1 Introduction

An organism depends on its ability to do useful work in order to grow and prosper. On the level of biomolecules the whole of life's activities has as its basis ion transport (neural activity) and muscle contraction (locomotion). To generate useful energy to support the appropriate work functions an organism relies on the metabolism of foodstuffs. It is the meaningful coupling of the generation and utilization of energy which allows a cell to maintain the delicate balance of life.

In 1941, Franz Lipmann (1) implicated adenosine triphosphate (ATP) as the molecule formed in energy production processes, such as oxidative phosphorylation, and the molecule necessary for a cell to do useful work, such as ion transport or muscle contraction. This central role for ATP is illustrated schematically in Fig. 1-1. The questions of stoichiometry and coupling of bioenergetic processes have, since 1941, rested on the relative rates of ATP generation and utilization.

The problem of the coupling of ATP utilization to its generation has been attacked in a variety of ways. Most of the enzyme systems which catalyze reactions responsible for regulating high energy phosphate metabolism have been isolated, purified, and extensively studied to determine important mechanistic and regulatory factors. However, the conditions exsisting within a living cell are different from those *in vitro*, and it remains an open question as to how bioenergetic processes are controlled *in vivo*. In particular, the ATP

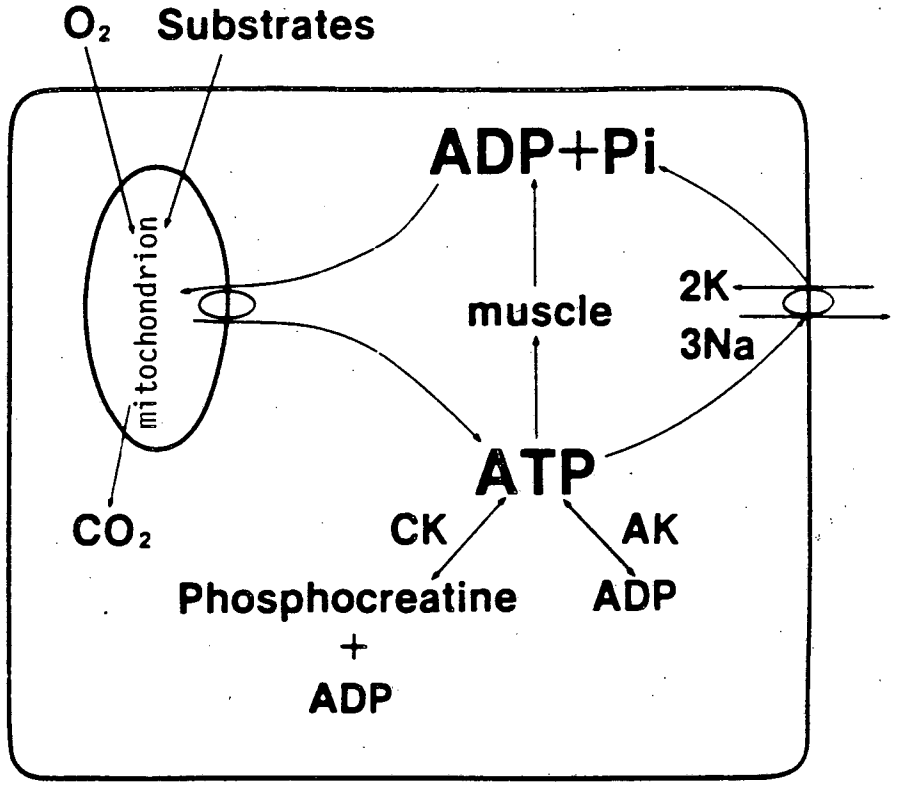

A Biological Cell

Figure 1-1. Schematic representation of the role of ATP in high energy phosphate metabolism. Metabolism of O_2 and substrates in the mitochondria produce ATP via oxidative phosphorylation. ATP is then transported to the cytosol in exchange for ADP. The hydrolysis of ATP to Pi and ADP in the cytosol can be used for muscle contraction or ion transport. Two additional enzymatic reactions which are important for ATP metabolism are also shown; CK represents creatine kinase and AK represents adenylate kinase.

turnover rate has been difficult to measure in an intact cell. The rapid and cyclical nature of bioenergetic reactions which utilize ATP has made conventional radiotracer techniques difficult to interpret (2). Isolated organelles have been prepared in vitro so that ATP turnover rates could be measured; but asssumptions concerning regulatory mechanisms, which may be disrupted as organelles are isolated, remain questionable. Physiologists, using analysis of an organ's inputs and outputs, have investigated the relationship of active transport and muscle contraction to oxidative metabolism in living tissue. In these studies regulatory mechanisms were intact but assumptions concerning stoichiometries of basic biochemical reactions determined in vitro were necessary to fill the gaps between inputs and outputs.

There has been a growing interest for the past three decades in bridging the gap between the reductionist approach of classical biochemistry and the black box approach of physiology. The growth in the application of spectroscopic techniques to living organisms has laid the groundwork so that the biochemist can study relevant problems in an intact cell or organ. Fluorescent techniques have found widespread application to bioenergetic problems by means of the intrinsic probes NADH and flavoproteins (3). Both are important participants in glycolysis and oxidative phosphorylation, thus allowing metabolic activation (workload increase) and deprivation (anoxia) to be studied in a relatively noninvasive manner. Radiography (4) and positron emmission tomography (5) have been used with the appropriately labeled substrates to investigate a variety of metabolic problems, eg. glucose metabolism using labeled deoxy-glucose. These techniques can

be used to obtain a three dimensional representation of metabolic activity in living organisms. While many new insights have been obtained with these techniques they suffer from two problems; 1) while the cell being studied remains alive, large doses of labeled material or high intensity light of a troublesome wavelength (UV) are necessary, and 2) the number of metabolites which can be studied is severely restricted. In particular, none of the above mentioned techniques allows unambiguous visualization of ATP.

In the past decade technical advances in the art of nuclear magnetic resonance (NMR) have increased sensitiviy to the point where spectra can be obtained from living tissue. Because the radiofrequencies usually used to perform NMR experiments are relativly harmless, NMR offers an excellent window into the biochemical functioning of living cells. Furthermore, the variety of nuclei which can be observed (Table 1-1) by NMR and which play an enormously important biochemical role lead to almost limitless possibilities for experimentation. This becomes particularly exciting to contemplate as magnets large enough to study humans become widely available.

Fig. 1-2b shows a ^{31}P NMR spectrum obtained from a free living protozoan, Tetrahymena thermophilia (6). The spectrum is a plot of intensity, in arbitrary units, vs. frequency, in parts per million (PPM). From the point of view of bioenergetic questions the exciting observation is that the three phosphates from ATP are easily discernible, as is a resonance due to inorganic phosphate (Pi). Furthermore, the spectrum is sensitive to metabolic perturbations such as oxygenation of an anoxic cell suspension (Fig 1-2). The application of magnetic labeling techniques, such as saturation

Table 1-1. NMR observable nuclei of biological interest.

Nucleus	Spin	Relative Sensitivity	Observe Frequency at 5.6 Tesla
^{1}H	1/2	1.00	240.0 MHz
^{2}H	1	9.65×10^{-3}	36.8
^{3}H	1/2	1.21	256.0
^{13}C	1/2	1.59×10^{-2}	60.3
^{14}N	3/2	1.01×10^{-3}	17.3
^{15}N	1/2	1.04×10^{-3}	24.3
^{19}F	1/2	0.83	225.8
^{23}Na	3/2	9.25×10^{-2}	63.5
^{31}P	1/2	6.63×10^{-2}	97.2
^{35}Cl	3/2	4.7×10^{-3}	23.5
^{39}K	3/2	5.08×10^{-4}	11.2
^{129}Xe*	1/2	2.12×10^{-2}	66.4

* in honor of Bob Tilton and the XL-100.

Figure 1-2. ^{31}P NMR spectra of Tetrahymena thermophilia showing the effect of perfusing the cell suspension with oxygenated buffer. Tetrahymena thermophilia BIV 1868 were grown to mid-log phase at 30° then harvested by centifugation at 200g at 4°. The resulting pellet was transfered into the flow cell for NMR or a duplicate chamber containing a Clarke type oxygen electrode (Yellow Springs Instruments). Spectra, obtained at 25°, are the sum of 4000 pulses, acquired at 109 MHz using a 45° pulse and a 206msec recycle time. (a) Spectrum obtained before buffer is passed through the cells. The cells were therefore anoxic. (b) Spectrum obtained 10 min after the perfusion apparatus had been switched on. Peaks shown are (1) methylene diphosphonate (pH 9), contained in an external cappillary; (2) Pi; (3) γATP; (4) αATP, NAD(H); (5) βATP. The inset shows the effect perfusion has on the oxygen tension of the cell pellet. (From reference. 6).

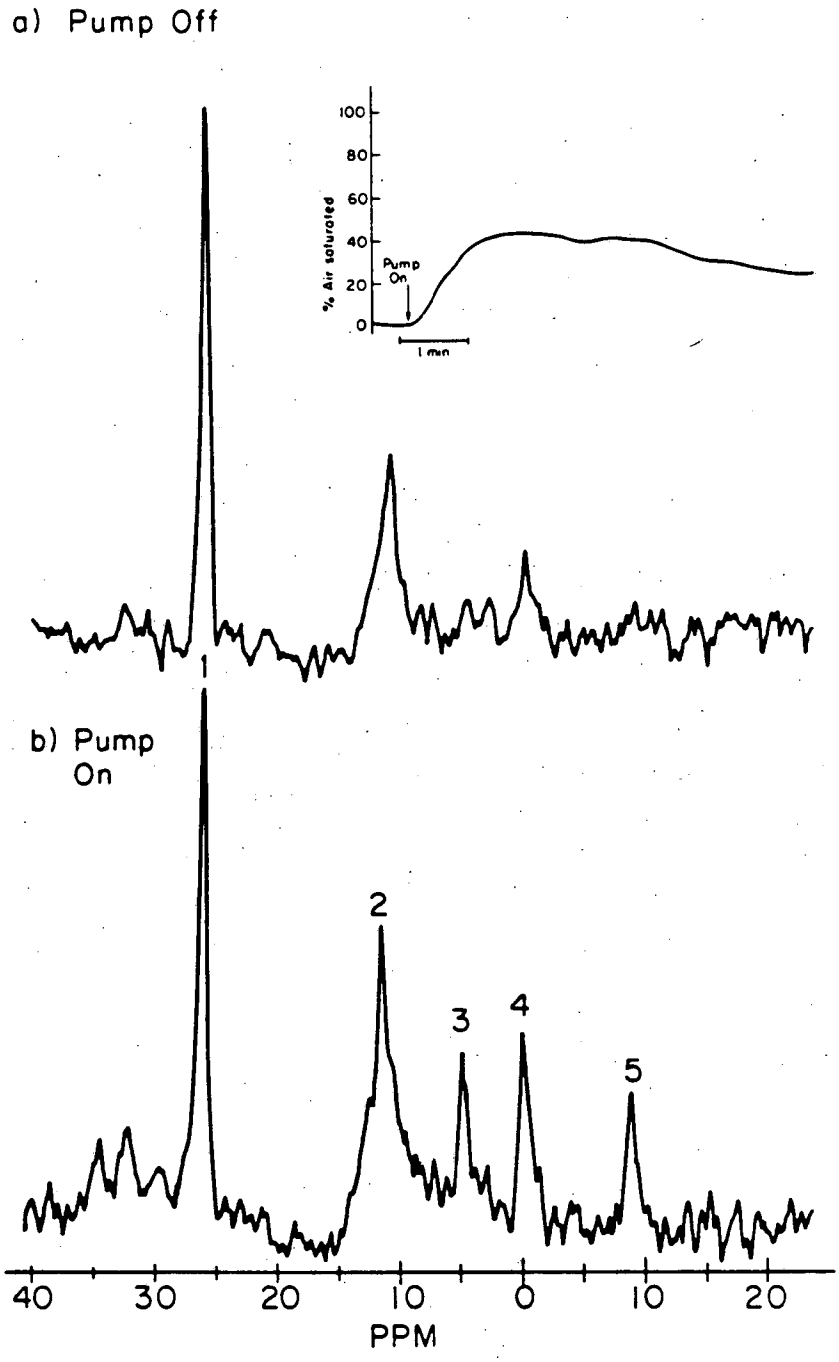
a) Pump Off
100
80
60
40
20
0
% Air saturated
Pump On
1 min
1
b) Pump On
2
3
4
5
40
30
20
10
0
10
20
PPM
XBL8210-4191

transfer, allow metabolite interconversion rates to be determined. This thesis is concerned with techniques to obtain NMR spectra from living systems, in particular rat organs in situ, and with the application of magnetization transfer techniques to measure reactions important in the regulation and control of high energy phosphate metabolism.

1.2 The Question of Stoichiometry: The Necessity of Measuring ATP Turnover Rates

The underlying question which motivated the work described in this thesis is the problem of stoichiometry. What is the ratio of ATP formed to oxygen consumed in an intact living cell, and is this ratio variable under changing physiologic conditions? What is the ratio of ATP consumed to the amount of work performed and is this ratio variable?

IN VITRO CONSIDERATIONS. Ochoa (7) was one of the first to measure the ratio of the ATP synthesis flux (J_{ATP}) to the oxygen consumption rate (J_O) in isolated mitochondria and found it to be 3 with NADH linked substrates. This along with Chance's (8) work on the electron transport chain showing three coupling sites between electron transport and ATP synthesis, led to a value of 3 for the J_{ATP}/J_O ratio to become widely accepted. Since then, many people have measured J_{ATP}/J_O ratios in isolated mitochondria or submitochondrial particles using a variety of techniques. A whole range of values have been obtained (Table 1-2) with the assumption that unavoidable losses in energy make the true value of 3 hard to reach. More recently Hinkle and Yu (9), taking great precautions to eliminate systematic errors and

Table 1-2. J_{ATP}/J_O ratios determined in isolated mitochondria. The incorporation of ^{32}Pi into ATP was compared to the rate of oxygen consumption. Data is from reference 9.

Author	Substrate	J_{ATP}/J_O
Kalckar (1937)	Glucose	2.0
Ochoa (1943)	Pyruvate	3.1
Lehninger (1949)	β-hydroxybutyrate	1.8
Lardy (1952)	β-hydroxybutyrate	2.5
Lenaz (1956)	Pyruvate	2.9
Slater (1973)	β-hydroxybutyrate	1.7
Wilson (1973)	Glutamate	3.2
Hinkle & Yu (1978)	β-hydroxybutyrate	2.0

account for all sources of ATP production and utilization, obtained values closer to 2. They pointed out that with the acceptance of the chemiosmotic theory it was possible to accommodate fractional values for the J_{ATP}/J_O ratio (the question of H^+/ATP stoichiometry is a hotly debated one, with some experimental results implying a variable H^+/ATP depending on the pH gradient and flux through the electron transport chain. For a recent review see Hansford (10)).

To further complicate matters, Klingenburg and co-workers (11,12) have shown that the transport of ADP into mitochondria occurs with the exchange of ATP out of mitochondria and is dependent on membrane potential. It is also known that Pi transport occurs in an antiport exchange with an hydroxide ion or symport with a proton (13). Thus some of the energy generated by electron transport is necessary for transport of nucleotides.

Very recently Duzynski et al. (14) found that the J_{ATP}/J_O ratio changed depending on whether ATP was utilized extra- or intra-mitochondrially. They concluded that half an equivalent of ATP is needed to transport ATP from inside to outside the mitochondria. The energy needed for this transport process is expected to depend on intra- and extra-mitochondrial concentrations of nucleotides, making conditions under which the measurements are made an important consideration. It is the energy needed for transport of ATP, ADP, and Pi which Hinkle and Yu (9) used to rationalize the value of 2 that they measured for an extra-mitochondrial J_{ATP}/J_O.

Using a non-equilibrium thermodynamic model for oxidative phosphorylation, Lemasters (15) deduced an upper limit of 4 for the J_{ATP}/J_O ratio. They used data derived from inverted mitochondrial

membranes. Their value represents an intra-mitochondrial ratio, making the traditionally accepted value of 3 for an extra-mitochondrial ratio plausible. Rottenberg (16), using a similar non-equilibrium thermodynamic theory derived an expression which indicated that the J_{ATP}/J_O ratio was dependent on the free energy change associated with the reaction, ADP + Pi$\rightleftharpoons$ATP. This again points to the problem of accurately defining the conditions under which these measurements are made.

The question of the J_{ATP}/J_O stoichiometery is an open one even for the case of isolated mitochondria. To extend these results to intact cells is troublesome especially when the problems of working with isolated mitochondria are considered:

1. It is hard to isolate highly coupled mitochondria because they are easily uncoupled by the presence of fatty acids.

2. The intra-organelle volumes of isolated mitochondrial preparations may be as small as one third that found in vivo (17); possibly indicating a very different osmotic environment in the two cases.

3. Mitochondria accumulate bivalent cations, especially Ca^{2+}. These transport processes require energy from electron transport via the proton gradient. The ionic environment could effect measured J_{ATP}/J_O values.

IN VIVO CONSIDERATIONS. To get at the question of stoichiometry in vivo, one basic type of experiment has been performed. The rate at which an epithelial tissue pumps ions is modulated and the concomitant changes in oxygen consumption are measured. Zerahn did this experiment in frog skin and found, on a plot of Na^+ flux vs oxygen consumption a

slope of 17-18 (18). Assuming a ratio of three Na^+/ATP, a J_{ATP}/J_O ratio of 3 was deduced. The results from other tissue are summarized in Table 1-3. It can be seen that some tissues deviate from the expected ratio. In particular the dog kidney has a very high Na^+/O_2 ratio. Most explanations for the large amount of Na^+ which is pumped per O consumed, have invoked the passive diffusion of Na^+ (19). Because the kidney is a leaky epithelial tissue it is possible that a portion of the Na^+ diffuses without the need of energy derived from oxygen consumption. Alternatively, the J_{ATP}/J_O ratio or the J_{Na^+}/J_{ATP} ratio may be different from the value of 3 commonly accepted. The enzyme which is primarily responsible for pumping Na^+ in the kidney is the Na-K ATPase (20). It is widely accepted that <u>in vivo</u> the number of Na^+ pumped by this enzyme per ATP hydrolized is fixed at 3. However, there is a recent report indicating that under certain circumstances this ratio is variable (21). The discussion presented above concerning the J_{ATP}/J_O stoichiometry supports the possibility that this ratio is also variable.

The essential measurement which has been lacking in attempts to answer the above questions, is the ATP turnover rate, determined <u>in vivo</u>. Comparison of O_2 consumption rates and ATP turnover rates in an intact cell or organ under various metabolic conditions would allow evaluation of the J_{ATP}/J_O ratio as well as the determination of whether it is a fixed or variable quantity. Furthermore, comparison of O_2 consumption, Na^+ reabsorption, and ATP turnover rates in the intact kidney would reveal at which stage of high energy phosphate metabolism the added efficiency is occuring.

Table 1-3. in Vivo determination of bioenergetic stoichiometries in various tissues. In each case ion transport rates were varied and the changes in O_2 consumption monitored. Data is from reference 19.

Tissue	Ion	$\frac{\text{Ions}}{O_2}$	$\frac{ATP}{O}^{*}$	$\frac{\text{Ions}}{ATP}^{**}$
Frog skin	Na^+	18	3	3
Toad bladder	Na^+	18	3	3
Dog kidney	Na^+	28	4.5	4.6
Bullfrog Cornea	Na^+	24	4	4

* assumes Na^+/ATP of 3.

**assumes ATP/O of 3.

1.3 Other Enzymatic Reactions Important To ATP Metabolism

Besides the synthesis of ATP, catalyzed by oxidative phosphorylation, and the hydrolysis of ATP, predominantly catalyzed by Na-K ATPase (ion transport) or myosin ATPase (muscle contraction), there are two other enzymes which play a major, not yet fully understood, role in high energy phosphate metabolism.

CREATINE KINASE. Creatine kinase (CK) catalyzes the reaction, phosphocreatine (PCr) + ADP$\rightleftharpoons$ATP + creatine (Cr) (22). This enzyme is primarly found in muscle and nervous tissue and is the only enzyme known to catalyze reactions involving PCr. Its major role is thought to be the rapid synthesis of ATP from increased levels of ADP during periods of increased workloads, eg. muscle contraction (23). During periods of ATP availability CK functions to generate high levels of PCr, to be used as a high energy phosphate reservoir. CK exsists at such high activities in cells that it is believed that the reaction it catalyzes is maintained close to equilibrium (24), lending further support to the notion that PCr acts as a high energy phosphate reservoir.

In addition to its role as a high energy phosphate reserve system, the CK catalyzed reaction has been proposed to act as a shuttle system in muscle for high energy phosphate (25). ATP formed in mitochondria is believed to react rapidly with Cr to form PCr and ADP. The ADP is then readily available for rephosphorylation to ATP via oxidative phosphorylation. Meanwhile, PCr diffuses to the site of energy utilization to phosphorylate ADP formed by muscle contraction to make ATP. Experiments performed on isolated mitochondria (26) and isolated

myofibrils (25) have indicated that this system is more effective in sustaining muscle contraction and oxidative phosphorylation than is the diffusion of ATP and ADP.

To help clarify these proposed roles for CK, a measurement of its reaction rate in an intact tissue under various workloads would be helpful. If the reaction is in equilibrium the measured forward rate should equal the reverse rate. Furthermore, to function adequately as a high energy phosphate reserve the rate of the CK catalyzed reaction should be significantly faster than the rate of ATP production or utilization.

ADENYLATE KINASE. Adenylate kinase (AK)(27) catalyzes the reaction, $2ADP \rightleftharpoons ATP + AMP$. AK is found in all mammalian tissue at high enough activities so as to be thought to be in equilibrium (24). This reaction functions to generate ADP from AMP as well as provide an alternative source of ATP if ADP levels become appreciable. In the NMR spectrum of anoxic Tetrahymena (Fig. 1-2) no ATP or ADP is detected. As oxygen is introduced ATP appears without any ADP ever being detectable. Presumably the AK catalyzed reaction is partially responsible for maintaining such large ATP/ADP ratios. Once again, a measurement of the rates of this reaction in an intact tissue in different metabolic states should help to better clarify the role of this enzyme.

1.4 The Approach: in Vivo ^{31}P NMR

For the past 10 years there has been increasing application of ^{31}P NMR to study the metabolic state of various cells and organs. The non-invasive nature of the technique and the ease of obtaining metabolic

information, as compared to conventional freeze clamp techniques, makes *in vivo* NMR a promising tool. For an excellent monograph describing the basic principles, technical considerations, and results obtained *in vivo* with ^{31}P NMR (as well as ^{13}C, ^{1}H, ^{23}Na, and other nuclei) the interested reader is referred to the recent book by Gadian (28).

Representative ^{31}P NMR spectra from various sources are shown in Fig. 1-3. The peaks seen represent the major phosphorus-containing metabolites, such as Pi, PCr, the α, β, and γ phosphates of ATP, resonances from phosphomonoesters (PME), such as sugar phosphates, and peaks from phosphodiesters (PDE). Signals from phospholipids, DNA, or RNA are expected to be broad (approximately 20PPM) and thus not easily distinguished from noise under the conditions commonly used to acquire metabolite spectra. In the case of the *in situ* brain spectrum (Fig. 1-3c) a broad component arising from bone is readily seen owing to the large amount of phosphate in bone. These spectra illustrate that reasonably good signal-to-noise ratios can be obtained from viable tissue providing care is taken both to keep the tissue alive in the NMR spectrometer (6) as well as to define where signals are coming from (Chapter 3).

^{31}P NMR of cells and organs has primarily been used to obtain three classes of information:

1. The intensity of each peak in the spectrum is proportional to the concentration of the respective metabolite. If care is taken to calibrate peak areas with standards of known concentration and data are acquired so that the peaks represent their full intensities, i.e. not partially saturated, concentrations of metabolites can be determined.

In a few cases, concentrations obtained from NMR spectra have been

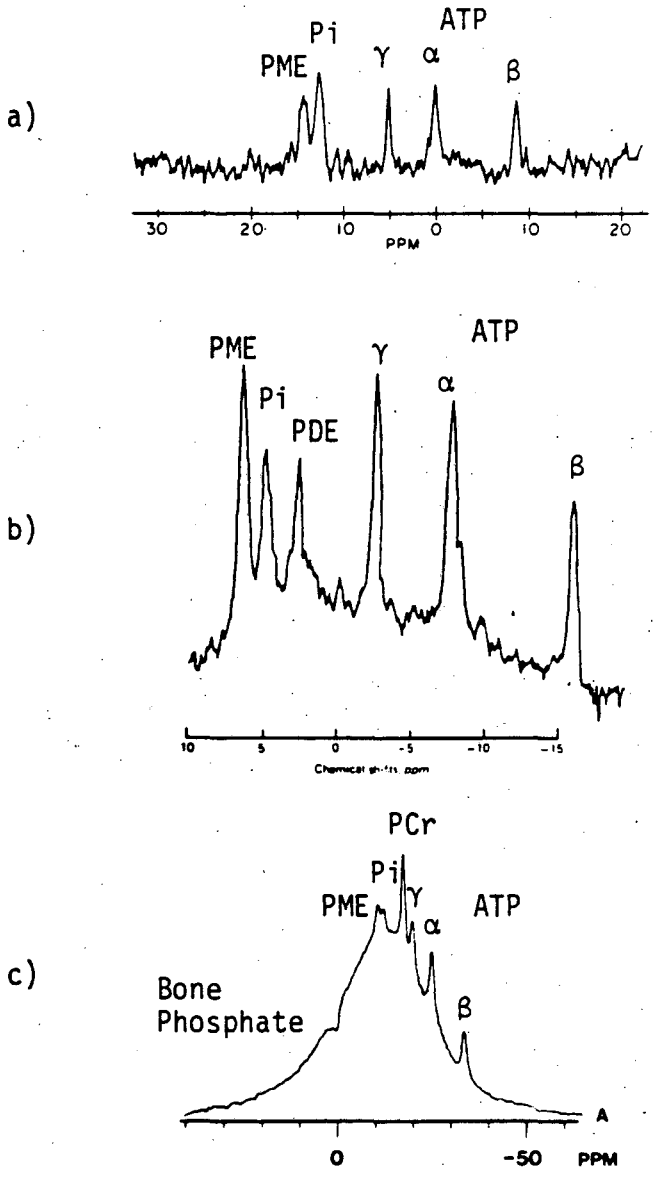

Figure 1-3. in Vivo ^{31}P NMR spectra obtained from various sources. (a) spectrum obtained from secondary cultures of chicken embryo fibroblasts (from reference 29); (b) spectrum obtained from perfused kidney (from reference 30); spectrum obtained from rat brain, in situ (from reference 31).

compared to values obtained by acid extract and enzymatic analysis. While values for ATP and PCr concentrations obtained by the two methods have agreed, there have been discrepancies found with other metabolites. In muscle, the ADP concentration inferred from NMR turns out to be at least twenty times lower than the values obtained from extracts (32). This discrepancy has beeen attributed to bound ADP, whose ^{31}P resonances are broadened due to restricted moblilty of the molecule and thus not detectable under normal situations. A similar discrepancy between tissue extract and NMR determined concentrations has been reported for Pi (30, 32). In perfused rat kidney as much as 75% of the extractable Pi was not detected in the NMR spectrum (30a). This cannot be explained by hydrolysis of ATP during the extraction process because ATP concentations by the two techniques are comparable. A proposed explanation is that a great deal of Pi exsists as a CaPi precipitate in mitochondria. Solid phosphate would tend to give broad lines (eg. the bone in the brain spectrum of Fig. 1-3) and thus not be easily detected.

2. In solution at pH 7, Pi exists as roughly equal amounts of $H_2PO_4^-$ and HPO_4^{-2}. These two species are in rapid exchange on the NMR time scale so only one peak is seen in the ^{31}P NMR spectrum. The resonance position of this peak depends on the relative amounts of the two species and thus depends on pH. As the second pK of Pi is titrated the resonance shifts approximately 2.5 PPM. Because this pK (6.7) is in the physiologically relevant pH range, the shift of the Pi resonance is an excellent in vivo pH meter.

Determining intracellular pH has been the most frequently used application of in vivo ^{31}P NMR. The intracellular pH of red blood cells

(33), human muscle (34), Rhodopseudomonas sphaeriodes (35), freshly fertilized Xenopus eggs (36) and the pH gradient across membranes (37) are just a few of the systems which have been studied.

The major drawback with this technique is that the pK of Pi depends on the concentration of magnesium ion, ionic strength, and protein composition of the intracellular envoironment (39). Calibration curves have been made in solutions which mimic intracellular conditions as well as possible, however uncertainties concerning intracellular environments lead to an inherent inaccuracy of approximately 0.05 pH units. In one case a cell suspension has been titrated by the addition of a proton ionophore (35); in this case it was assumed that the intracellular pH was equal to the extracellular pH.

3. The final class of information commonly obtained by in vivo ^{31}P NMR experiments are the rates of metabolic reactions. For reactions which are relatively slow it has been possible to perturb the system and monitor changes in peak intensities. Because it takes on the order of one minute, in the best of situations, to obtain a spectrum with adequate signal-to-noise, the reactions observed have been limited. Nontheless, interesting results studying the fall in PCr or ATP levels in exercising muscle (39,40), tissue made ischemic or anoxic (41,42), and glucose- loaded chicken embryo fibroblasts (29) have extended our understanding of high energy phosphate metabolism.

Unfortunately the reactions catalyzed by ATPases, CK, and AK in organs such as kidney and heart are much too fast, compared to the time it takes to acquire a spectrum, to use jump-type experiments to obtain kinetic information. For example, based on the rate of oxygen consumption of the rat kidney in situ, approximately 50% of the ATP

pool is hydrolysed and resynthesized every second.

Due to the ingenuity of two generations of magnetic resonance spectroscopists there are techniques which allow these faster rates to be measured. These techniques rely on the notion that peaks in the spectrum can be selectively, magnetically labeled. The effects of chemical exchange on the label can then be followed. The theory of these magnetization transfer techniques, as it pertains to in vivo NMR spectroscopy, is presented in the next chapter with a brief review of work done in this area by other investigators.

1.5 References

1) Lipmann, F. (1941) Adv. Enzymol. 1,99.

2) Ottaway, J.H., and Mowbray, J. in Current Topics in Cellular Regulation Vol. 12 Horecker, B.L., and Stadtman, E.R. (eds.) pp.107-208 Academic Press, N.Y., 1977.

3) Chance, B., Barlow, C., Nakase, Y., Takeda, H., Mayevsky, A., Fischetti, R., Graham, N., and Sorge, J. (1978) Am. J. Physiol. 235, H809-H820.

4) Sokoloff, L., Reivich, M., Kennedy, C., DesRosiers, H., Patlak, C.S., Pettigrew, K.D., Sakurada, O., and Shinohara, M. (1977) J. Neurochem. 28, 897-916.

5) Phelps, M.E., Kuhl, D.E., and Mazziotta, J. (1980) Science 211, 1445-1448.

6) Karczmar, G.S., Koretsky, A.P., Bissell, M.J., Klein, M.P., Weiner, M.W. (1983) J. Magn. Reson. 53, 123-128.

7) Ochoa, S. (1943) J. Biol. Chem. 151, 493-505.

8) Chance, B. and Williams, G.R. (1956) Adv. Enzymol. 17, 65-124.

9) Hinkle, P.C., and Yu, M.L. (1979) J. Biol. Chem. 254, 2450-2455.

10) Hansford, R.G. in Current Topics in Bioenergetics Vol. 10 Sanadi, D.R. (ed.) pp.217-278 Academic Press, N.Y., 1980.

11) LaNoue, K., Mizani, S.M., and Klingenberg, M. (1978) J. Biol. Chem. 253, 191-198.

12) Klingenberg, M. and Rottenberg, H. (1977) Eur. J. Biochem. 73, 125-130.

13) Palmieri, F., Prezioso, G., Quagliariella, E., and Klingenberg, M. (1971) Eur. J. Biochem. 22, 66-74.

14) Duszynski, J., Bogucka, K., Letko, G., Kuster, U., Kunz, W., and Wojtczak, L. (1981) Biochim. Biophys. Acta. 637, 217-223.

15) Lemasters, J.J. (1980) FEBS Letts. 110, 96-100.

16) Rottenberg, H. (1979) Biochim. Biophys. Acta. 549, 225-253.

17) Holian, A. and Wilson, D.F. (1980) Biochemistry 19, 4213-4221.

18) Zerahn, K. (1956) Acta. Physiol. Scand. 36, 300-318.

19) Mandel, L. and Balaban, R.S. (1981) Am. J. Physiol. 240, F357-F371.

20) Hokin, L.E. and Dahl, J.L. in Metabolic Pathways, Vol. 6, 3rd ed.: Metabolic Transport. Hokin, E. (ed.) pp.270-315 Academic Press, N.Y., 1972

21) Garner, W.H., Garner, M.H., and Spector, A. (1983) Proc. Natl. Acad. Sci. USA 80, 2044-2048.

22) Kenyon, G.L. and Reed, G.H. (1983) Adv. Enzymol. 54, 367-426.

23) Watts, D.C. in The Enzymes, Vol. VIII, 3rd ed. Boyer, P.D. (ed.) pp.385-455 Academic Press, N.Y., 1973.

24) Veech, R.L., Lawson, J.W.R., Cornell, N.W., and Krebs, H.A. (1979) J. Biol. Chem. 254, 6538-6547.

25) Bessman, S.P. and Geiger, P.J. (1981) Science 211, 448-452.

26) Jacobus, W.E. and Lehninger, A.L. (1973) J. Biol. Chem. 248, 4803-4810.

27) Noda, L. in The Enzymes, Vol. 8, 3rd ed. Boyer, P.D. (ed.) pp.279-305 Academic Press, N.Y., 1973.

28) Gadian, D.G. NMR and its Applications to Living Systems Clarendon, Oxford, 1982.

29) Karczmar, G.S. Personal Communication.

30) Balaban, R.S., Gadian, D.G., and Radda, G.K. (1981) Kidney Int. 20, 575-579.

30a) Freeman, D., Bartlett, S., Radda. G., and Ross, B. (1983) Biochim. Biophys. Acta. 762, 325-336.

31) Gonzalez-Mendez, R., Litt, L., Koretsky, A.P., von Colditz, J., Weiner, M.W., and James, T.L. (1984) J. Magn. Reson. 57, 526-533.

32) Leigh Jr., J.S., Chance, B., Eleff, S., D'Ambrosio, C., Radda, G.K., and Gadian, D. (1980) Fed. Proc. 39, 2113.

33) Moon, R.B., and Richards, J.H. (1973) J. Biol. Chem. 248, 7276-7278. This paper is generally considered to be the one which generated interest in applying ^{31}P NMR to living systems.

34) Taylor, D.J., Bore, P.J., Styles, P., Gadian, D., and Radda, G.K. (1983) Mol. Biol. Med. 1, 77-94.

35) Nicolay, K., Kaptein, R., Hellingwerf, K.J., and Konings, W.N. (1981) Eur. J. Biochem. 116, 191-197.

36) Nuccitelli, R., Webb, D.J., Lagier, S.T., and Matson, G.B. (1981) Proc. Natl. Acad. Sci. USA 78, 4421-4425.

37) Ogawa, S., Rottenberg, H., Brown, T.R., Shulman, R.G., Castillo, C.C., and Glynn, P. (1978) Proc. Natl. Acad. Sci. USA 75, 1796-1800.

38) Roberts, J.K.M., Wade-Jardetzky, N., and Jardetzky, O. (1981) Biochemistry 20, 5389-5394.

39) Dawson, M.J., Gadian, D.G., and Wilkie, D.R. (1977) J. Physiol. 267, 703- 735.

40) Chance, B., Eleff, S., Leigh Jr., J.S., Sokolow, D., and Sapega, A. (1981) Proc. Natl. Acad. Sci. USA 78, 6714-6718.

41) Seymour, A., Bailey, I.A., and Radda, G.K. (1983) Biochim. Biophys. Acta. 762, 525-530.

42) Prichard, J.W., Alger, J.R., Behar, K.L, Petroff, O.A.C., and Shulman, R.G. (1983) Proc. Natl. Acad. Sci. USA 80, 2748-2751.

CHAPTER 2: IN VIVO MAGNETIZATION TRANSFER: THEORY AND PREVIOUS WORK

2.1 Introduction and Historical Background

A unique feature of NMR is the ability to measure chemical exchange reactions at steady-state in a noninvasive manner. Radioisotope techniques have the disadvantage that the tracer must enter and equilibrate with the desired pool. NMR techniques can be used to perturb directly the magnetization of desired populations of nuclei and the chemical transfer of the perturbed nuclei can be measured. Thus, NMR can be used to measure enzyme exchange rates within living organisms. This chapter will consider the basic principles of various magnetization transfer techniques including satuation transfer, inversion transfer, and two-dimensional (2D) NMR. The use of these techniques to investigate high energy phosphate metabolism, in vivo, will be reviewed.

McConnell and Thompson (1) first suggested that chemical exchange of nonequilibrium nuclear spin magnetization between two populations of nuclei with different resonant frequencies could be measured, and that inversion might be used to study chemical exchange. Forsén and Hoffman (2-4) demonstrated the feasibility of double-irradiation methods using continuous wave techniques. This approach was expanded to Fourier transform NMR using inversion transfer (5,6) and saturation transfer (7,8) to measure chemical exchange rates. Campbell et al. (9) reviewed the use of NMR pulse methods to measure slow exchange rates, specifically considering inversion transfer, saturation transfer, and Carr-Purcell sequences. The technical aspects of these techniques were

thoroughly discussed. Experiments were described using these techniques to measure the exchange between the two dipolar-coupled sites in valium. Recently, 2D NMR techniques have been used to measure many exchange reactions simultaneously, without the need for selective irradiation (10).

2.2 Principles of Magnetization Transfer

The basis for magnetization transfer experiments is best illustrated by considering a simple two-site exchange between species A and B, $A \rightleftharpoons B$. The concentrations of A and B are assumed to be in a steady-state for the duration of an experiment. As is the case for all metabolic reactions discussed in this thesis, the rate of exchange between A and B is assumed to be very slow compared to the inverse chemial shift difference between A and B, giving rise to two well resolved resonances (Fig. 2-1a). In this case it is most fruitful to consider the effects of exchange on the Z component of each spin magnetization, as described by the modified Bloch equations (11):

$$\frac{dM_A}{dt} = \frac{M_A^o - M_A}{T_{1A}} - k_1 M_A + k_2 M_B \qquad [2\text{-}1]$$

$$\frac{dM_B}{dt} = \frac{M_B^o - M_B}{T_{1B}} - k_2 M_B + k_1 M_A \qquad [2\text{-}2]$$

Where M^o is the equilibrium magnetization of the appropriate spin.

M is the magnetization of the spin at time t.

T_1 is the longitudinal relaxation time of the appropriate spin.

k_1 is the first order unidirectional rate constant for the reaction A→ B, with the equilibrium rate just equal to $k_1 M^o_A$.

Figure 2-1. Illustration of a steady-state saturation transfer experiment. A) is a spectrum obtained without any saturation of resonance B. The arrow indicates where a selective rf pulse would be placed to perform the appropriate control to account for the effects of stray irradiation on resonance A when resonance B is saturated. B) is a spectrum obtained after resonance B has been saturated until the magnetization of A has reached a new steady-state, M^{ss}_{A}. Because B is saturated, it is absent from the spectrum. The arrow indicates where the selective rf field would be placed to saturate resonance B. C) is the difference spectrum obtained by subtracting spectrum B) from spectrum A). The intensity of A equals $(M^{o}_{A}-M^{ss}_{A})$.

SATURATION TRANSFER EXPERIMENT

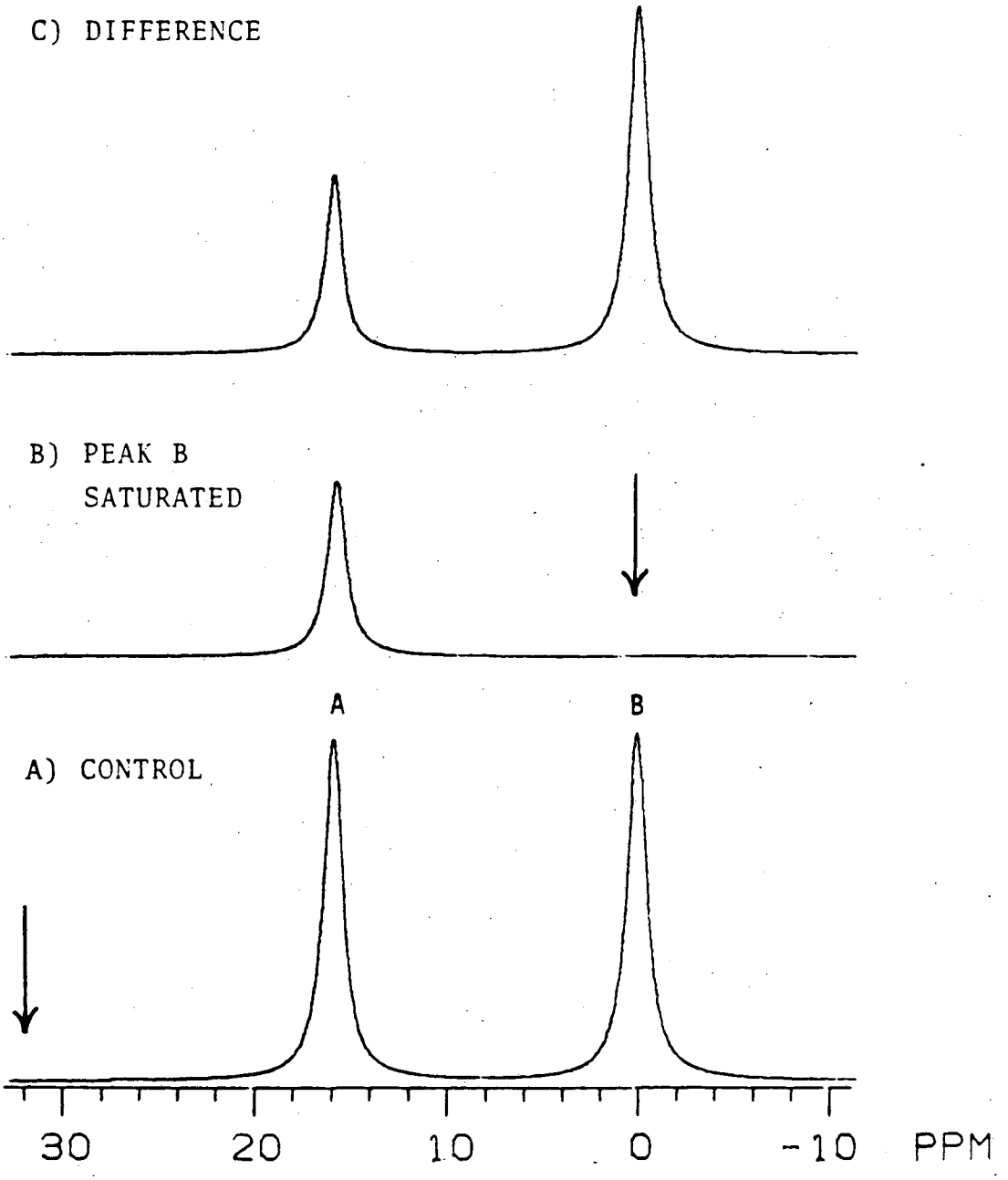

k_2 is the first order unidirectional rate constant for the reaction B→ A, with the equilibrium rate just equal to $k_2 M^o_B$.
Any dipole coupling between A and B is assumed to be negligible so that the effects of cross-relaxation can be ignored.

Chemical exchange has the effect of coupling the time dependent behavior of the Z magnetization of spins A and B. While the general solution for these coupled differential equations can be obtained (2) it is cumbersome to use in practice. This is especially true for cases when the two spins have different T_1 values and the equilibrium constant for the reaction does not equal 1. These are the conditions usually found with in vivo rate measurements.

2.3 Saturation Transfer

The most commonly used approach to simplify the exchange problem has been to uncouple the two spins by placing a selective radiofrequency (rf) field on a spin, B for example, so as to saturate that spin. The requirements which the selective rf pulse must meet are twofold. First, $(\gamma H_1)^2 >> (T_1 T_2)^{-1}$ so the peak becomes completely saturated. The time that it takes for B to become saturated depends on T_{1B}, T_{2B}, H_1, and the chemical exchange rate (Appendix 1). Second, γH_1 << the difference in frequency between A and B $(\omega_A - \omega_B)$) so that the saturating rf field does not effect A. To account for any effects that stray irradiation may have on A a suitable control (Fig. 2-1a) is usually performed. After saturation has occurred, the magnetization of spin B is zero ($M_B = 0$) and only the resonance due to A is observed (Fig. 2-1b). The effects of exchange between spin A and, the magnetically invisible, spin B can then be monitored. For this case

the Z magnetization of spin A is described by:

$$\frac{dM_A}{dt} = \frac{M_A^o - M_A}{T_{1A}} - k_1 M_A \qquad [2\text{-}3]$$

If spin B is kept saturated until the magnetization of A reaches a steady- state, $dM_A/dt = 0$, then:

$$\frac{M_A^{ss}}{M_A^o} = \frac{1}{1+k_1 T_{1A}} \qquad [2\text{-}4]$$

Where M_A^{ss} is the steady-state magnetization of A (Fig. 2-1b).

It can be seen that two processes tend to affect the magnetization of A. First, chemical exchange between A and invisible B nuclei will decrease the intensity of A. If this were the only process occurring, the signal intensity of A would decrease to zero as B is kept saturated, at a rate defined by k_1. However, spin-lattice relaxation processes will cause the saturated nuclei to reappear when they exchange to site A, at a rate defined by T_{1A}. Thus, exchange between A and B has the effect of lowering the signal intensity of A by an amount dependent on k_1 and T_{1A}. If the value for T_{1A} is known, k_1 can be easily extracted from a comparison of spectra obtained without and with B saturated to the steady-state. The situation is exactly analogous if spin A is saturated, so that k_2 can be determined.

Unfortunately, the value for T_1 is difficult to obtain <u>in vivo</u> because its measurement requires that there be no exchange taking place. Although some investigators have inhibited exchange reactions in order to measure T_1 in the absence of exchange (12), these maneuvers may alter the physiological state of the tissue, which may in turn effect T_1 (<u>eg.</u> Table 1 in Ref. 13). Alternatively, two NMR techniques

can be utilized which allow the simultaneous measurements of k_1 and T_1. Instead of saturating spin B until a steady-state develops, one can follow the time course of the decrease in M_A as B is saturated for variable lengths of time (2). Solution of equation 3 with the constraints that at t = 0, $M_A = M^o_A$ and $M_B = 0$, leads to the expression:

$$M_A = \frac{M^o_A}{1+k_1T_{1A}} (1+k_1T_{1A}\exp(-t\frac{(1+k_1T_{1A})}{T_{1A}})) \qquad [2\text{-}5]$$

Thus, the magnetization of A (M_A) decays from M^o_A to M^{ss}_A with an apparent time-constant (T_{1APP}) of:

$$T_{1APP} = \frac{T_{1A}}{1+k_1T_{1A}} \qquad [2\text{-}6]$$

Exchange has the effect of making T_{1APP} appear shorter than T_1.

Alternatively, the longitudinal relaxation of A can be measured, using typical experiments (e.g. inversion recovery, saturation recovery) while maintaning steady-state saturation of B (14). The measured time constant for the relaxation of A is also given by equation 2-6. Thus, a combination of a steady-state measurement of M_A^{ss} with a time dependent measurement of T_{1APP} allows the rate constant k, to be determined. In terms of these measurable quantities, k_1 is given by:

$$k_1 = \frac{M^o_A - M^{ss}_A}{M^o_A\, T_{1APP}} \qquad [2\text{-}7]$$

Once the first-order rate constant, k, for the reaction is known, it is easy to calculate the reaction rate by multiplying k by the

appropriate concentration of the reactant. In arbitrary intensity units, $k_1 M^o_A$ equals the rate A⟶B. Therefore, it can be seen from equation 2-7 that the rate A⟶B (in arbitrary intensity units) equals $(M_A^o - M_A^{ss})/T_{1APP}$.

In addition to the above approaches, the initial rate of change in M_A upon saturation of B may be used to obtain a direct measurement of the rate A⟶B. This is illustrated by the behavior of equation 2-3 as t approaches 0. At t = 0, $M_A = M_A^o$ and equation 2-3 becomes:

$$\left(\frac{dM_A}{dt}\right)_{t=0} = -k_1 M_A^o \qquad [2\text{-}8]$$

In this way a direct measurement of the rate A⟶B can be obtained without the necessity of calculating T_1 or k_1.

2.4 Inversion Transfer and 2D NMR

Besides saturation transfer, other approaches, such as inversion transfer (15) and 2D techniques (16, 17) have been applied to measure exchange in vivo. An inversion transfer experiment is performed by applying a selective 180° pulse to a specific spin, e.g. spin B. Immediately following this selective pulse, a spectrum will show resonance A as usual, but resonance B will be inverted. As was the case for the saturation transfer experiment, chemical reaction will cause the inverted spins (B) to exchange with the noninverted spins (A); this will tend to decrease the intensity of A and increase the intensity B. Using the initial conditions that $M_B = -M_B^0$ and $M_A = M_A^0$ at t = 0, the time dependence for M_A and M_B can be deduced from equations 2-1 and 2-2 and the rate constants determined. The resulting

equations are complicated, and once again a procedure for simplifying data analysis is available (9). If the initial rate of change of A is measured after the selective inversion of B, equation 1 can be simplified to:

$$\left(\frac{dM_A}{dt} \right)_{t=0} = -2k_1 M_A^o \qquad [2\text{-}9]$$

Thus the rate of reaction, A$\longrightarrow$B can be readily determined from the initial rate of decrease in A following inversion of B. One difference between saturation transfer and inversion transfer is that saturation transfer is a continuous labelling approach while inversion transfer utilizes a pulse label.

2D NMR techniques to study exchange processes were introduced by Jeener et al. (10). 2D NMR relies on the application of three non-selective 90^o pulses. The first two are separated by a so-called, evolution time, and the last two by a mixing time (t_{mix}). A series of spectra are obtained by systematically varying the evolution time while leaving the mixing time fixed. A two-dimensional Fourier transform can then be performed resulting in a 2D spectrum which has on its diagonal the peaks seen in the normal, one-dimensional spectrum. The effects of exchange show up as cross peaks between the species which are in exchange. If a set of two dimensional spectra are obtained with different mixing times, the intensities of the diagonal and cross peaks will vary, allowing rate constants and T_1s to be deduced. Similar to inversion transfer, 2D NMR is a pulse labelling technique. The main advantage of the 2D technique is that all exchange reactions can be monitored simultaneously without the need for selectively perturbing

individual resonances. The major disadvantage is that 2D NMR is, in general, time consuming, and peak volumes are difficult to quantitate. Recently a 2D technique has been described which eliminates the need to collect many 2D spectra at varying mixing times (18). This technique has not yet been used to study biochemical reactions.

To simplify the analysis of two-dimensional data for in vivo applications, the initial rate of increase of the cross peaks has been studied for short mixing times, leading to the following expression (19):

$$\left(\frac{dM_{AB}}{dt} \right)_{t_{mix}=0} = X_A k_1 \qquad [2\text{-}10]$$

where M_{AB} is the normalized intensity of the cross peak appearing between A and B, X_A is the mole fraction of spin A, and k_1 is the rate constant for the reaction A→B.

2.5 Unidirectional Rate Constants and the Order of a Reaction

The rate constants derived from magnetization transfer experiments are always unidirectional and first order, no matter what the actual order of the chemical reaction might be. Because the relaxation rate, T_1, represents a first order rate constant it is most convenient to express the effects of exchange as a first order rate constant. That this can always be done is due to the fact that the magnetization transfer experiments are performed under steady-state conditions from the point of view of the chemistry occuring. For example, if the synthesis of ATP is described by the following equation:

$$ADP + Pi \underset{k_r}{\overset{k_f}{\rightleftharpoons}} ATP$$

then the Bloch equation to describe the change in Pi mgnetization is given by:

$$\frac{dM_{Pi}}{dt} = \frac{M^{o}_{Pi} - M_{Pi}}{T_{1Pi}} - k_f[ADP]M_{Pi} + k_r M_{ATP} \qquad [2\text{-}11]$$

If the γATP resonance is saturated to measure k_f, comparison of equation 2-11 with equation 2-3 indicates that the measured k would equal $k_f(ADP)$. This measured k is pseudo first order in the sense that the dependence of k on the concentration of ADP is hidden. It appears to be first order because chemically the system is in a steady-state, so the concentration of ADP is a constant and can be combined with k_f to form the measured rate constant. Whether the measured rate constant can be related to the true rate constants depends on prior knowledge of the reaction mechanism. This does not affect the calculated value for the rate of the reaction being studied. No matter what the order of the reaction the rate can always be determined by multiplying the measured pseudo first order rate constant by the appropriate concentration. For the above example this means multiplying the measured k by the Pi concentration.

It is interesting to consider how the rate constant measured in a biological system, by magnetization transfer experiments, relates to enzyme kinetic parameters. Consider the simple scheme usually used to derive Michaelis-Menton kinetics:

$$E + S \underset{k_2}{\overset{k_1}{\rightleftharpoons}} ES \underset{k_4}{\overset{k_3}{\rightleftharpoons}} E + P$$

The unidirectional rate of the reaction from substrate to product is

given by:

$$V = \frac{k_3 E_T[S]}{[S]+K_m} = \frac{V_{max}[S]}{K_m+[S]} \qquad [2\text{-}12]$$

where E_t is the total enzyme concentration, K_m is defined in the usual way as $(k_2 + k_3)/k_1$, and V_{max} is the maximal rate of the reaction. The modified Bloch equation to describe the change in S magnetization upon saturating P is simply:

$$\frac{dM_s}{dt} = \frac{M_s^0 - M_s}{T_{1s}} - k_{measured} M_s \qquad [2\text{-}13]$$

where $k_{measured}(M_s)$ is directly proportional to the unidirectional rate from substrate to product, V in equation 2-12. It is readily apparent that $k_{measured}$ is proportional to $k_3 E_t/(K_m+(S)) = V_{max}/(K_m+(S))$. If $k_{measured}$ was determined as a function of (S) it would be possible to obtain estimates of V_{max} and K_m. Similar expressions could be derived for more complicted mechanisms and would be interesting to do for the enzyme reactions which have been studied in vivo. This example illustrates the need to have a model of the reaction mechanism to extract anything other than unidirectional rates from magnetization transfer experiments.

2.6 Limitations and Complications of Magnetization Transfer Measurements of Reaction Rates

A fundamental limitation to all magnetization transfer studies is the range of exchange rates which can be measured. On one end of the scale there is the frequency separation between peaks. If exchange between sites is fast compared to this separation ($k > 100$ sec $^{-1}$ for

phosphorus nuclei at commonly used magnetic field strengths) only one resonance representing an average of the two sites, will be detected. An example of this is the single Pi peak observed in most ^{31}P NMR spectra of living tissue, which represents the sum of mono and dibasic phosphate. Kinetic information for the case of fast exchange can be derived from lineshape calculations (20). However, most biochemical reactions are much slower than this frequency separation. In fact they are so slow that $k<<1/T_1$. In this case any magnetic perturbation to a spin will relax before any significant exchange has occurred. For the case of steady-state saturation it can be seen from equation 2-4 that unless $k_1 T_{1A}$ is on the order of unity, M_A^{ss}/M_A^o will not be (within the limits of achievable signal-to-noise) different from unity. For phosphorus spectra obtained from organs, an optimistic assessment is to say that $M_A^{ss}/M_A^o = 0.95$ is measurable. This implies a lower limit on k of 0.05 sec^{-1}, assuming that phosphorus metabolites have a T_1 of approximately 1 sec. For the biologist, it is fortunate that certain important reactions for bioenergetics occur at rates which are sufficiently rapid that they can be analyzed by magnetization transfer.

COMPARTMENTATION. A cell is not a well stirred homogeneous solution. Compartmentation of metabolites and enzymes complicates analysis of exchange reactions. Only in some instances can metabolites in different compartments be distinguished in the NMR spectrum. It may not be obvious how much of the total signal obtained is involved in the reaction. Furthermore, enzymes in different compartments may be reacting at different rates, but the NMR exchange experiment will measure only a bulk reaction rate which represents some weighted average of all these different rates. There are approaches to this

problem for the case where a resonance contains an exchanging and a non-exchanging fraction.

If the T_{1APP} of the exchanging and the non-exchanging fractions are assumed to be equal, then the effect of the non-exchanging fraction is to cause an underestimate of $(M^o-M^{ss})/M^o$. The difference (M^o-M^{ss}) will be correct because the non-exchanging fraction is not effected by saturation of the appropriate peak. However, M^o will be overestimated, leading to an underestimate of $(M^o-M^{ss})/M^o$ and an underestimate of k. The unidirectional rate, kM^o, will be correct because the underestimated rate constant will be balanced by the overestimated value of M^o. If the T_{1APP} of the two fractions are not equal then the best way to determine T_{1APP} of the exchanging fraction is to vary the length of the saturating pulse. In this case the decrease in peak intensity will be due only to the exchanging fraction and will change with the appropriate T_{1APP}. Alternatively, an inversion transfer (15) or a 2D experiment can be performed. The buildup of the cross peaks in the 2D experiment and the change in the noninverted peak intensity in the inversion transfer experiment will be due to the exchanging fraction only. The case where the observed peak may contain two significant populations which are exchanging at different rates is beyond the scope of this thesis and is probably characterized by too many parameters for magnetization transfer experiments to be used alone to define the rates.

In the extreme case were one of the exchanging pools is very small (below the sensitivity of NMR to detect) some interesting differences between magnetization transfer techniques arise. These are discussed in Chapter 5, with some implications for myocardial

bioenergetics.

LIMITATIONS OF A SIMPLE TWO-SITE EXCHANGE MODEL. The analysis so far has assumed that exchange occurs between just two magnetically inequivalent sites. It is more difficult to analyze magnetization transfer studies when the species invovlved are exchanging between more than two sites. In a living cell multiple exchange pathways are common, so caution must be exercized when analyzing data using a two-site model.

Reactions occurring in vivo are all catalyzed by enzymes. On the reaction pathway from free substrate to product there may be enzyme-bound intermediates. Magnetization transfer techniques will measure the correct rate for the reaction if free reactants and enzyme-bound intermediates are in fast exchange on the NMR time scale, and the rate limiting step is the interconversion of substrate to product. However, if the lifetime and relaxation rate of enzyme bound intermediates become significant, the magnetization transfer experiment will only measure partial reactions, instead of net rates. Recently, Brindle et al. (21) compared the rates of phosphate transfer from PCr to the γ phosphate of ATP (γATP), catalyzed by creatine kinase, using saturation transfer and an NMR isotope dilution technique. The forward rate of the reaction (PCr + ADP$\longrightarrow$ATP + Cr) measured by both techniques were the same indicating that, at least for this enzyme, saturation transfer measured the proper rate. Whether or not this is true for other enzymes, such as the ATP synthetase complex, remains to be tested.

EFFECTS OF COMPETING REACTIONS. Besides the problem of enzyme bound intermediates, substrates are usually involved in more than one reaction. For example, γATP is in exchange with both PCr and Pi in

muscle tissue. To examine the effects of competing reactions consider the simple two site exchange model, $A \rightleftharpoons B$, where now B is involved in a second or competing reaction which converts it to C.

$$A \underset{k_2}{\overset{k_1}{\rightleftharpoons}} B \underset{k_4}{\overset{k_3}{\rightleftharpoons}} C$$

The modified Bloch equations for this case are:

$$\frac{dM_A}{dt} = \frac{M_A^0 - M_A}{T_{1A}} - k_1 M_A + k_2 M_B \qquad [2\text{-}14]$$

$$\frac{dM_B}{dt} = \frac{M_B^0 - M_B}{T_{1B}} - (k_2+k_3) M_B + k_1 M_A + k_4 M_C \qquad [2\text{-}15]$$

$$\frac{dM_C}{dt} = \frac{M_C^0 - M_C}{T_{1C}} - k_4 M_C + k_3 M_B \qquad [2\text{-}16]$$

Exact solutions for this three-site exchange example, and indeed for the n-site case, are obtainable (22), but are complicated and difficult to use in practice. Saturation of B to measure k_1 leads to the proper result, because equation 2-14, describing the behavior of M_A, is the same as that for the simple two-site exchange (equation 2-1). However, saturation of A to measure k_2 is now complicated by the dependence of M_B on the reaction involving C. If A is saturated (M_A= 0) equations 2-15 and 2-16 become:

$$\frac{dM_B}{dt} = \frac{M_B^0 - M_B}{T_{1B}} - (k_2+k_3) M_B + k_4 M_C \qquad [2\text{-}17]$$

$$\frac{dM_C}{dt} = \frac{M_C^0 - M_C}{T_{1C}} - k_4 M_C + k_3 M_B \qquad [2\text{-}18]$$

In the extreme case where k_3 and k_4 = 0 (the competing reaction rate approaches 0), equation 2-14 reduces to the two-site case (equation 2-3). In the case where the competing reaction is much faster than any relaxation at site C (k_3M_B and k_4M_C >> $(M_C^o - M_C)/T_{1C}$), then in the steady state (dM_B/dt, dM_C/dt = 0), k_4M_C equals k_3M_B. For this case equation 2-17 reduces to the same equation as did the two site case (equation 2-3). Therefore, the effect of the competing reaction depends not only on its rate but also on the rate of relaxation which can occur at site C. The steady-state solution for M_B is given by:

$$\frac{M_B^{ss}}{M_B^o} = \frac{1 + k_4T_{1C} + k_3T_{1B}}{1 + (k_2+k_3)T_{1B} + k_4T_{1C} + k_2k_4T_{1B}T_{1C}} \qquad [2\text{-}19]$$

Where all reactions were assumed to be in equilibrium. Comparison of this equation with the result for the two-site case (equation 2-4) indicates that M_B^{ss}/M_B^o would lead to an underestimate of k_2.

Thus far, this analysis considers only the effect of the competing reaction on M_B^{ss}/M_B^o. Measurement of T_{1APP} of B with A saturated will also be affected by the reaction with C. In this case the relaxation of B will, in general, be a double exponential with time constants dependent on k_2, k_3, k_4, T_{1B}, and T_{1C}. A simple two-site analysis leading to a single exponential fit to the relaxation of B could either underestimate or overestimate the T_{1APP} of B, depending on T_{1C}, k_3 and k_4.

MEASUREMENTS TO ACCOUNT FOR COMPETING REACTIONS. Fortunately, if the exchange network is known experiments can be performed to simplify the analysis of the situation. The pertinent parameters to be measured are given by:

$$\frac{M_B^{SS}}{M_B^O} = \frac{1 + \frac{M_C^{SS}}{M_C^O} k_3 T_{1B}}{1 + (k_2+k_3)T_{1B}} \quad ; \quad \text{A saturated} \qquad [2\text{-}20]$$

$$\frac{M_B^{SS}}{M_B^O} = \frac{1 + \frac{M_A^{SS}}{M_A^O} k_2 T_{1B}}{1 + (k_2+k_3)T_{1B}} \quad ; \quad \text{C saturated} \qquad [2\text{-}21]$$

$$T_{1APP} = \frac{T_{1B}}{1 + (k_2+k_3)T_{1B}} \quad ; \quad \text{A and C saturated} \qquad [2\text{-}22]$$

Thus, monitoring B and C with A saturated, A and B with C saturated and measuring the T_{1APP} of B with both A and C saturated allows calculation of k_2 (and k_3) with the competing reaction properly accounted for. A similar multiple saturation technique has been used to measure proton exchange rates (23).

Another approach to the problem of competing reactions would be to monitor the initial change in M_B after perturbation of A, either by inversion, saturation, or a 2D experiment. At short times after the perturbation in A, the change in B would be due entirely to the reaction $A \rightleftharpoons B$, because there would not have been enough time for the competing reaction, $B \rightleftharpoons C$, to scramble the label. This technique is commonly applied to the measurement of nuclear Overhauser effects in macromolecules (24,25), where the potential for spin diffusion between many spins is equivalent to the problem of competing reactions.

2.7 Review of Magnetization Transfer Studies to Investigate High Energy Phosphate Metabolism

Owing to the unique information available from magnetization transfer experiments, interest in applying these techniques in vivo has

grown steadily. Brown, Ugurbil, and Shulman (26) first demonstrated that a reaction could be studied using saturation transfer in living cells. Since then reactions catalyzed by ATP synthesis, creatine kinase, and adenylate kinase, have been studied in isolated cells, perfused organs, and tissue in situ. Fig. 2-2 illustrates the phosphate groups which are exchanged due to reactions catalyzed by these three enzymes. In this section the results obtained, and the problems associated with studies to measure these exchange rates are reviewed. No attempt has been made to make an exhaustive review and the reader is referred to two recent articles (27,28) for a more thorough review.

ATP SYNTHESIS. Brown et al. (26) measured high energy phosphate kinetics in intact cells using saturation transfer. Thick suspensions (approximately $5x10^{11}$ cells/ml) of Escherichia coli were studied at 145.7 MHz; 20 ml/min O_2 was bubbled through the cells. The γNTP resonance (50% of NTP was stated to be ATP) was saturated, and control spectra were obtained by placing the selective irradiation halfway between the γNTP and Pi resonances. Saturation of the γNTP resonance reduced the Pi peak by 20±5%; no other peak was affected. When dicyclohexylcarbodiimide (DCCD) was added to inhibit the ATPase reaction, saturation of the γNTP signal had no effect on the Pi resonance, suggesting that the DCCD sensitive ATPase was responsible for the exchange. Saturation of the Pi peak produced a 25-37% decrease of the γNTP magnetization, which was assumed to be equivalent to a 50-75% decrease in the γATP magnetization; no other peak was affected. T1 measurements were made in the presence of DCCD to eliminate the effects of exchange. The T_1 of γNTP was about 0.2 sec and the T_1 of Pi

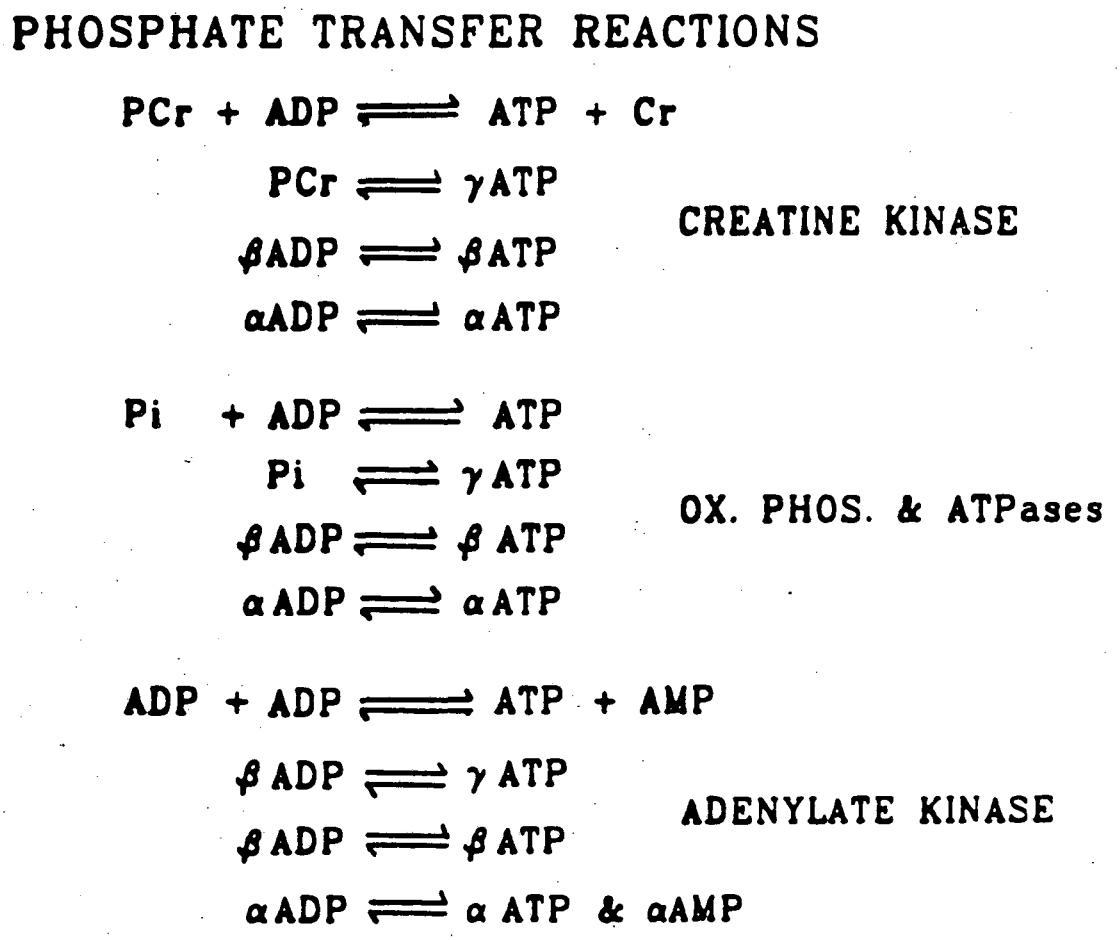

Figure 2-2. Illustration of the different phosphate group exchanges which occur during reactions catalyzed by creatine kinase, ATP synthesis and hydrolysis, and adenylate kinase.

was 0.43±0.08 sec. The calculated unidirectional rate constant for Pi incorporation into γATP was 0.6 sec^{-1}, and the k for the reaction γATP→ Pi ranged from 5-15 sec^{-1} due to the errors involved in the measurements. The unidirectional rates for both reactions were roughly similar, suggesting that ATP synthesis rates were equal to ATP hydrolysis rates. The interpretation of these results is complicated by the presence of peaks overlapping the γATP resonance (e.g. γGTP, γUTP, etc ...) which may or may not contribute to the exchange. The authors considered this problem and estimated that 50% of the NTP pool was not contributing to the exchange. Furthermore, the measured T_1 of the γNTP peak is a reflection of all components and may not accurately reflect the T_1 of γATP. No attempt was made to compare measured rates of ATP synthesis and O_2 consumption.

Alger, den Hollander, and Shulman (29) performed experiments similar to the above using Saccharomyces cerevisae. The γATP resonance was saturated for 2 sec prior to acquisition, and a control was performed by saturating at a point downfield from Pi equal to the distance that γATP resonates from Pi. To increase the efficiency of signal averaging pulse delays shorter than $5T_1$ were used with pulses less than 90°, resulting in partially saturated spectra. While this procedure could give erroneous values of $(M^{o}-M^{ss})/M^{o}$, the authors compared the values obtained under partially saturated and fully relaxed conditions and found no difference. Saturation of the γATP signal caused a decrease in the intracellular Pi peak (29±3% drop), as well as a decrease in the intensity of the βATP peak. A small change in the αATP signal was attributed to the effects of stray irradiation, because a similar change was produced by the appropriate control. The

apparent T_1 of Pi, measured by inversion recovery while saturating the γATP resonance, was 0.7 sec.

The authors considered the possibiltiy that Pi might be involved in reactions other than ATP synthesis (e.g. synthesis of polyphosphates and glycolytic intermediates). However, because anaerobiasis and an inhibitor of oxidative phosphorylation reduced the decrease in Pi magnetization upon saturating γATP to 10% of the aerobic value these, additional exchange pathways were considered negligible.

The k for ATP synthesis was 0.44 sec^{-1}. Assuming an intracellular volume to deduce Pi concentrations, the unidirectional rate was calculated to be 3.5±1.0 μmol/sec/gm. Interpreting the change in βATP intensity to be due to saturation of βADP when the γATP peak was saturated, the rate of ATP hydroysis was calculated and found to be similar to the rate of synthesis. O_2 consumption was 0.02 μmol/sec/gm, which implies an ATP synthesis rate of 0.12 μmol/sec/gm, assuming a J_{ATP}/J_O of 3. The NMR measured rate was thus approximately 30 times larger than the rate expected from O_2 consumption. Therefore, in yeast it appears that saturation transfer measures a rapid exchange rather than net synthesis. These results illustrate that caution should be exercised when attributing unidirectional exchange rates to net rates.

The first measurement of ATP synthesis in a perfused organ was performed by Matthews et al. working with a Langendorff perfused heart (12). The γATP peak was saturated until a steady-state change in the Pi peak was obtained. The Pi peak fell to 64% of its control value. A small transfer to the βATP peak was also observed. The T_1 of Pi was obtained following total global ischemia to eliminate the effects of exchange. The T_1 was 1.9 sec and assumed to be equal to the T_1 of Pi

in the well functioning heart. The steady-state rate of ATP synthesis was calculated to be 2.8±0.3 μmol/sec/gm dry weight. Oxygen consumption of these perfused hearts was found to be 0.34±0.02 μmol/sec/gm dry weight. A J_{ATP}/J_O of 3.5±0.8 was measured making corrections for the amount of ATP produced from glycolysis, estimated from lactate release. In contrast to the yeast results discussed above, the NMR measured ATP synthesis rate in perfused heart gives reasonable results. Irradiation of the Pi peak, to measure the rate of ATP hydrolysis, gave no change in the γATP peak intensity. This was attributed to the short T_1 of γATP (0.9 sec.).

Freeman et al. (30) performed saturation transfer measurements of the perfused kidney to investigate the stoichiometric relationship between ATP turnover, oxygen consumption, and sodium transport. Saturation of the γATP signal produced a 42% decrease in the Pi magnetization. In addition to Pi, the βATP resonance was reduced by 18%. This was attributed to adenylate kinase activity, or a negative NOE, but could have been due to βADP$\rightleftharpoons$βATP exchange. The rate of ATP synthesis was compared to oxygen consumption and a J_{ATP}/J_O of 2.45 was calculated. Comparison of the rate of ATP synthesis to the rate of Na^+ reabsorption led to a value of 4.5 for the J_{Na^+}/J_{ATP}, indicating that in the perfused kidney the large J_{Na^+}/J_O is due to efficient coupling of ATP hydrolysis to Na^+ reabsorption.

Comparison of NMR data with enzymatic analysis indicated that 100% of the ATP, but only 25% of ADP and 27% of Pi in the kidney was NMR visible. The finding that the measured value of 2.45 for the J_{ATP}/J_O ratio is similar to the accepted value of 3, was interpreted to show that the NMR invisible pools of Pi and ADP do not significantly

participate in oxidative phosphorylation.

The only saturation transfer studies performed on a mammalian organ in situ, other than those presented in Chapter 4 of this thesis, were performed on rat brain (31) and very recently on rat kidney (31a). In brain, saturation of the γATP peak produced a 35% fall of the Pi magnetization as well as a change in the α and βATP peaks. The rate of ATP synthesis was 0.33 μmol/sec/gm wet weight which agrees with results derived from previously published values of cerebral oxygen consumption assuming a J_{ATP}/J_O of 3.

Recently 2D exchange techniques have been applied to the perfused heart (16), as well as to rat brain and muscle (17). Interestingly, no cross peaks were observed between the Pi and γATP signals, in contrast to the saturation transfer results presented above. One possibility is that the short T_1 of the γATP peak made the cross peaks too small to detect. Another possibility, based on the differences between saturation transfer and 2D techniques to detect small exchanging metabolite pools, is presented in Chapter 5.

CREATINE KINASE. Magnetization transfer studies of CK have been performed in skeletal muscle (32,33), heart (12,13,32,34-38), and brain (31). These studies have all been concerned with two questions. First, does the enzyme behave kinetically the same in vivo as it does when it is isolated and studied in vitro? Second, can measurement of the steady-state kinetics of the enzyme define its role in vivo?

To investigate the important parameters which regulate CK in vivo Radda and co-workers have studied the perfused heart (34,35). Heart metabolism was altered with different substrates, by changing perfusion pressure, or by producing KCl arrest (34). The forward rate of CK was

measured by saturating the γATP and observing the PCR peak. The T_{1APP} of PCr was measured using saturation recovery techniques while saturating the γATP peak. The free cytosolic ADP concentration was calculated assuming that CK was in equilibrium and using the *in vitro* determined equilibrium constant. The effect of increasing ADP concentration, due to changing metabolic conditions, on the forward rate was analysed using an Eadie-Hofstee plot; a linear relationship between the forward flux and the forward flux/(ADP) was demonstrated. The calculated K_m for ADP was found to be in good agreement with the value determined *in vitro*. The authors concluded that free ADP was the primary factor regulating the CK flux.

To determine the activation energy for the CK catalyzed reaction *in vivo*, Matthews et al. (35) studied the temperature dependence of the forward rate in perfused heart. Lowering the temperature from 37 to $4^{o}C$ reduced the steady-state flux through CK by 80%. The apparent activation energy was calculated to be 42 kJoules/mole, which, the authors claimed, was in good agreement with previously published values. From this data it was concluded that the reaction is not diffusion limited *in vivo* and that extraction and dilution of the enzyme for study *in vitro* does not alter its fundamental kinetic properties. To further support this conclusion, Meyer et al. (15) measured the same forward flux through CK in isolated cat bicep muscle and isolated enzyme in a solution mimicking intracellular conditions of ionic strength.

To gain a deeper understanding of the role of CK in muscle energetics most investigators have studied the relation of flux through CK to oxygen consumption and workload. Nunnally and Hollis (13) were

the first to demonstrate a correlation between the rate through CK and the physiological state of an organ in their studies of perfused rabbit heart. They performed a series of measurements in which the time of saturation was varied in order to derive T_{1APP}. This, combined with a steady-state measurement of $(M^O-M^{SS})/M^O$, allowed the appropriate rate constant to be calculated. Under control conditions the forward direction of CK was greater than the reverse rate, similar to results obtained by Brown et al. (32) using perfused rat hearts. Measurements were also performed during KCl arrest and after recovery from ischemia. The pulse pressure and the rate of rise in pressure per beat were reduced following ischemia, however, the forward and reverse rates through CK were markedly increased and were now equal. Ischemia produced differing effects on the T_1s; the T_1 of γATP was reduced from 1.2 sec (control) to 0.6 sec after ischemia, whereas the T_1 of PCr was increased from 1.8 to 2.2 sec. These results indicate that it is important to perform magnetization transfer experiments so that both T_{1APP} and $(M^O-M^{SS})/M^O$ are measured. KCl arrest, which reduces the energy demands, also markedly reduced the unidirectional rates for the CK catalyzed reaction. The T_1 of PCr was prolonged by KCl arrest, but there was no significant effect on the T_1 of γATP. To show that the measured discrepancy between the forward and reverse rate through CK was not intrinsic to the enzyme, studies were performed on purified muscle CK; the forward and reverse directions were the same.

The discrepancy between the forward and reverse rates of CK has been measured by a number of investigators in skeletal muscle (33), perfused heart (32,34), and brain <u>in situ</u> (31). Because levels of PCr were in a steady-state during these experiments, and CK is believed to

be the only enzyme which utilizes PCr, the net forward rate must equal the net reverse rate through CK. Explanations for why there is a discrepancy have taken two forms. Brown et al. (32) and Gadian et al. (33) suggested that because ATP was involved in other reactions (competing reactions) besides that catalyzed by CK, a simple two-site analysis to the saturation transfer data was underestimating the reverse rate. Matthews et al. (34) attempted to account for this by including the effects of exchange between γATP and Pi and found that this exchange was not sufficient to explain the discrepancy. They pointed out that there were other reactions (e.g. adenylate kinase) which should also be taken into account. Their analysis accounted only for the effects of the additional exchange on $(M^O-M^{SS})/M^O$ and not T_{1APP} and so was not strictly correct. Nunnally and Hollis (13) also considered the effects of competing reactions but, besides an effect on PCr, saturation of γATP reduced only the βATP magnetization. This effect was too small to explain the measured discrepancy in rates.

Nunnally and Hollis (13) suggested that the forward and reverse rates were different because of compartmentation of cellular pools of metabolites and enzymes. Their observation of near equality in rates in the reperfused ischemic heart was interpreted to indicate the loss of ATP from one compartment. The shortening of the T_1 for the γATP peak in these studies was suggested to confirm this result. While Nunnally and Hollis suggested the possibility of compartmentation, it was not clear precisely why the reverse rate should be smaller than the forward rate. Chapter 5 of this thesis proposes a detailed explanation for why saturation transfer measures unequal forward and reverse rates for the CK reaction. The model was inspired by contrasting the 2D

exchange results with saturation transfer results in brain. Balaban et al. (17) found that the forward rate through CK was equal to the reverse rate in rat brain using 2D exchange techniques. This is in contrast to the findings of Shoubridge et al. (31) who measured a significantly larger forward than reverse rate using saturation transfer techniques in rat brain.

If PCr is to fulfill its role as a high energy phosphate reservoir the forward rate through CK should be larger than ATP turnover rates. That this is true has been demonstrated by performing magnetization transfer studies in perfused heart (12,13,32,34-38) and brain in situ (31). Results from heart indicate that the rate of phosphate incorporation into ATP from PCr ranges from 3-15 times faster than ATP synthesis rates depending on the physiological state of the organ. In brain the forward flux through CK was 5 times larger than the rate of ATP synthesis.

ADENYLATE KINASE. In many of the studies described above an effect on the βATP peak was observed when the γATP was saturated. While the role of AK in causing this exchange has been acknowledged it has been explicitly studied only by Gupta (39) in red blood cells. This has been the only saturation transfer study reported to date on isolated mammalian cells. Saturation of the βATP peak produced a 12±3% decrease in the intensity of the γATP signal. Besides a negative NOE, the only explanation for this exchange depends on two cycles of the AK reaction (Fig. 2-2). First βATP is transferred to βADP (below detectable levels in red blood cells) and then the βADP phosphate is transferred to the γATP position. By accounting for the two cycles which the reactants must go through to carry the magnetic label and by

measuring the T_{1APP} of γATP (1.3 sec) with βATP saturated, a unidirectional rate of 0.3 μmol/sec/ml cells was determined. Similar experiments were performed on isolated AK to show that this enzyme could explain the observed transfer. No saturation transfer was observed between γATP and Pi or 2,3-diphosphoglycerate suggesting that these exchanges were occurring too slowly to be measured, which also implies that competing reactions were not an important concern.

2.8 Conclusions

Magnetization transfer experiments can be performed on living cells although the interpretation of these experiments is not without its problems. The need to account for competing reactions, formulate testable models of compartmentation, as well as appreciate the differences between the various versions that magnetization transfer can take has been illustrated by results obtained by other workers. Furthermore, the need to compare results of experiments from in vitro preparations and living tissue is emphasized. In particular, an understanding of what precisely is being measured when the exchange between Pi and γATP is being studied will probably occur only when studies are performed on isolated mitochondria and the isolated ATP synthetase complex.

Finally, as the reader has probably appreciated, errors involved in these measurements are large. This is partly due to the instability of the preparations used. Perfused organs are generally considered to be dying organs, so sufficient time is not available to perform lengthy magnetization transfer studies without an appreciable change in physiological state. A remedy to this situation is to perform these

experiments on the organ in situ. This has been hampered by the lack of adequate ways of obtaining ^{31}P NMR spectra from heart and kidney. The next chapter presents a technique which allows good NMR spectra to be obtained so that magnetization transfer studies can be performed.

2.8 References

1) McConnell, H.M., and Thompson, D.D. (1957) J. Chem. Phys. 25, 958-959.

2) Forsén, S., and Hoffman, R.A. (1963) J. Chem. Phys. 39, 2892-2901.

3) Forsén, S., and Hoffman, R.A. (1964) J. Chem. Phys. 40, 1189-1196.

4) Forsén, S., and Hoffman, R.A. (1963) Acta Chem. Scand. 17, 1787-1788.

5) Dahlquist, F.W, Longmuir, K.J., and DuVernet, R.V. (1975) J. Magn. Reson. 17, 406-410.

6) Alger, J.R., and Prestegard, J.H. (1977) J. Magn. Reson. 27, 137-141.

7) Gupta, R.J., and Redfield, A.G. (1970) Science 169, 1204-1206.

8) Glickson, J.D., Dadok, J., and Marshal, G.R. (1974) Biochemistry 13, 11-14.

9) Campbell, I.D., Dobson, C.M., Ratcliffe, R.G., and Willaims, R.J.P. (1979) J. Magn. Reson. 29, 397-417.

10) Jeener, J., Meier, E.H., Bachmann, P., Ernst, R.R. (1979) J. Chem. Phys. 71, 4546-4553.

11) McConnell, H.M. (1958) J. Chem. Phys. 28, 430.

12) Matthews, P.M., Bland, J.L., Gadian, D.G., and Radda, G.K. (1981) Biochem. Biophys. Res. Comm. 103, 1052-1059.

13) Nunnally, R.L., and Hollis, D.P. (1979) Biochemistry 18, 3642-3646.

14) Mann, B.E. (1977) J. Magn. Reson. 25, 91-94.

15) Meyer, R.A., Kushmerick, M.J., and Brown, T.R. (1982) Am. J. Physiol. 242, C1-C11.

16) Garlick, P.B., and Turner, C.J. (1983) J. Magn. Reson. 51, 536-539.

17) Balaban, R.S., Kantor, H.L., and Ferretti, J.H. (1983) J. Biol. Chem. 258, 12787-12789.

18) Bodenhausen, G., and Ernst, R.R. (1982) J. Am. Chem. Soc. 104, 1304-

19) Balaban, R.S., and Ferretti, J.A. (1983) Proc. Natl. Acad. Sci. USA 80, 1241-1245.

20) Johnson, C.R. (1965) Adv. Magn. Reson. 1, 33-

21) Brindle, K.M., Porteous, R., and Radda, G.K. Biochem. Biophys. Acta (in press).

22) Schotland, J., and Leigh, J.S. (1983) J. Magn. Reson. 51, 48-55.

23) Perin, C.L., and Johnson, E.R. (1979) J. Magn. Reson. 33, 619-626.

24) Wagner, G., and Wuthrich, K. (1979) J. Magn. Reson. 33, 675-680.

25) Kumer, A., Wagner, G., Ernst, R.R., and Wuthrich, K. (1981) J. Am. Chem. Soc. 103, 3654-3658.

26) Brown, T.R., Ugurbil, L., and Shulman, R.G. (1977) Proc. Natl. Acad. Sci. USA 74, 5551-5553.

27) Alger, J.R., and Shulman, R.G. (1984) Quart. Rev. Biophys. (in press).

28) Koretsky, A.P., and Weiner, M.W. in Biomedical Magnetic Resonance James, T.L. and Margulis A. (eds) 1984, in press.

29) Alger, J.R., den Hollander, J.A., and Shulman, R.G. (1982) Biochemistry 21, 1957-1963.

30) Freeman, D., Bartlett, S., Radda, G.K., and Ross, B. (1983) Biochim. Biophys. Acta 762, 325-336.

31) Shoubridge, E.A., Briggs, R.W., and Radda, G.K. (1982) FEBS Lett.

140, 288-292.

32) Brown, T.R., Gadian, D.G., Garlick, P.B., Radda, G.K., Seeley, P.J., and Styles, P. in Frontiers of Biological Energetics vol 2. Dutton, P.L., Leigh, J.S., and Scarpa, A. (eds) pp.1341-1349. Academic Press, N.Y., 1978.

33) Gadian, D.G., Radda, G.K., Brown, T.R., Chance, E.M., Dawson, M.J., and Wilkie, D.R. (1981) Biochem. J. 194, 215-228.

34) Matthews, P.M., Bland, J.L., Gadian, D.G., and Radda, G.K. (1982) Biochim. Biophys. Acta 721, 312-320.

35) Matthews, P.M., Bland, J.L., and Radda, G.K. (1982) Biochim. Biophys. Acta 763, 140-146.

36) Seymour, A.L., Keough, J.M., and Radda, G.K. (1983) Biochem. Soc. Trans. 11, 376.

37) Bittl, J.A., and Ingwall, J.S. (1984) Personal communication.

38) Miceli, M.V., Hoertez, J.A., and Jacobus, W.E. (1983) Circulation 68, III-65.

39) Gupta, R.K. (1979) Biochim. Biophys. Acta 586, 189-195.

CHAPTER 3: THE ART AND SCIENCE OF IMPLANTED RF COILS

3.1 Introduction

There has been growing interest in the use of NMR to obtain biochemical information from animal tissue, in situ (1-9). Studying an intact organ in situ offers the advantages of prolonged stability and normal physiologic functioning as compared to perfused organs or isolated cells. A major obstacle to such endeavors has been distinguishing signals due to the tissue of interest from those of nearby tissue. Organs lying close to the surface of animals have been studied using surface coils (5-8). Unfortunately, spectra from deeper lying organs, such as the heart, suffer from problems of sensitivity and discrimination. The addition of static field focussing to define a small region of homogeneity (6) has the potential to overcome some of the difficulties encountered with surface coils. However, specialized gradient coils, not found on most spectrometers, are required and they are often difficult to use. Other approaches have relied on acute surgical intervention to position an organ in the NMR receiver coil, concurrently removing it from surrounding tissue (2,3,9). These surgical maneuvers may have adverse physiological consequences and limit the viability of the organ or animal during the course of NMR measurements.

To circumvent some of these problems a technique for implanting rf coils around rat kidney, liver, and heart several days prior to NMR experiments has been developed (10-12a) and is described in this chapter. These chronically implanted coils allow ^{31}P NMR spectra to be

obtained from organs under homeostatic conditions with any spectrometer which has a magnet large enough to accommodate the animal.

3.2 Materials and Methods

SURGICAL PROCEDURES. Sprague Dawley rats (180-220 gm) maintained on a standard diet were used throughout. Animals were anesthesized with an intraperitoneal injection of a mixture of Ketalar (87mg/kg body weight, Parke-Davis, Morris Plains, N.J.) and Rompun (3mg/kg body weight, Cutter Lab., Shawnee, Ka.). The left kidney was exposed by a flank incision and the coil placed around the organ. To separate surrounding muscle from the coil, a thin layer of biologically inert material, Gortex (Gore Assoc., Sunnyvale, Ca.), was placed between the coil and the muscle. The coil was held in place by tightly suturing the muscle and skin around the coil leads during closure. Liver coils were placed between the hepatic lobes through an abdominal incision. No Gortex was needed as the coil was surrounded on all sides by liver.

For heart coil implantation, the animal was anesthesized and received positive pressure ventilation via tracheal intubation through the mouth using an intra-arterial puncture tube (Angiocath, Deseret Co., Sandy, Utah). Ventilation was maintained with a tidal volume of 0.6-3 ml at 80-140 respirations per minute using a respirator (Harvard Instruments, Cambridge, Ma.). The diaphragm was exposed through a mid-abdominal incision, and then opened with an arc shaped incision. The coil was placed around the heart and the diaphram was then closed around the leads using sutures and liquid adhesive (Locktite Superbonder 495, Locktite Corp., Newington, Ct.). The coil leads were exteriorized through the abdominal skin. After the animal was removed

from the respirator, a soft polyethylene tube (Angiocath, Deseret Co.) was left in the thoracic cavity and negative suction was applied for 2-6 hours following surgery. Prophylactic antibiotics (Tobramycin, 10 mg/ kg body weight/day, Eli Lilly Ind. Inc., Carolina, Puerto Rico and Ampicillin, 6.5 mg/kg body weight/day, Bristol Lab., Syracuse, N.Y.) were administered to the rats for 2-4 days after heart surgery. Recovery from all surgery was monitored by daily measurement of weight.

For NMR measurements the rat was continually anesthesized with a mixture of Ketalar (43.5 mg/hour/kg body weight) and Rompun (1.5 mg/hour/kg body weight) through an intraperitoneal line (PE-50, Clay Adams). A venous line, for continual infusion of saline and an arterial line, to monitor blood pressure and heart rate, were inserted. The animal was placed on a holder, the coil leads soldered to the rest of the tuning circuit, and the circuit tuned to the appropriate frequency. The holder was then placed in a shielded casing and positioned so that the organ of interest was centere in the static magnetic field (B_o field). At the end of an experiment the organ was preserved for histological examination.

COIL DESIGN. Coils were made from 22 gauge, copper wire insulated with polyethylene tubing (PE 100, Clay Adams, Parsippany, N.J). To minimize loss in sensitivity associated with the wire leads, which run from the coil to the tuning circuit outside the rat, fixed value capacitors (American Technical Ceramics, Huntington Station, NY) were attached close to the coil to partially tune and match the circuit (Appendix 2, 13). The capacitors were insulated with silicone sealant and covered with Teflon tape. Examples of coils used for heart and kidney implantation are shown in Fig. 3-1.

Figure 3-1. Rf coils used to obtain NMR spectra from rat organs in situ. A two turn phosphorus coil and a single turn proton coil, in a crossed configuration are shown in a. These coils were used to obtain phosphorus spectra from kidney while simultaneously monitoring protons to lock the magnetic field of the Varian XL-100. A two turn coil used to obtain phosphorus spectra from heart at 97 MHz is shown in b. Capacitors used to partially tune and match the circuit are shown insulated with silicone sealant. A coil used to obtain spectra from rat kidney at 97 MHz is shown in c. A kidney is displayed between the coil turns to illustrate the orientation of the coil with respect to the organ. A capillary containing MDPA and Gortex used to prevent skeletal muscle from touching the coil are also shown. Ruler markings are in cm.

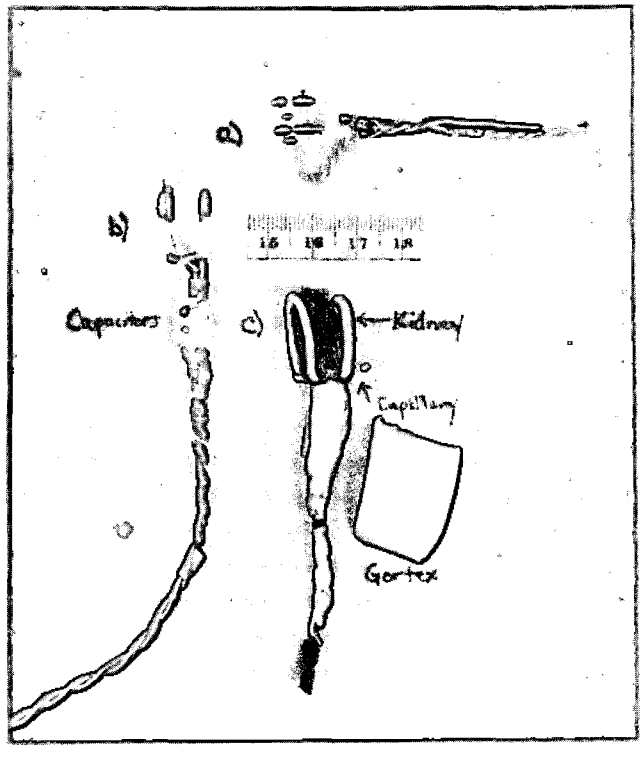

In some cases a capillary containing methylene diphosphonic acid (MDPA, Sigma Chemical, St. Louis, Mo.) buffered at pH 8.9 was attached to the coil during surgery to provide a chemical shift and integration standard.

NMR MEASUREMENTS. ^{31}P NMR measurements were performed at 40.5 MHz, on a Varian XL-100 with a MONA accessory (Nicolet, Fremont, Ca.) and at 97.3 MHz on a homebuilt spectrometer utilizing a superconducting magnet with a 3 in. diameter bore (Cryomagnet Systems, Indianapolis, Ind.) and a Nicolet 1180/293B data system. The XL-100 was locked to either an external D_2O sample or with protons detected from the organ using a second, roughly crossed coil tuned for protons. The fixed frequency ^{2}H lock channel of the XL-100 was converted to observe protons using a mixer placed between the ^{2}H preamp and the probe. An additional frequency synthesizer was used to mix the ^{2}H pulse frequency up for excitation and back down for detection. Because the proton signal is so strong, the loss in sensitivity associated with this scheme is tolerable. No lock was used with the superconducting magnet. The proton signal arising primarily from water in the tissue, obtained through the phosphorus coil without additional tuning, was used to shim. Typically a ^{1}H linewidth of 45-70 Hz (Fig. 3-2) was achieved prior to acquiring ^{31}P spectra.

In order to quantitate peak areas and chemical shifts the Nicolet simulation routine NTCCAP was used (Fig. 3-3). Linewidths, heights and peak positions were varied until a minimum rms error fit was obtained. No resolution enhancement techniques, such as left shifting or convolution difference, were used to remove broad components associated with any of the spectra.

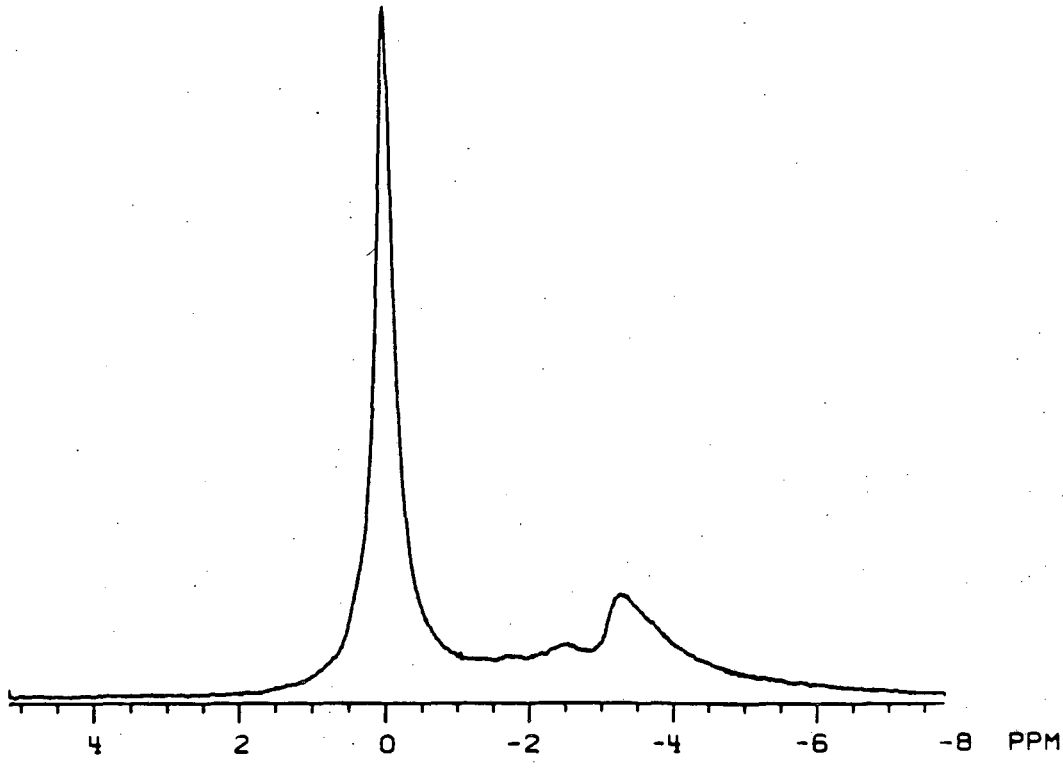

Figure 3-2. Typical ^{1}H spectrum obtained after shimming the magnetic field using the water signal from the organ of interest. The spectrum is the sum of 4 acquisitions obtained at 240 MHz from a kidney using a 40 μsec pulse (10^{o}) and a 2.3 sec recycle time. Larger peak at 0 PPM is from water protons in the kidney and the smaller peak at -3.4 PPM is from - CH_2- protons in fat. Water linewidth is 62 Hz at half-height.

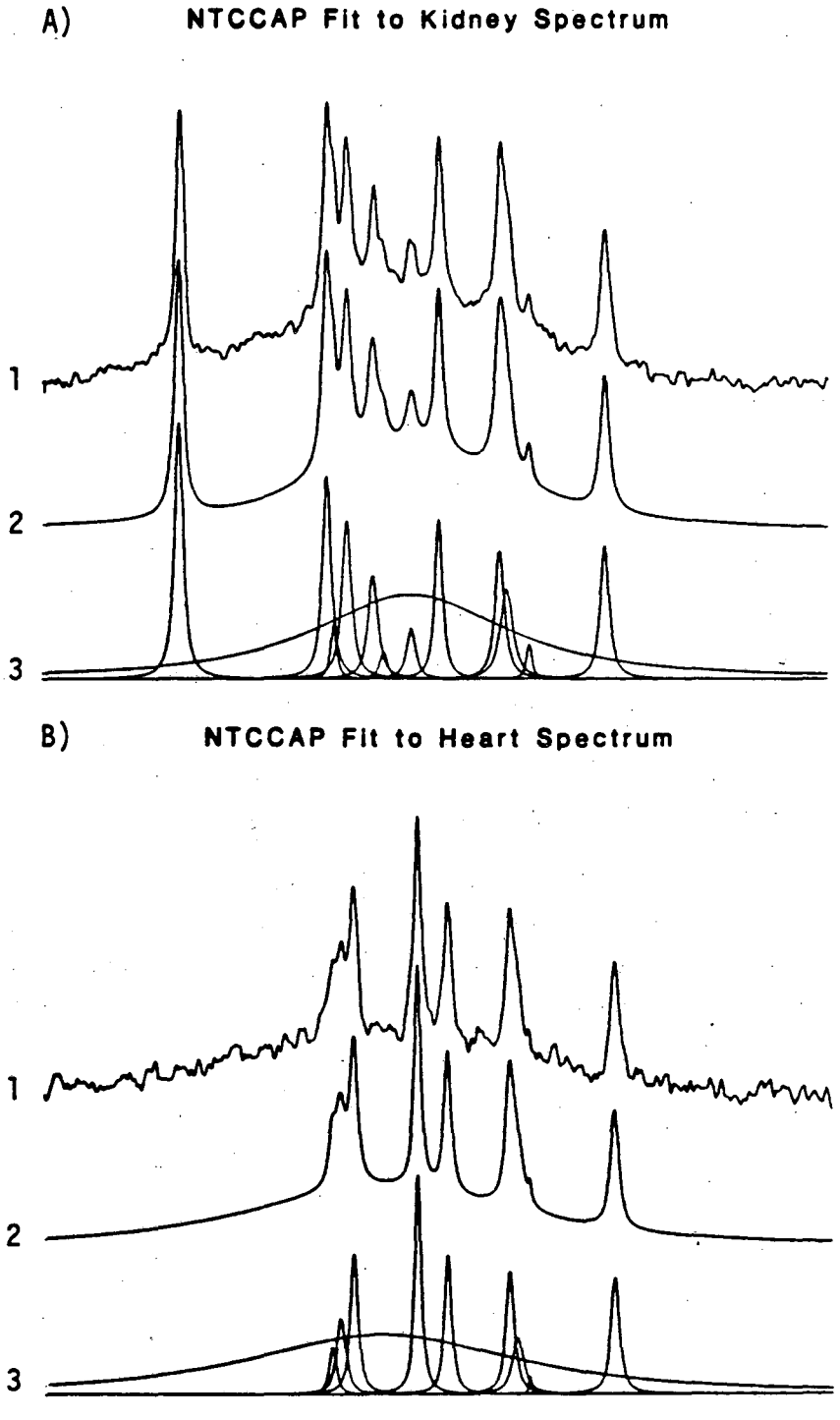

Figure 3-3. Examples of NTCCAP simulation of ^{31}P NMR spectra from A) kidney and B) heart. Upper trace (1) represents original spectrum, middle trace (2) is simulated spectrum, and lower trace (3) shows each individual line used to produce the simulated spectrum.

3.3 Results and Discussion

COIL IMPLANTATION. Surgical implantation of NMR rf coils is an invasive procedure, the effects of which were largely reversible when the animals were allowed to recuperate for several days. All rats survived kidney and liver surgery and were gaining weight within two days. The survival rate from heart coil surgery was approximately 80%, with weight gain beginning within four days. Histological examination revealed that minor surface fibrosis of kidney, liver, and heart occurred in tissue which touched the coil. Fig. 3-4 shows two rats, one with a kidney and one with a heart coil. As can be seen the rats were happy and free to move about.

X-rays (Fig. 3-5) show that both kidney and heart coils maintained their proper orientation so that the B_1 field produced was perpendicular to the B_o field, even though the rats were allowed to move about freely. Coils placed in the liver also maintained proper orientation.

QUANTITATIVE ANALYSIS OF SPECTRA. ^{31}P NMR spectra of kidney, heart and liver obtained at 97.3 MHz (Fig. 3-6), indicate the relative concentrations (Table 3-1) of observed metabolites. There was no significant difference in the intensities of the β and γATP peaks in any of the organs, indicating that free ADP concentrations were below 3% of ATP concentrations.

Peaks observed <u>in vivo</u> and their chemical shifts are in agreement with those detected in perfused organs (3,14-18), although there are some differences. In the phosphodiester region of the kidney spectrum a previously unreported peak (Fig. 3-6a, peak 6) is seen along with

Figure 3-4. A) shows a rat with a coil implanted around the kidney. B) shows a rat with coil implanted around the heart. In both cases the coil leads can be seen coming from inside the rat.

A)

B)

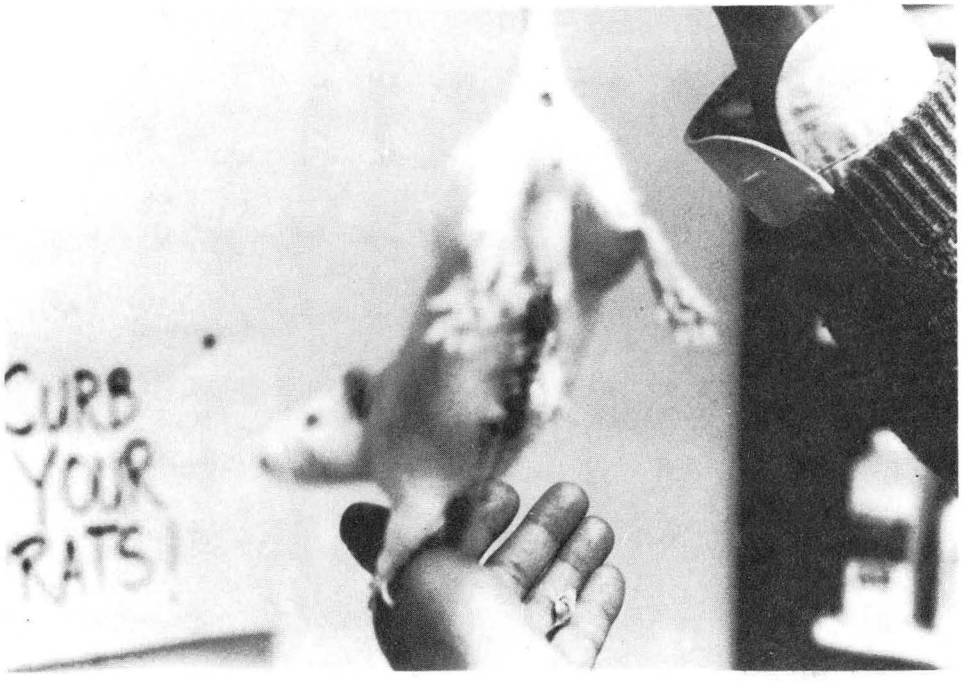

Figure 3-5. X-rays of rats two days following coil implantation showing the orientation of the coils. In experiments performed at 40.5 MHz (a & c) the B_o field runs perpendicular to the plane of the page; at 97.3 MHz (b & d) the B_o field runs parallel to the long axis of the rat. a) Coils implanted around kidney. The two turn coil was used to detect ^{31}P and the single turn coil for ^{1}H to shim and lock the B_o field. b) Kidney coil. c) Heart coil. The coil external to the rat contained a capillary of D_2O for locking the field. d) Heart coil.

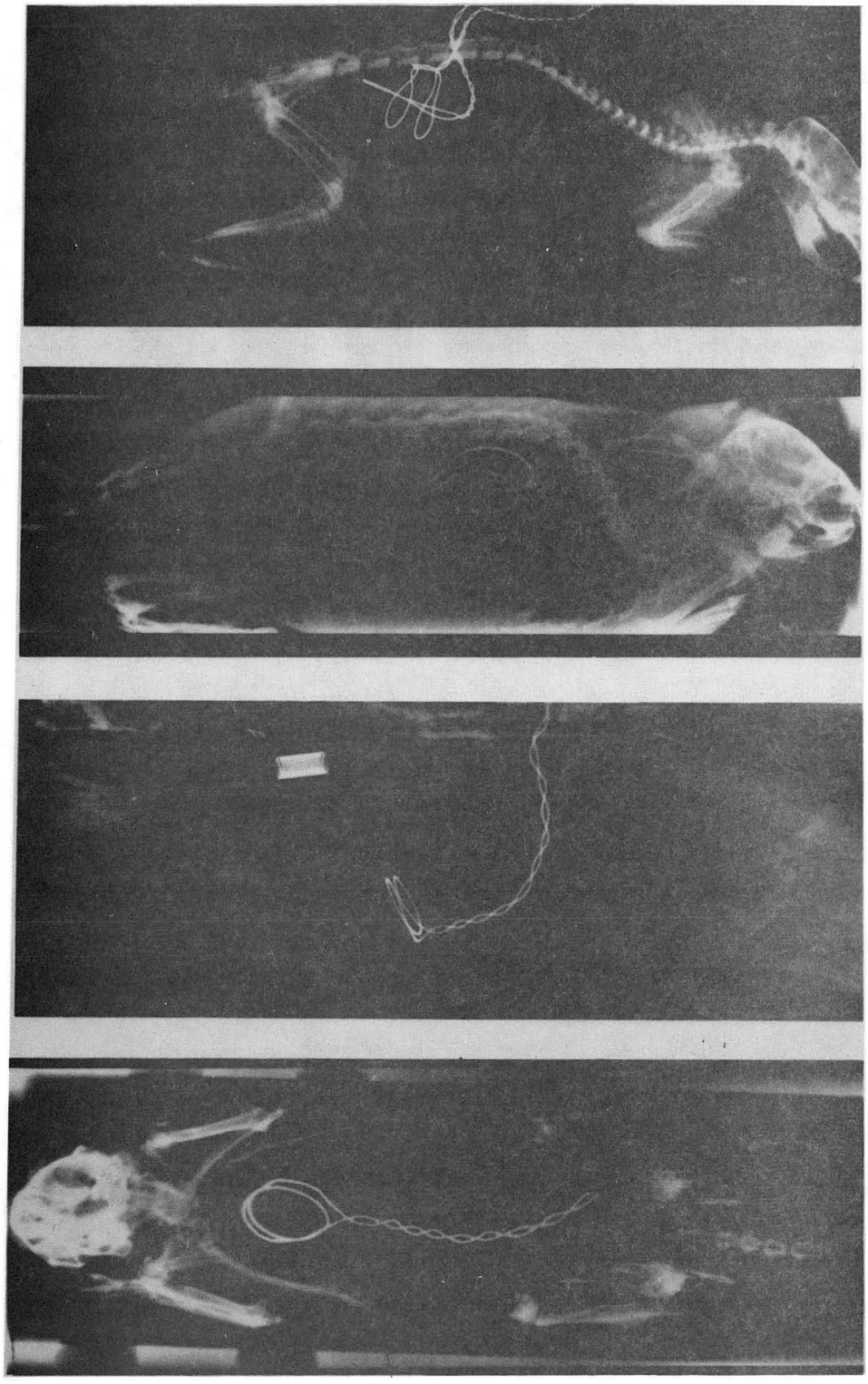

XBB 836-5333

Figure 3-6. Spectra obtained from a) kidney, b) heart, and c) liver using chronically implanted coils. Spectra are the sum of 128 acquisitions using a 30 μsec. pulse (75^{o}) and a 10 sec. recycle time. A 30 Hz exponential filter was applied to the free induction decay prior to Fourier transformation. Chemical shifts were referenced to the αATP peak, which was set equal to 0 PPM. Peaks are: 1) βATP, 2) αATP + NAD(H), 3) γATP, 4) PCr, 5) PDE 6) Ur Pi, 7) Pi, 8) PME, 9) Unknown, and 10) MDPA.

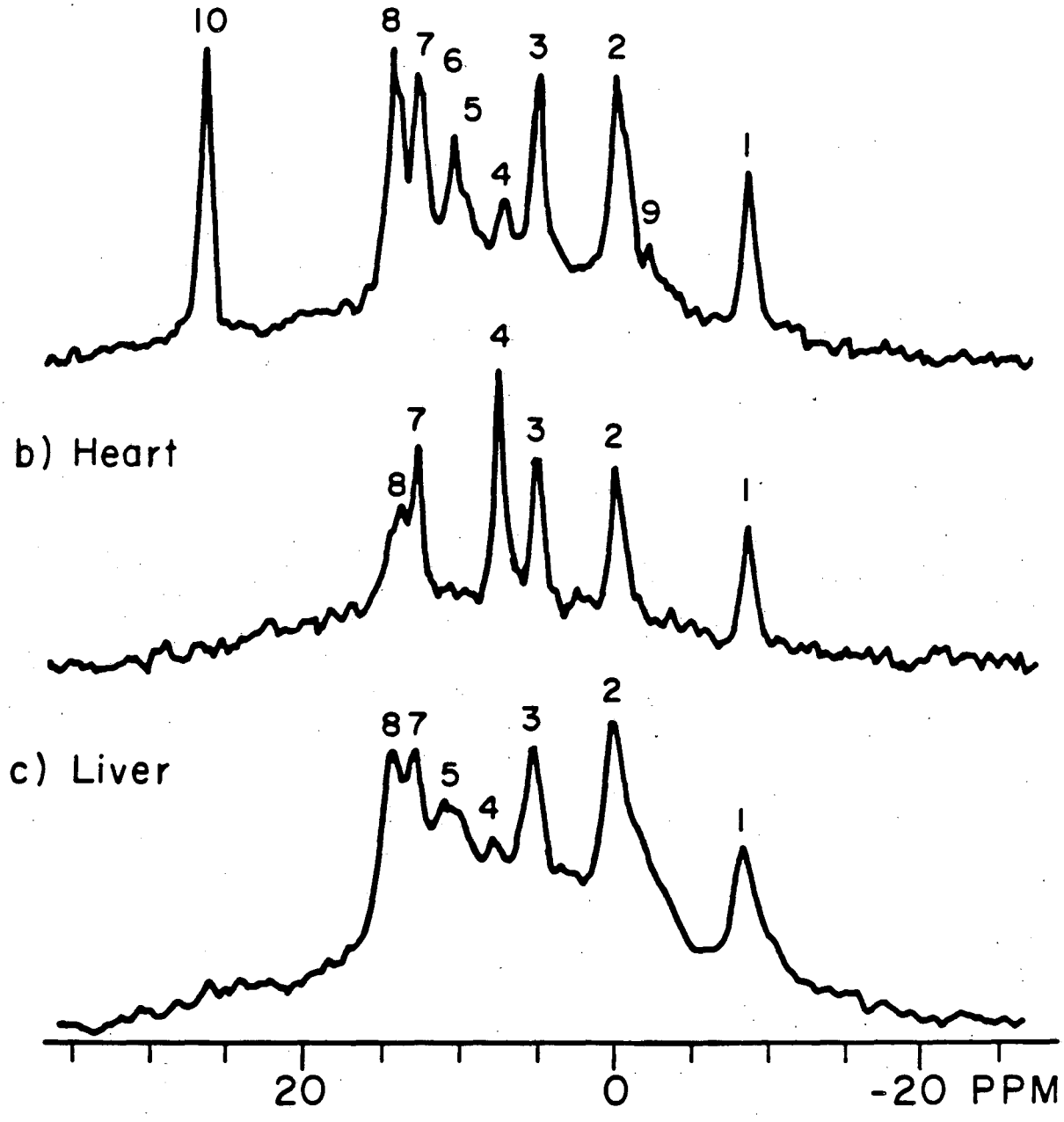
a) Kidney
10
8
7
6
5
4
3
2
9
1
b) Heart
8
7
4
3
2
1
c) Liver
8
7
5
4
3
2
1
20
0
-20 PPM

Table 3-1. Relative Intensities and Chemical Shifts of Metabolites.

	βATP	αATP + NAD(H)	γATP	PCr	PDE	P_i	SP
Shift*	-8.64	0	5.15	7.55	10.55	12.76	14.22
Kidney	100	208±26+	99±2	30±16	31±25	103±26	150±19
Heart	100	182±15	103±3	133±15	3±5	116±8	107±37
Liver	100	191±14	101±1	14± 9	90±84	57±19	106± 9

Intensities are in arbitrary units; βATP set equal to 100.

Errors are ± one standard deviation with n=10 for kidney, n=6 for heart, and n=2 for liver.

*Chemical shift in PPM with αATP set equal to zero.

+Contains intensity of unknown peak at -2.31 PPM.

contributions from a previously reported (7) phosphodiester (PDE) peak (Fig. 3-6a,peak 5). This new peak changed in intensity and chemical shift concomitantly with changes in urine (Ur) pH suggesting that it is due to Ur P_i contained in the kidney pelvis. In the in vivo kidney an unidentified peak is detected, (Fig. 3-6a, peak 9), where nucleotide sugars, such as UDP-glucose, are expected to resonate.

PCr is detected neither in the perfused liver nor kidney (3,14,17,18), so the amounts of PCr seen in vivo allow the contribution of surrounding muscle to be assessed. Rat skeletal muscle contains PCr/ATP ratios of 4:1 and PCr/P_i ratios of 15:1 (5). The PCR/ ATP ratio detected in kidney was approximately 1:3.3 and less in liver (Table 3-1). If all the PCR were coming from muscle then other muscle metabolites, such as P_i and ATP, would make less than a 10% contribution to the spectrum. To verify this assertion, the renal artery was ligated; the level of ATP, monitored by the height of the βATP peak, dropped to zero within 15 min (Fig. 3-7a), with a complementary increase in P_i. Were surrounding tissue contributing to the spectra, one would expect to observe some residual ATP signal. Furthermore, when the kidney was removed and replaced with a phantom containing only MDPA, no narrow metabolite peaks were detected (Fig. 3-7b). A broad feature which persisted, is suggested to arise both from metabolites in surrounding tissue residing in inhomogeneous portions of the B_o field as well as from phosphorus containing molecules in the organ which would be expected to give a broad signal (e.g. phospholipids, RNA, DNA, etc...).

Besides the tissue of interest, blood circulating through the organ can contribute to the spectra. In particular, the

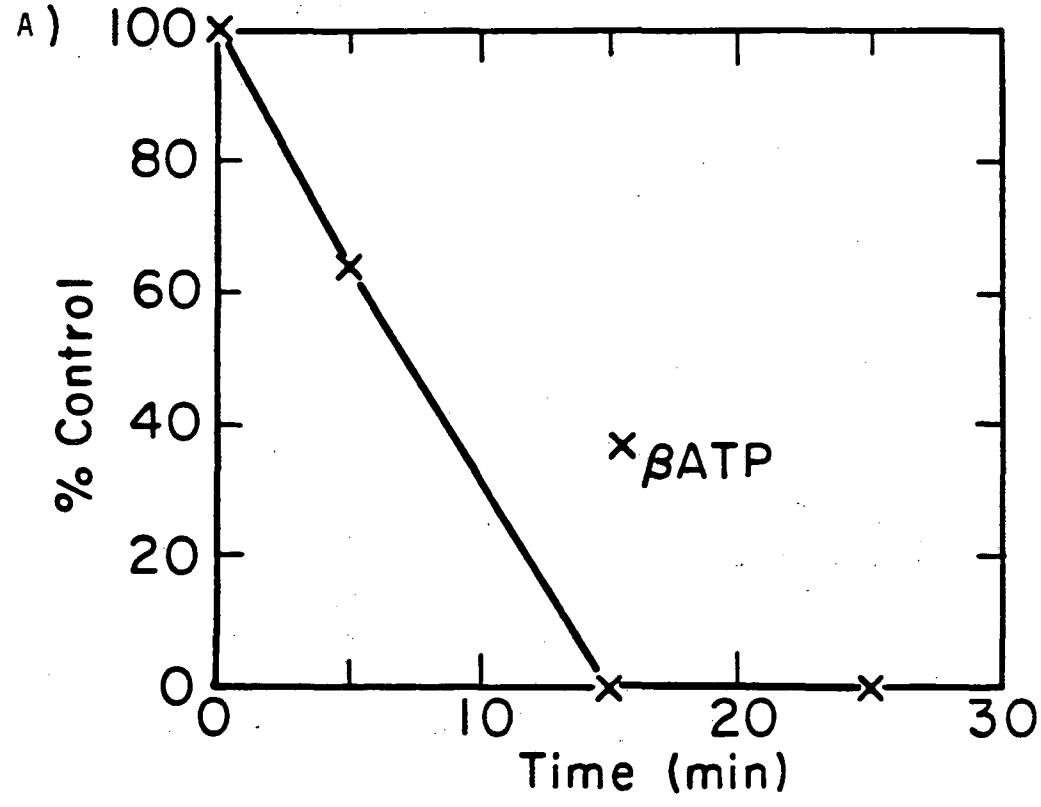

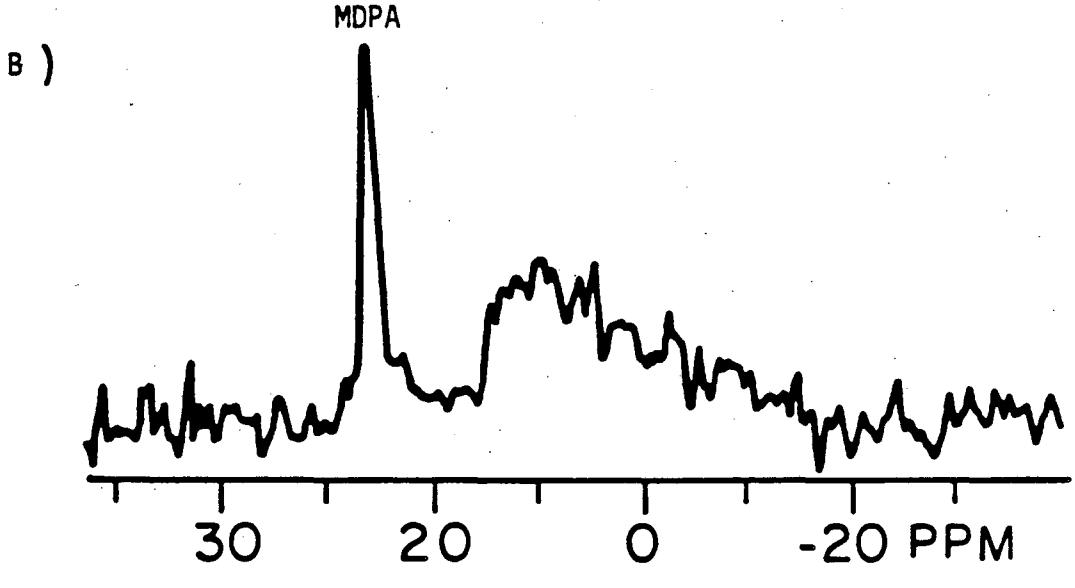

Figure 3-7. A) plot of βATP intensity vs. time after occluding the renal artery. B) ^{31}P NMR spectrum of a kidney phantom containing MDPA. The orginal kidney was removed and replaced with a similar sized phantom just prior to obtaining the spectrum at 40.5 MHz.

phosphomonoester (PME)-P_i region of the in vivo heart spectra has more intensity than observed in the working heart perfused with phosphate-free medium (15). This suggests either that there is a significant contribution to the spectra from 2,3 diphosphoglycerate (2,3-DPG) and P_i in blood within the heart chamber or that changes in cardiac metabolism account for the differences. However, even if all the PME-P_i intensity in the heart spectra were due to blood, the concentration of ATP occurring in rat blood is too small to make a significant contribution to the spectrum. The effect of blood on the liver and kidney spectra is harder to estimate since the in vivo spectra closely resemble those obtained from the perfused organs. It is estimated that blood and extracellular fluid comprise approximately 15% of the wet weight of liver and kidney (19). From the concentration of 2,3-DPG of rat blood (20) and the 2,3-DPG/P_i ratio, determined from NMR of whole rat blood, it can be estimated that blood contributes approximately 25% of the PME-P_i intensity in both kidney and liver. This implies that other metabolites in blood make negligible contributions to the organ spectra. Recently there has been a fluorocarbon blood substitute developed which can essentially replace the whole blood volume of a rat with no adverse effects (20a). This has been used to demonstrate that blood makes a negligible contribution to the ^{31}P NMR spectrum of rat brain (20b). A similar approach to quantitating the contribution of blood to kidney, heart, and liver spectra would be useful.

MAGNETIC FIELD EFFECTS. To determine the effects of field strength on resonance linewidths from organs in vivo, spectra were obtained at 40.5 and 97.3 MHz (Fig.3-8). Linewidths increased roughly in proportion to the field strength, explaining why no improvement in

Figure 3-8. Comparison of kidney (a & b) and heart (c & d) ^{31}P NMR spectra at 40.5 MHz (a & c) and 97.3 MHz (b & d). Acquisition parameters were: a) 45° pulse, 130 msec recycle time, 30 min total acquisition time, with a 15 Hz filter, b) 45° pulse, 130 msec recycle time, 8 min total acquisition time, and a 30 Hz filter, c) 60° pulse, 3 sec recycle time, 30 min total acquisition time, and a 15 Hz filter. d) 90° pulse, 10 sec recycle time, 20 min total acquisition time, and a 30 Hz filter. Peaks are: 1) βATP, 2) αATP + NAD(H), 3) γ ATP, 4) PCr, 5) Ur Pi + PDE 6) Pi, 7) PME, and 8) MDPA.

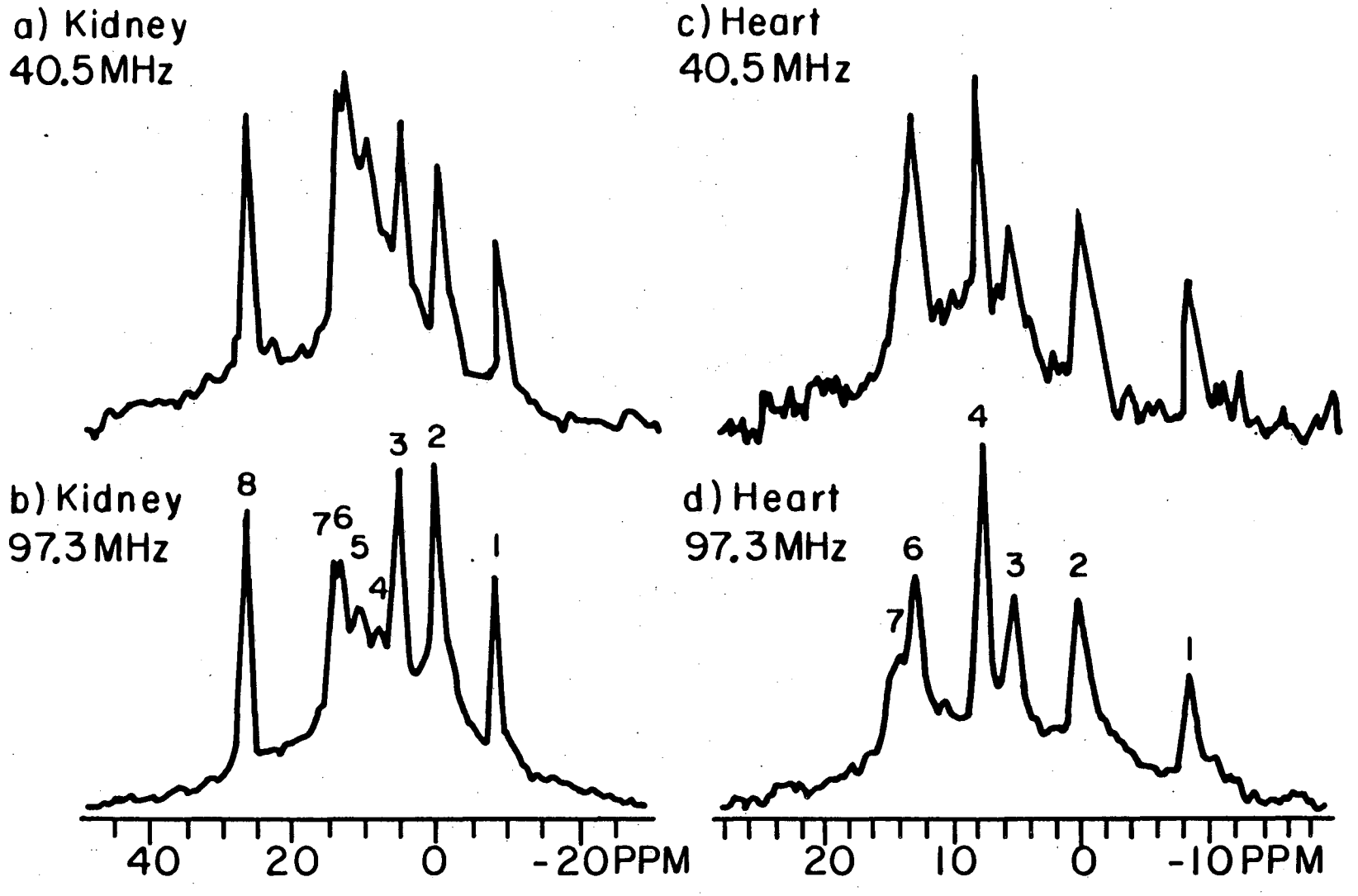
a) Kidney
40.5 MHz
c) Heart
40.5 MHz
b) Kidney
97.3 MHz
8
7
6
5
4
3
2
1
40
20
0
-20 PPM
d) Heart
97.3 MHz
6
7
4
3
2
1
20
10
0
-10 PPM

resolution was obtained at the higher field. This result is consistent with results obtained on cell suspensions (21). A quantitative description of linewidth dependence on field is difficult with such complicated systems because there are many mechanisms which may contribute to the linebroadening, eg. chemical shift dispersion arising from pH heterogeneity, paramagnetic ions, and residual chemical shift anisotropy. In addition micro- and macrostructural heterogeneity in an organ can lead to linebroadening induced by geometrical effects or differences in susceptibilities or both.

STABILITY OF SPECTRA. An advantage of in vivo experiments over studies of perfused organs, is metabolic stability and integrity. With implanted coils, NMR spectra can be obtained continuously for 18-24 hours, with only a 10±3% variation in the βATP intensity in kidney or the PCr/ATP ratio in heart. This permits a wide variety of manuevers and observations to be performed on a single animal. The lengths of experiments were limited by variability of animal response during anesthesia. Unanesthetized animals could be used to obtain excellent spectra but small movements were frequent and required continual reshimming or repositioning. It is anticipated that the use of tranquilizers would minimize movements and eliminate the adverse effects of prolonged anesthesia.

EFFECTS OF FRUCTOSE. In order to check that the spectra would indicate the metabolic response of an organ to a biochemical perturbation, fructose was administered and ^{31}P NMR spectra were obtained from kidney, liver, and heart. Previous work, employing both freeze clamp techniques (22-25) and NMR (4,11,26), has shown that fructose administration depletes ATP and P_i levels, while increasing

sugar phosphate levels in kidney and liver. A comparison of the time course of metabolite levels in both kidney and liver after an intraperitoneal injection of fructose is shown in Fig. 3-9. In both organs levels of P_i drop rapidly as sugar phosphate levels increase. The effect was much more pronounced in liver than in kidney, which is in agreement with freeze clamp data (23,25) and is presumably due to the larger fructokinase activity in liver. The parallel changes in the β and γATP resonances indicate that ADP levels never become detectable, probably because oxidative phosphorylation regenerates ATP from ADP formed from fructose phosphorylation. However, levels of ATP did fall indicating that the net pool of adenylates decreases. The fact that ATP levels recovered slowly, relative to P_i and sugar phosphates, is consistent with the idea that adenine nucleotides must be resynthesized to replace the depleted pool (22,25). Fructose loading did not alter the heart spectrum indicating that the heart was unable to metabolize fructose, consistent with the fact that heart has no fructokinase activity. That the heart spectrum did not change with fructose administration was evidence that liver did not contribute appreciable signal to the heart spectrum.

A hope for the future is that <u>in vivo</u> NMR will aid in the diagnosis and treatment of disease. Initial work on human muscle (26a) has indicated that NMR spectroscopy will, at least in certain instances, be helpful. However, these findings indicate that a resting spectrum is not very sensitive to the biochemical differences of normal and diseased states. Biochemical abnormalities were detected only when patients were put through an exercise routine. This was quite easy for the case of muscle metabolism. As the technical expertise develops

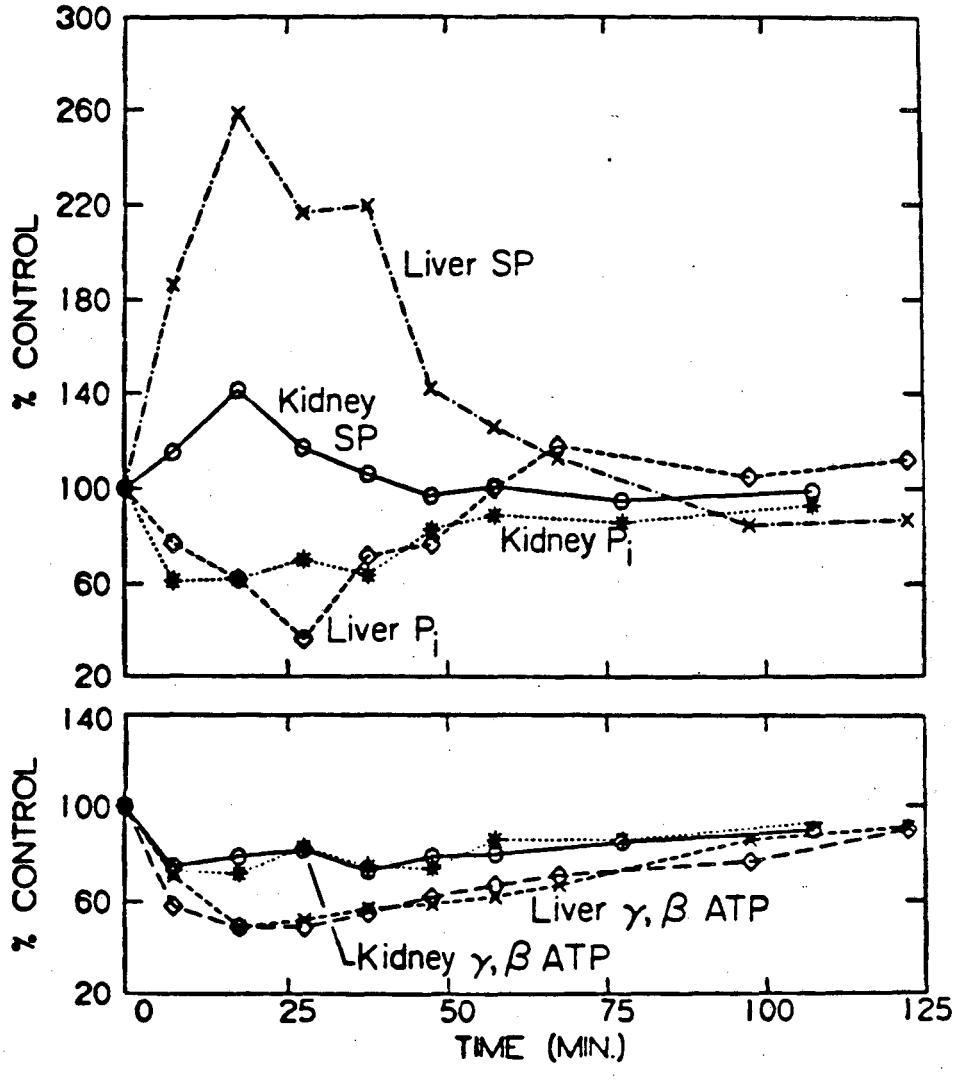

Figure 3-9. An intraperitoneal injection of 10 umol/gm body weight of fructose was administered and the metabolite levels monitored in kidney and liver. After obtaining three control spectra, acquisitions were averaged for five minutes every ten minutes beginning five minutes after the fructose injection. Spectra were acquired at 97.3 MHz using 286 90° pulses, a 1 sec recycle time, and a 30 Hz filter. Metabolites shown are; in a) o= kidney sugar phosphate, *= kidney Pi, x= liver sugar phosphate, and ◇ = liver Pi and in b) o=kidney γATP, *= kidney βATP, x= liver γATP, ◇ = liver βATP

which will allow kidney and liver spectra to be obtained from humans, it will be important to develop metabolic stress tests for these organs as well. Fructose administration seems like an excellent candidate to provide an exercise test for liver and kidney.

NMR GATED TO THE CARDIAC CYCLE. Using gated NMR, Fossel et al. (27) have reported cyclical concentration changes of phosphate metabolites in the glucose-perfused, working heart. To determine if these cyclical changes occur in vivo, gated heart spectra were obtained. Fig. 3-10a shows the aortic pressure wave from the rat heart while Fig. 3-10b shows the acquisition interval of the spectrometer. Two time intervals were monitored: peak systole and a point 200 msec later, during diastole. The relative position of the diastolic point varied 10% with respect to peak systole due to variations in heart rate. There was no difference (Fig. 3-10e) between the spectra obtained at diastole (Fig. 3-10c) and systole (Fig. 3-10d). The inconsistencies between the results obtained on the perfused heart (27) and the in situ heart are possibly due to the better nutrient supply available in vivo. That this is the most likely explanation for the difference between the in situ and the perfused heart is supported by the recent freeze-clamp work of Wikman-Coffelt et al. (28). Using a fast freeze-clamp technique they found cyclical variations in phosphate metabolites with glucose perfused hearts but none when pyruvate was used in the perfusate. Studying the onset of fluctuations in a stressed or a diseased heart by NMR offers the potential for understanding the biochemical limits of cardiac performance.

EXTENSION TO OTHER NUCLEI. Besides the phosphorus nucleus there are many other nuclei which can be detected by NMR and which play an

FIGURE 3-10. Gated ^{31}P NMR spectra obtained from the rat heart, in vivo. a) Aortic pressure wave obtained with a polyethylene line in the carotid artery and a Stentor pressure transducer. To insure that the line introduced no significant time delay, the pressure wave was compared to the EKG in a parallel experiment outside the magnet. b) Nmr acquisition interval displayed on the same scale as the pressure wave, demonstrating the ability of the gating device to properly couple the pressure wave to the 293B pulse programmer. Spectra obtained at peak systole (d) and 200 msec later, diastole (c), were acquired at 97.3 MHz by alternating four acquisitions (45° pulse, 2 sec delay, 30 Hz filter) at each interval until 480 scans at each point were obtained. e) Diastole minus systole. Peaks are: 1) βATP, 2) αATP + NAD(H), 3) γATP, 4) PCr, 5) Pi, and 6) PME.

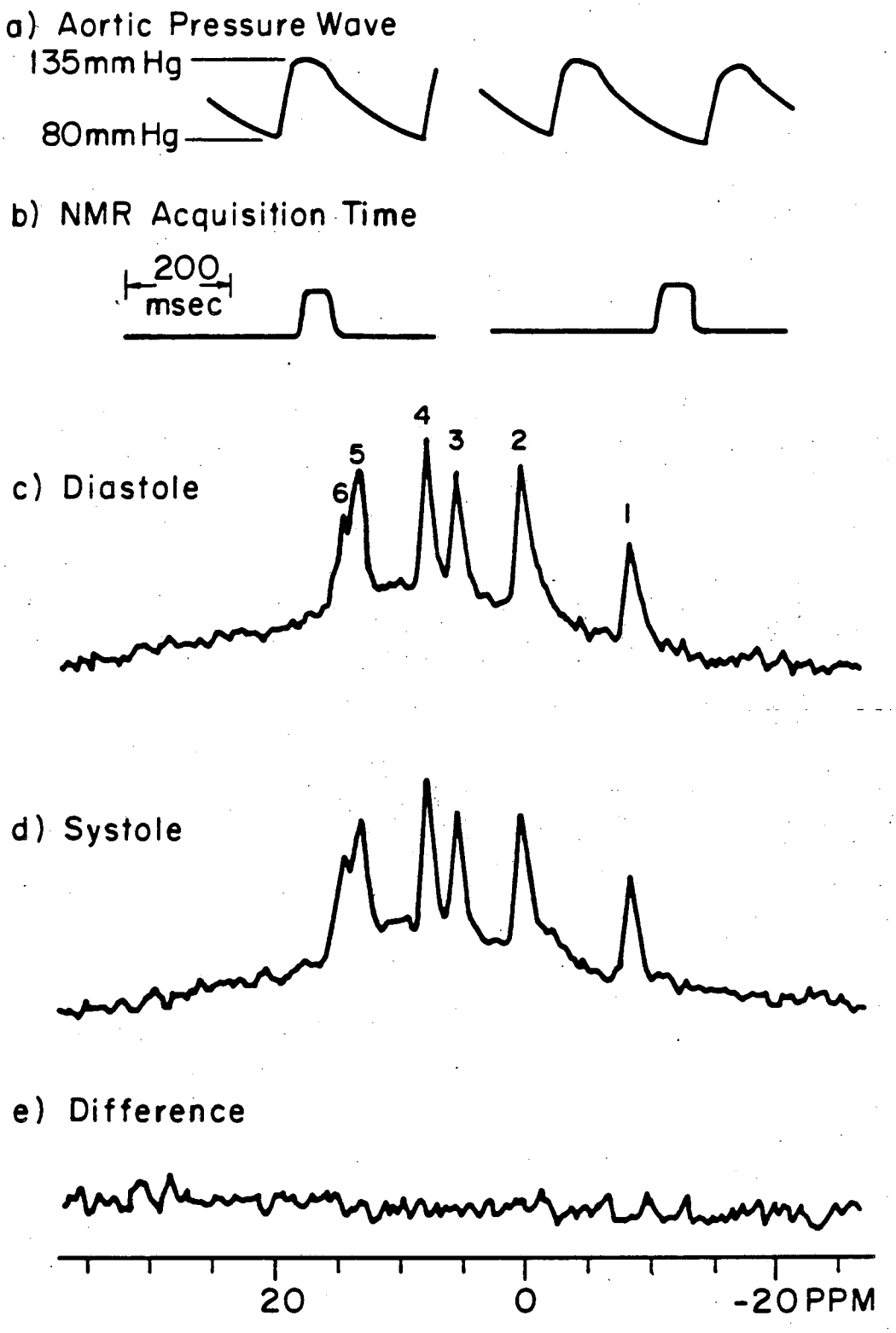
a) Aortic Pressure Wave
135mm Hg
80mm Hg
b) NMR Acquisition Time
200 msec
c) Diastole
6
5
4
3
2
1
d) Systole
e) Difference
20
0
-20 PPM

important role in biological processes (Table 1-1). Both ^{1}H and ^{13}C NMR studies have found widespread applications (29,30). The implanted coil approach should work for any nucleus desired as long as the coil can be tuned to the appropriate frequency. An example of a nucleus from which, owing to its low gyromagnetic ratio, it is more difficult to obtain spectra, but is important to biological processes, is ^{39}K. Fig. 3-11 shows the first ^{39}K spectra obtained from rat kidney and skeletal muscle in situ using implanted coils. These spectra demonstrate that implanted coils can be used to obtain information from nuclei other than phosphorus.

3.4 Conclusions

Stable ^{31}P NMR spectra from the heart, kidney, and liver of laboratory rats can be obtained using chronically implanted coils. Rats have been observed to tolerate the coils for up to six months, the longest time monitored, allowing the possibility of repeated study of a single animal. Signal-to-noise ratios obtained were comparable to those achieved with perfused organs (3, 14-18) making possible a wide variety of experiments. The extension of this technique to larger animals, other organs and other nuclei, such as ^{13}C or ^{23}Na, should be easily accomplished. The use of these coils to perform saturation transfer studies in rat heart and kidney is the subject of the next chapter.

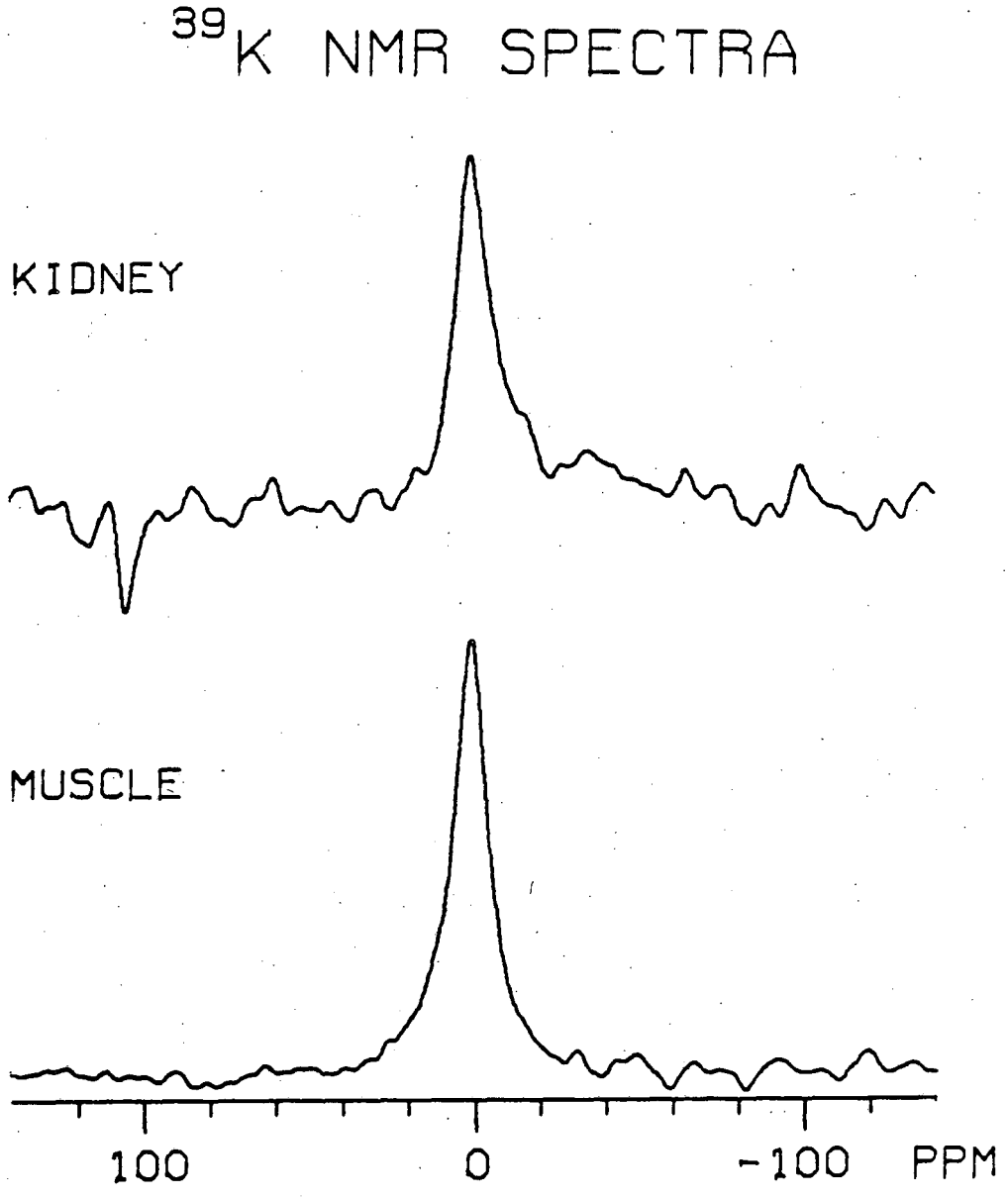

Figure 3-11. ^{39}K spectrum from a) rat kidney and b) skeletal muscle obtained with a six turn coil tuned to the observation frequency of 11.05 MHz. Both spectra represent the sum of 1000 acquisitions using a 60 μsec pulse and a 558 msec recycle time. 50 Hz exponential linebroadening was applied to the FID prior to Fourier transformation. The linewidth at half-height is approximately 120 Hz.

3.5 References

1) Chance, B., Nakasa, Y., Bond, M., Leigh, J.S. Jr. and McDonald,G. (1978) Proc. Natl. Acad. Sci. USA 75, 4925-4929.

2) Grove, T.H., Ackerman, J.J.H., Radda, G.K. and Bore, P.J. (1980) Proc. Natl. Acad. Sci. USA 77, 299-302.

3) Radda, G.K., Ackerman, J.J.H., Bore, P.J., Sehr, P., Wong, G.G., Ross,B.D., Green, Y., Bartlett, S. and Lowry, M. (1980) Int. J. Biochem. 12, 277-281.

4) Chan, L., Ledingham, J.G.G., Dixon,J.A., Thulburn, K.R., Waterton, J.L., Radda, G.K. and Ross, B.D. (1982) in Acute Renal Failure, ed. H.E. Eliahu (John Libbey, London) pp. 35-41.

5) Ackerman, J.J.H., Grove, T.H., Wong, G.C., Gadian, D.G. and Radda, G.K. (1980) Nature (London) 283, 167-170.

6) Gorden, R.E., Hanley, P.E., Shaw, D., Gadian, D.G., Radda, G.K., Styles, P., Bore, P.J. and Chen, L. (1980) Nature (London) 287, 736-738.

7) Balaban, R.S., Gadian, D.G. and Radda, G.K. (1981) Kidney Int. 20, 575-579.

8) Ross, B.D., Radda, G.K., Gadian, D.G., Rocker, G., Esin, M. and Falconer-Smith, J. (1981) N. Eng. J. Med. 304, 1338-1342.

9) Neurohr, K.J., Barrett, E.J. and Shulman, R.G. (1983) Proc. Natl. Acad. Sci. USA 80, 1603-1607.

10) Weiner, M.W., Greene, K., Vreman, H., Wemmer, D., Wade-Jardetzky, N., and Jardetzky, O. (1980) IRCS Med. Sci. 8, 671.

11) Koretsky, A.P., Strauss, W., Basus, V., Murphy, J., Bendel, P., James,T.L. and Weiner, M.W. (1982) in Acute Renal Failure, ed. H.E.

Eliahu (John Libbey, London) pp 42-46.

12) Koretsky, A.P., James, T.L., & Weiner, M.W. (1982) Clin. Res. 30, 397A.

12a) Koretsky, A.P., Wang, S., Murphy-Boesch, J., Klein, M.P., James, T.L., and Weiner, M.W. (1983) Proc. Natl. Acad. Sci. USA 80, 7491-7495.

13) Murphy-Boesch, J., and Koretsky, A.P. (1983) J. Magn. Reson. 54, 526-532.

14) Ackerman, J.J.H., Lowry, M., Radda, G.K., Ross, B,D. and Wong, G.C. (1981) J. Physiol. 319, 65-79.

15) Jacobus, W.E., Taylor, G.J., Hollis, D.P. and Nunnally, R.L. (1977) Nature (London) 265, 756-758.

16) Garlick, P.B., Radda, G.K., Seeley, P.J. and Chance, B. (1977) Biochem. Biophys. Res. Commun. 74, 1256-1262.

17) Salhany, J.M., Stohs, S.J., Reinke, L.A., Pieper, G.M. and Hassing, J.M. (1979) Biochem. Biophys. Res. Commun. 86, 1077-1083.

18) McLaughlin, A.C., Takeda, H. and Chance, B. (1979) Proc. Natl. Acad. Sci. USA 76, 5445-5449.

19) Blouin, A., Bolender, R.P., and Weibel, E.R. (1977) J. Cell Biol. 72, 441-455.

20) Sasaki, R., Ikura, K., Sugimoto, E., and Chiba, H. (1974) Analyt. Biochem. 61, 43-47.

20a) Goodin, T.H., Clarke, W.P., Taylor, K., Eccles, R., Geyer, R.P., and McCoy, L.E. (1983) Am. J. Physiol. 245, H519-H523.

20b) Ackerman, J.J.H., Berkowitz, B.A., and Deuel, K. (1984) Biochem. Biophys. Res. Comm. 119, 913-919.

21) Evans, F.E. (1979) Arch. Biochem. Biophys. 193, 63-75.

22) Maenpaa, P.H., Raivio, K.O., and Kekomaki, M.P. (1968) Science 161,

1253-1254.

23) Burch, H.B., Lowry, O.H., Meinhardt, L., Max Jr.,P., and Chyu, K-J., (1970) J. Biol. Chem. 245, 2092-2102.

24) Woods, H.F., Eggleston, L.V., and Krebs, H.A. (1970) Biochem. J. 119, 501-510.

25) Morris Jr., R.C., Nigon, K., and Reed, E.B. (1978) J. Clin. Invest. 61, 209-220.

26) Iles, R.H., Griffiths, J.R., Stevens, A.N., Gadian, D.G. and Porteous, R. (1980) Biochem. J. 192, 191-202.

26a) Taylor, D.J., Bore, P.J., Styles, P., Gadian, D.G., and Radda, G.K. (1983) Mol. Biol. Med. 1, 77-94.

27) Fossel, E.T., Morgan, H.E. and Ingwall, J.S. (1980) Proc. Natl. Acad. Sci. USA 77, 5445-5449.

28) Wikman-Coffelt, J., Sievers, R., Coffelt, R.J., and Parmley, W.W. (1983) Am. J. Physiol. 245, H354-H362.

29) Brown, F.F., Campbell, I.D., Kuchel, P.W., and Rabenstein, D.L. (1977) FEBS Letts. 82, 12-16.

30) Shulman, R.G., Brown, T.R., Ugurbil, K., Ogawa, S., Cohen, S.M., and den Hollander, J.A. (1979) Science 205, 160-166.

CHAPTER 4: SATURATION TRANSFER STUDIES OF RAT HEART AND KIDNEY *IN SITU*

4.1 Introduction

A detailed understanding of the regulation and control of metabolic pathways requires an estimate of the rates of each individual reaction. For the case of the generation of ATP by oxidative phosphorylation and utilization for various work functions (eg. Na^+ transport and muscle contraction) most kinetic information comes from *in vitro* studies of isolated subcellular systems (1). However, functioning of *in vivo* regulatory mechanisms may be altered *in vitro*. Physiologic experiments performed on intact tissue have produced information concerning the coupling of oxidative metabolism to work demands (2). These studies have had to rely on assumptions concerning detailed reaction mechanisms, such as the stoichiometry of ATP formation from oxidative phosphorylation. To bridge the gap between *in vitro* studies of isolated mitochondria and physiologic studies it is important to know the rate of metabolic reactions, such as ATP formation and utilization, *in vivo*. NMR techniques can be used to measure the rates of enzyme reactions *in vivo* (3,4). In particular, using ^{31}P NMR magnetization transfer techniques, the rate of the creatine kinase reaction has been measured in perfused heart (5-7), isolated muscle (5,8) and in rat and turtle brain *in situ* (9,10,11). Additionally, the rate of ATP synthesis has been measured in the perfused heart and kidney (12,13,13a) as well as the rat brain (10).

Techniques have been developed which allow ^{31}P NMR spectra to be

obtained from rat kidney, heart, and liver, in situ (14-16, Chapter 3). The stability of the animals and the high metabolic rates which occur in these organs in situ offer advantages over perfused organs for magnetization transfer studies. The results of the experiments reported here represent the first in situ measurements of the rates of exchange between the phosphorus moiety of PCr and ATP in heart and between Pi and ATP in kidney.

4.2 Materials and Methods

SURGICAL PROCEDURE. Details of animal methods for NMR experiments have been described previously (Chapter 3, 16). Female Sprague-Dawley rats (180-220 gm) were used throughout. Two-turn radiofrequency coils were made from 22 gauge copper wire and insulated with polyethylene tubing (Clay-Adams, PE-100). Small ceramic chip capacitors (American Technical Ceramics) were placed close to the coil to partially tune and match the circuit, as well as minimize losses associated with implantation (Appendix 2, 18). These coils were surgically implanted around the heart or kidney, 3-5 days prior to NMR experiments. Two days prior to implantation of the kidney coil, the kidney which was not used for NMR experiments was removed.

On the day of NMR experiments, animals were kept anesthetized with a continuous dose of a Ketamine/Rompun mixture, administered through an intraperitoneal line. A venous line for administering saline and an arterial line to monitor blood pressure were also used. Just prior to kidney experiments, the rats were volume expanded (4% of body weight) over the course of 30 minutes with freshly prepared plasma.

NMR MEASUREMENTS. All measurements were performed at a phosphorus

frequency of 97.2 MHz in a 3" diameter vertical bore superconducting magnet (Cryomagnets Corp.), equipped with a homebuilt spectrometer and a Nicolet 1180/293B data system.

Rats were placed in a specially designed holder, and the coil leads were soldered to the remainder of the tuning and matching circuit. The coil was tuned to the appropriate frequency and the holder placed in the magnet so that the organ was centered in the magnetic field. For the kidney experiments, this meant securing the rat in an upside-down position, because the spinner assembly prevented placing the rat head up. The ^{1}H signal from water in the organ was used to shim the magnetic field before phosphorus spectra were obtained. No field frequency lock was employed.

Saturation transfer experiments were performed following Forsén and Hoffman (19). The unidirectional exchange of phosphate from ATP to PCr is used to briefly describe the technique. The PCr resonance was selectively saturated long enough so that the intensity of the γATP peak reached a steady-state ($M^{SS}_{\gamma ATP}$). This steady-state level was compared to the equilibrium magnetization of γATP ($M^{O}_{\gamma ATP}$) by obtaining a spectrum with the selective rf irradiation at a control frequency, displaced an equal distance as the PCr resonance is from the γATP signal but on the upfield side. To minimize the effects of any biological variations, control and saturated spectra were obtained concurrently by alternating eight pulses with the rf power in each position.

The apparent T_1 (T_{1APP}) of the γATP resonance was then measured using saturation recovery techniques (20) with the PCr peak saturated throughout the measurement. Saturation of the whole spectrum was

accomplished by a burst of 90° pulses of alternating phase (21) separated by 10 msec homospoil pulses. A sequence of time intervals between spectral saturation and observation of the γATP resonance, while maintaining the PCr peak saturated, were used to construct a T_1 plot. A best three parameter, single exponential fit, performed on the spectrometer's Nicolet computer, was used to extract T_{1APP} from the data. That this method gave accurate T_1s was demonstrated by comparing the T_1 of methylene diphosphonic acid (MDPA) obtained from a capillary attached to a kidney coil in a rat to the T_1 of MDPA obtained from a conventional probe using standard inversion recovery techniques. The two values agreed within experimental error.

The unidirectional rate constant for the reaction ATP⟶PCr was derived from the above measurements using the expression:

$$k_{ATP\longrightarrow PCr} = \frac{M^{o}_{\gamma ATP} - M^{SS}_{\gamma ATP}}{M^{o}_{\gamma ATP} T_{1APP}} \qquad [4\text{-}1]$$

The rate of the reaction, ATP ⟶ PCr was obtained by multiplying $k_{ATP\rightarrow PCR}$ by a suitable quantity of ATP expressed in arbitrary intensity units, obtained from the NMR spectra.

Specific spectral acquisition parameters are given in the figure legends. The pulse used to saturate specific peaks in the spectrum was generated using the decoupler channel of the spectrometer. Typically, peak-to-peak voltages of from 0.1-0.3 volts representing from 4-18 mgauss were employed.

Apart from an exponential filter of 30 Hz, applied to the free induction decay prior to Fourier transformation, no other data massage techniques, eg. convolution difference or left shifting, were used. To

quantitate peak areas, two procedures were used. For heart spectra, where the peaks were resolved and there was not much contribution from an underlying broad component, the Nicolet integration routine was employed. For kidney spectra, not all the peaks were well resolved, and there was a larger broad component that made use of the integration routine difficult; therefore, the Nicolet simulation routine NTCCAP was used. All the peaks, including the broad component, were fit by varying position, intensity, and linewidth until a minimum root mean square residual was obtained. Comparison of the two procedures for heart spectra yielded the same results within experimental error. All errors are reported as ± one standard deviation.

4.3 Results

Fig. 4-1 shows typical spectra obtained from kidney (a) and heart (b) using chronically implanted coils. The peaks seen, their relative magnitude, and the signal-to-noise ratios obtained are similar to spectra obtained from perfused organs.

KIDNEY. Fig. 4-2 shows the saturation transfer experiment performed on the rat kidney, in situ. In this case, spectra with the YATP peak saturated (Fig. 4-2b) and with the selective rf irradiation in the control position (Fig. 4-2a) were alternated every eight pulses until a total of 128 acquisitions were obtained. The arrows indicate the position of the selective rf field. Comparison between spectra with no selective irradiation and spectra in which irradiation was applied in the control position, indicated that the Pi peak was not significantly affected by stray irradiation from the saturation pulse. The saturation pulse did reduce the intensity of the broad component.

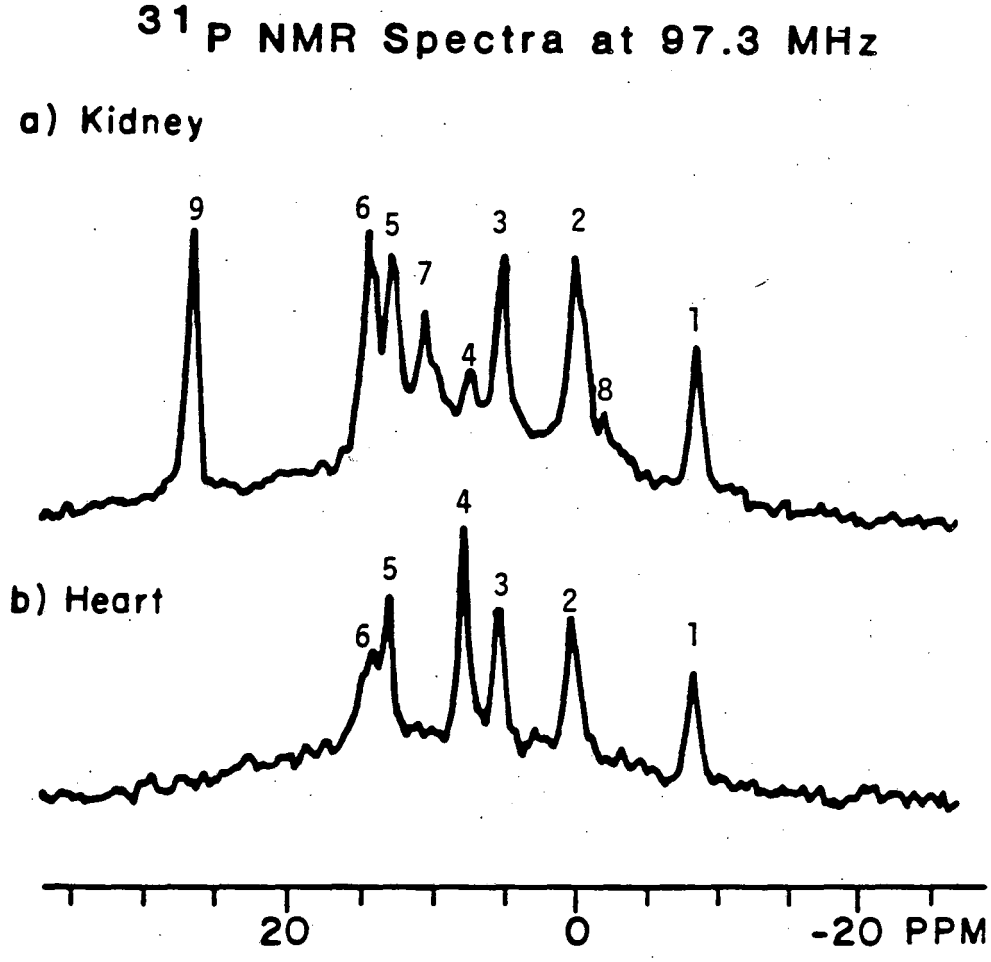

Figure 4-1. ^{31}P NMR spctra of a) kidney and b) heart in situ. Spectra are the sum of 128 acquisitions, using a 90^{o} pulse and a 10 sec recycle time. Numbers on peaks refer to: 1) βATP, 2) αATP and NAD(H), 3) γATP, 4) PCr, 5) Pi, 6) phosphomonoesters, 7) phosphodiesters and urine Pi in kidney, 8) Unidentified, 9) internal standard, MDPA.

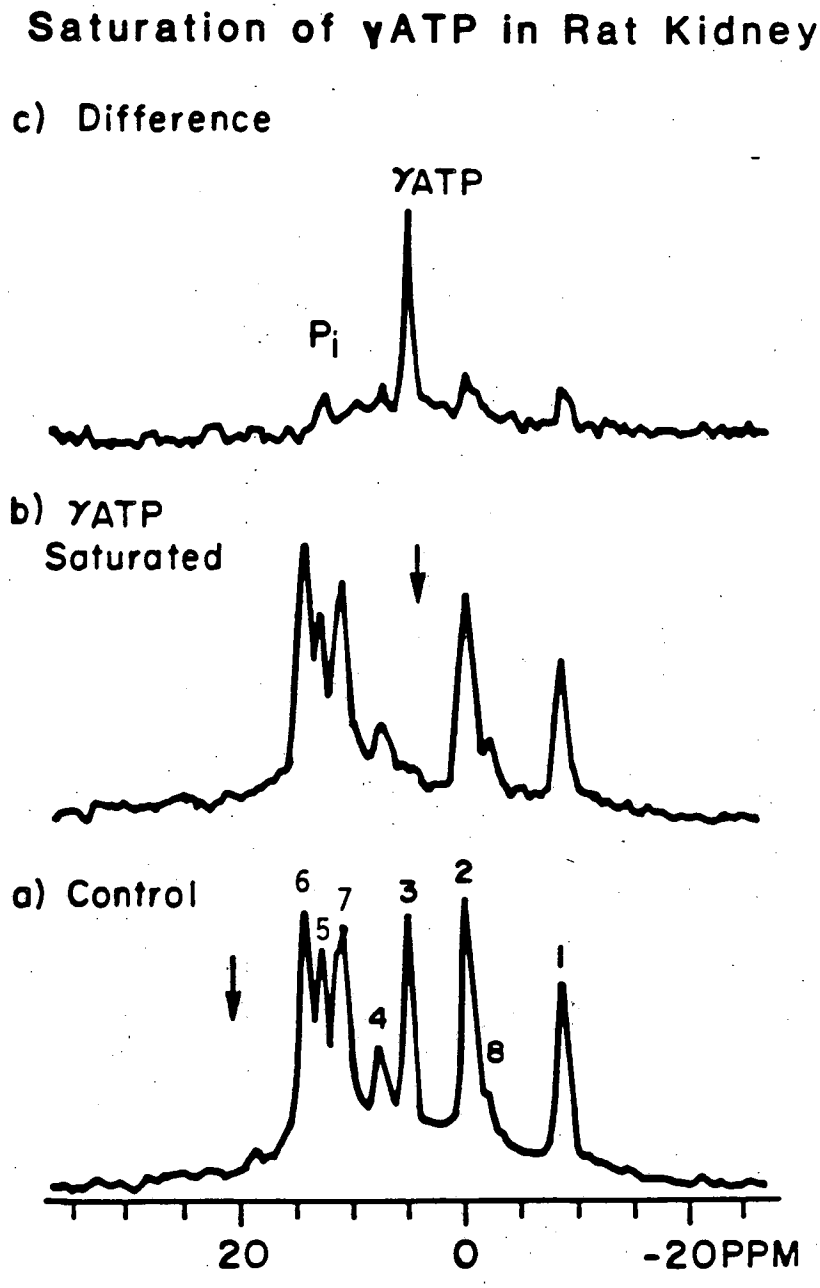

Figure 4-2. Saturation transfer measurement of the Pi→ ATP reaction in rat kidney. Spectra (a) and (b) are sums of 128 acquisitions using a 90° pulse and 10 sec recycle time during which the saturation pulse was left on. Eight spectra were alternated with the rf irradiation on a) the control frequency and b) the γATP peak (arrows) until 128 acquisitions for each spectrum had been obtained. C) is a difference spectrum obtained by subtracting b) from a). Peaks are numbered as in Fig. 4-1.

To determine whether non-selective effects of saturating the broad component could produce artifacts resembling the effects of exchange, the broad component was saturated at various positions where there were no visible NMR peaks. Difference spectra using controls with no selective irradiation (Fig. 4-1a) showed no changes in the magnetization of narrow resonances, although the broad component was reduced to approximately 52% of its control value. This observation suggests a potential method for reducing the broad component associated with heart, kidney, and liver spectra. Recently, this approach has been used to reduce the broad component associated with bone when performing NMR of the brain (22,23).

The difference spectrum (Fig. 4-2c) shows a reduction of the Pi magnetization when the γATP peak is saturated. Saturation of the Pi resonance had no effect on the γATP signal, possibly due to the short T_1 of the γATP resonance. Besides Pi, saturation of the γATP peak caused a reduction in both the α and βATP resonances. This was confirmed by the appropriate control experiments for these peaks. Saturation of the γATP peak can lead to a decrease in the βATP intensity via; a) dipolar interactions between the γ and β phosphorus nuclei, b) chemical exchange between the γ and βATP catalyzed by two cycles of the adenylate kinase reaction (4), or c) simultaneous saturation of the nearby βADP resonance when the γATP peak is irradiated, which exchanges with βATP during reactions catalyzed by creatine kinase, ATPases, or adenylate kinase. The reduction in the αATP magnetization upon saturation of the γATP peak has no obvious explanation, although it has been observed in experiments performed on rat brain (10). Table 4-1 presents the experimental results which lead

Table 4-1. Results of saturation transfer experiments performed on the rat kidney in situ.

Reaction	$\frac{M^o - M^{ss}}{M^o}$	T_{1APP}* (sec)	k (sec^{-1})	T_1** (sec)
Pi⟶γATP	0.15±0.04	1.24±0.16	0.12±0.03	1.46±0.12
βATP→γATP	0.20±0.08 (n=8)	0.55±0.07 (n=3)	0.36±0.14	0.69±0.11

* T_{1APP} and T_1 values are for reactants on the left side of the equations.

** T_1 is the intrinsic T_1, or the T_1 calculated to account for the effects of exchange.

to a calculated rate constant, $k_{Pi \rightarrow ATP}$, of 0.12±0.03 sec^{-1}.

HEART. Fig. 4-3 illustrates the results of an experiment performed to measure the rate constant for the reaction PCr $\longrightarrow$ ATP ($k_{PCr \longrightarrow ATP}$). Two spectra were obtained by alternating the selective rf power in the control position (Fig. 4-3a) with the saturation pulse on the γATP signal (Fig. 4-3b). The arrows indicate the positions of the rf field. The difference between these two spectra (Fig. 4-3c) indicates the decrease in PCr magnetization resulting from exchange. From these measurements a value of 0.56±0.09 for $(M^{o}_{PCr}-M^{ss}_{PCr})/M^{o}_{PCr}$ was derived (Table 4-2).

To assess the non-selective effects that saturation had on the magnetization of PCr, spectra without any selective irradiation (Fig. 4-1b) were compared to spectra obtained with the rf field in the control position (Fig. 4-3a). Irradiation reduced the PCr intensity to 88±11% of its equilibrium value. Because the PCr peak appeared to be symmetrical, it was assumed that the effects of non-selective saturation were equivalent regardless of whether the selective rf pulse was in the control position or on the γATP resonance. As an indication that that the value of $(M^{o}-M^{ss})/M^{o}$ for PCr was not affected by non-selective irradiation, the γATP resonance was saturated to varying degrees from 0-100% by decreasing the power of the selective rf irradiation. At the lower power levels (γATP 0-50% saturated) there were no non-selective effects of saturation detected on the PCr magnetization. Using the values of $(M^{o}_{PCr}-M^{ss}_{PCr})/M^{o}_{PCr}$ with γATP partially saturated, a value of $(M^{o}-M^{ss})/M^{o}$ for PCr with γATP 100% saturated was extrapolated. This extrapolated value was equal, within experimental error, to that obtained with γATP saturated completely.

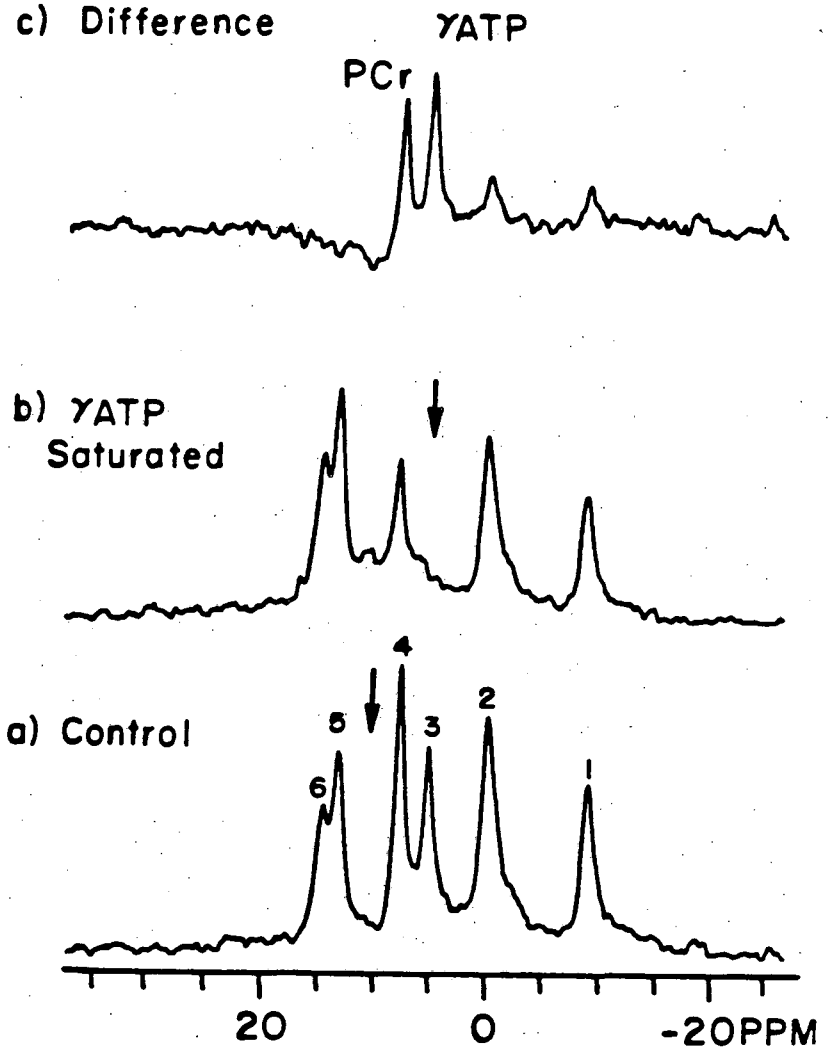

Figure 4-3. Saturation transfer measurement of the PCr → ATP reaction in rat heart. Spectra a) and b) are sums of 256 acquisitions each, using a 90° pulse and a 10 sec recycle time during which the saturation power was applied. Eight spectra were alternated with the rf irradiation on a) the control positon and b) the γATP position (arrows) until 256 acquisitions for each spectrum had been obtained. Spectrum c) is the difference obtained by subtracting b) from a). Peaks are numbered as in Fig. 4-1.

Table 4-2. Results of saturation transfer experiments performed on the rat heart *in situ*.

Reaction	$\frac{M^o - M^{ss}}{M^o}$	T_{1APP}* (sec)	k (sec^{-1})	T_1** (sec)
PCr→γATP	0.56±0.09	0.98±0.13	0.57±0.12	2.23±0.11
γATP→PCr	0.27±0.06	0.54±0.13	0.50±0.16	0.74±0.10
βATP→γATP	0.23±0.04	0.52±0.09	0.44±0.11	0.68±0.11
	(n=7)	(n=3)		

* T_{1APP} and T_1 values are for reactants on the left side of the equations.

** T_1 is the intrinsic T_1, or the T_1 calculated to account for the effects of exchange.

Similar to the kidney, saturation of the γATP peak led to a reduction in the α and βATP intensities (Fig. 4-3c). Saturation of the γATP peak had no effect on the Pi signal in contrast to results obtained in the perfused heart (12). This could be due to low levels of intracellular Pi in the heart in situ, especially when compared to the large contribution of 2,3-diphosphoglycerate in blood to this region of the spectrum.

Fig. 4-4 illustrates the saturation transfer experiment performed to measure the reverse rate, ATP⟶PCr, by saturating the PCr resonance and monitoring the reduction in γATP magnetization. As can be seen in the difference spectrum (Fig. 4-4c), saturation of the PCr resonance perturbs only the γATP peak. The negative peak in the αATP region was due to non-selective effects that the control irradiation (arrow Fig. 4-4a) had on peaks in this region. Typical data to derive T_{1APP} for both the PCr and γATP peaks are presented in Fig. 4-5.

Table 4-2 presents the experimental data and the calculated rate constants for the CK catalyzed reaction. For the forward direction (PCr⟶ ATP) a rate constant of 0.57±0.12 sec^{-1} was found. A value of 0.50±0.16 sec^{-1} was measured for the reverse direction (ATP⟶ PCr). Data are also included for the effect on the βATP peak.

To calculate the relative forward and reverse rates of the creatine kinase reaction, the rate constants derived above were multiplied by the concentration of PCr and ATP expressed in arbitrary intensity units. The PCr/ATP ratio was 1.29±0.13 (n=7). The forward rate, PCr⟶ATP, was 0.74±0.18 intensity units/sec and the reverse rate, ATP⟶ PCr, was 0.50±0.16 intensity units/sec. These rates were significantly different from one another ($P<0.05$), in agreement with

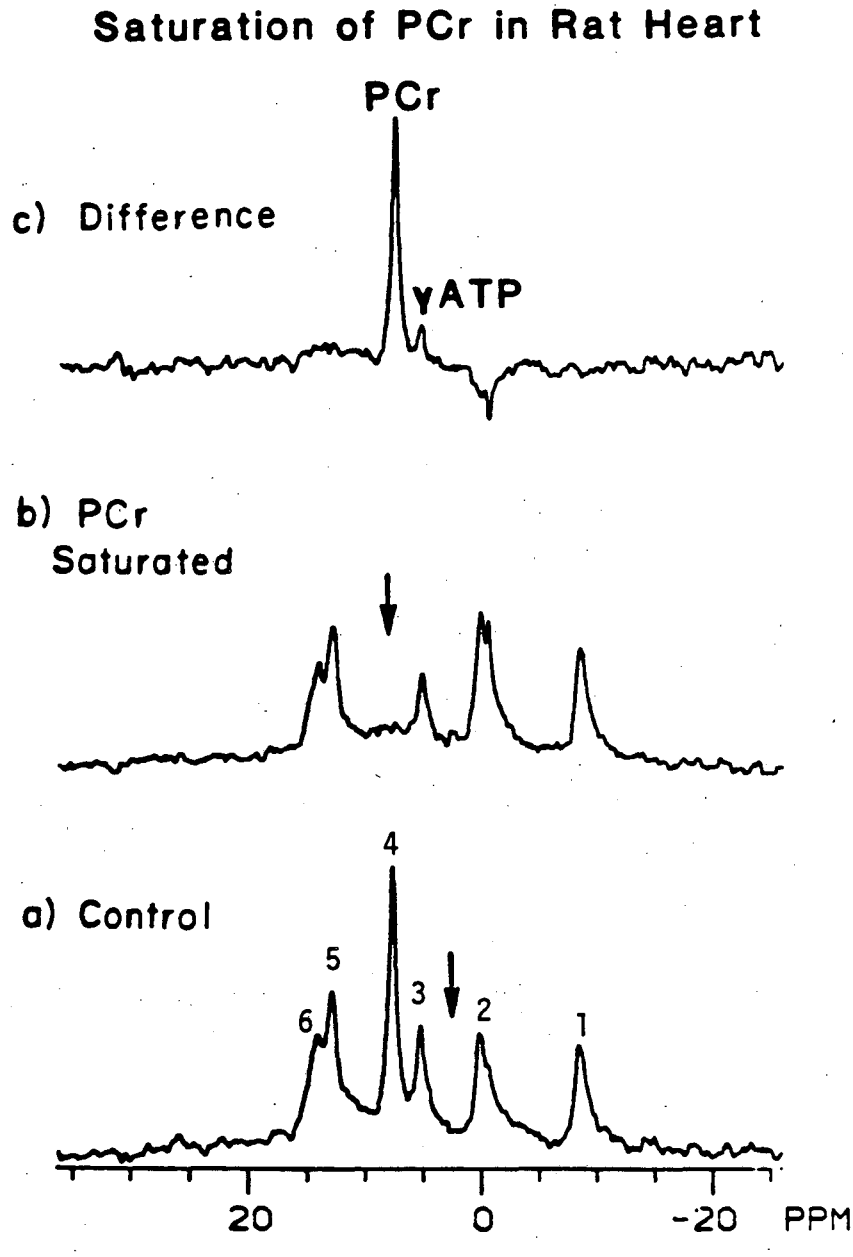

Figure 4-4. Saturation transfer measurement of the ATP⟶PCr reaction in rat heart. Experimental parameters were the same as those for Fig. 4-3. Arrows indicate the position of the selective rf irradiation; a) control, b) PCr saturated and c) differnce of a)-b). Peaks are numbered as in Fig. 4-1.

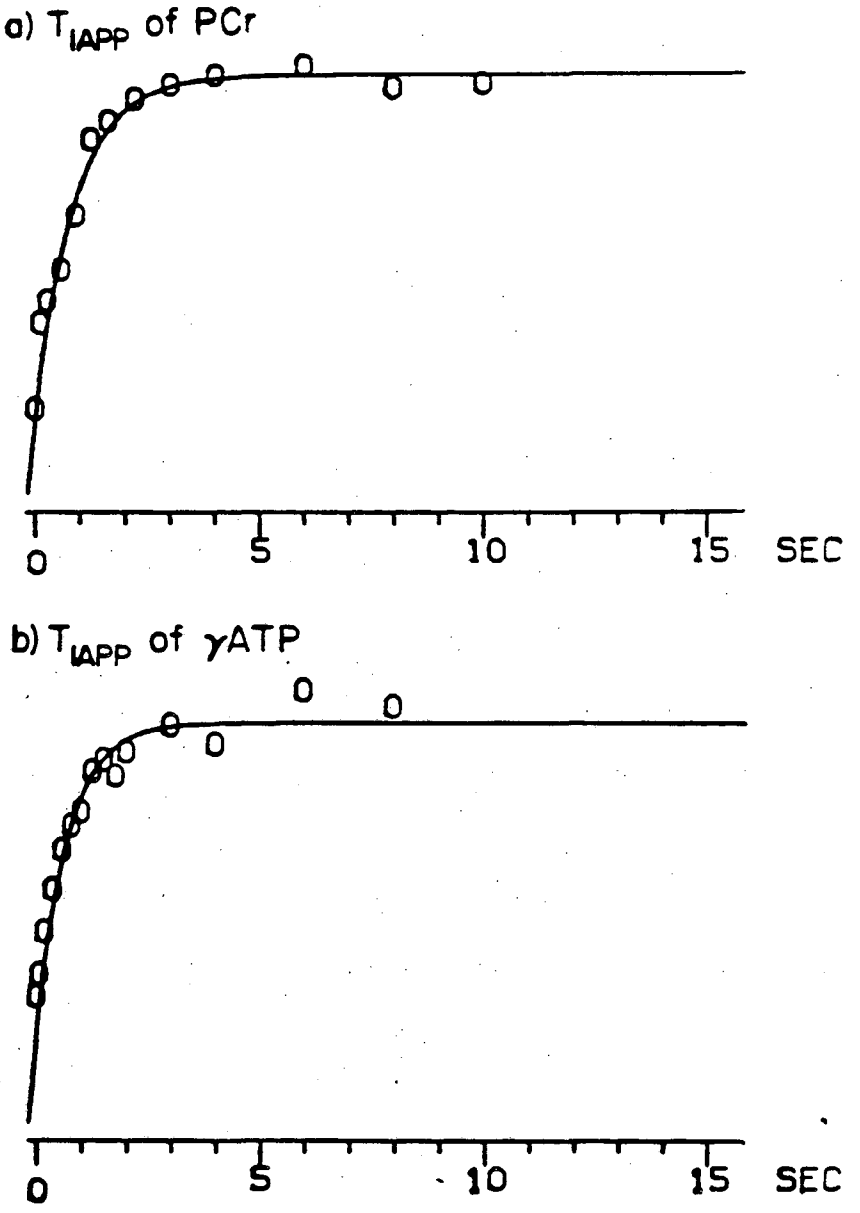

Figure 4-5. Data used for the determination of T_{1APP} of a) PCr and b) γATP in heart. Solid line represents the best single exponential fit to the data points (open cicles).

results previously reported for the perfused heart (5-7,24). Because creatine kinase is believed to be the only enzyme which utilizes PCr, and PCr appears to be in a steady-state, it is impossible for the rate of PCr production to be larger than the rate of PCr utilization. Two explanations have been offered for this discrepancy between the measured forward and reverse rates. One possibility is that subcellular compartmentation of metabolites and/or enzyme render the simple two-site exchange model, presented in Methods, inadequate (6). Another possibility is that the participation of ATP in other reactions (e.g. ATPase, adenylate kinase) causes a spurious reduction of the rate (5). This would occur because nuclei from metabolites other than PCr are exchanging with γATP and have not been included in the two-site analysis.

To test for the involvement of competing reactions, all metabolites in the spectrum were successively saturated while monitoring the effect on the γATP resonance. Saturation of the βATP peak caused a measurable change in the γATP peak; saturation of the other peaks (Pi, phosphomonoesters, αATP) had no effect on the γATP intensity. This indicates that the exchange between βATP and γATP is a significant competing reaction and could affect the measurement of exchange between PCr and γATP.

The following expressions, derived from the Bloch equations, for the steady-state magnetization of γATP, in the presence of saturation of the PCr or βATP peaks, account for the additional exhange reaction:

$$\frac{M^{SS}_{\gamma ATP}}{M^{O}_{\gamma ATP}} = \frac{1 + \frac{M^{SS}_{\beta ATP}}{M^{O}_{\beta ATP}}(k_{\gamma ATP \rightarrow \beta ATP} T_{1\gamma ATP})}{1 + (k_{ATP \rightarrow PCr} + k_{\gamma ATP \rightarrow \beta ATP}) T_{1\gamma ATP}} \qquad [4\text{-}2]$$

$$\frac{M^{o}_{\gamma ATP}}{M^{o}_{\gamma ATP}} = \frac{1 + \frac{M^{ss}_{PCr}}{M^{o}_{PCr}}(k_{ATP \rightarrow PCr} T_{1\gamma ATP}}{1 + (k_{ATP \rightarrow PCr} + k_{\gamma ATP \rightarrow \beta ATP}) T_{1\gamma ATP}} \qquad [4\text{-}3]$$

where,

$M^{ss}_{\gamma ATP}$ is the steady-state magnetization of γATP with PCr saturated in equation 4-2, and βATP saturated in equation 4-3.

$M^{o}_{\gamma ATP}$ is the equilibrium magnetization of the γATP signal measured with a suitable control irradiation pulse.

$M^{ss}_{\beta ATP}$ is the steady-state magnetization of βATP with PCr saturated.

$M^{o}_{\beta ATP}$ is the equilibrium magnetization of βATP.

M^{ss}_{PCr} is the steady-state magnetization of PCr with βATP saturated.

M^{o}_{PCr} is the equilibrium magnetization of PCr.

$T_{1\gamma ATP}$ is the intrinsic T_1 of γATP.

The T_{1APP} of γATP with both PCr and βATP saturated is given by:

$$T_{1APP} = \frac{T_{1\gamma ATP}}{1 + (k_{ATP \rightarrow PCr} + k_{\gamma ATP \rightarrow \beta ATP}) T_{1\gamma ATP}} \qquad [4\text{-}4]$$

Thus measurement of $M^{ss}_{\gamma ATP}/M^{o}_{\gamma ATP}$ and $M^{ss}_{\beta ATP}/M^{o}_{\beta ATP}$ with the PCr resonance saturated, $M^{ss}_{\gamma ATP}/M^{o}_{\gamma ATP}$ and M^{ss}_{PCr}/M^{o}_{PCr} with the βATP resonance saturated and the T_{1APP} of γATP with both the PCr and βATP signals saturated (Fig. 4-6) (an extra rf synthesizer was used for this purpose) allows the rate constant, $k_{ATP \rightarrow PCr}$ to be determined. A similar approach has been used previously to measure proton exchange (25).

Table 4-3 presents values for the different parameters measured in three different hearts . The rate constant derived from these measurements is 0.44±0.08, which is not significantly different from that measured assuming a two-site exchange between PCr and γATP. These

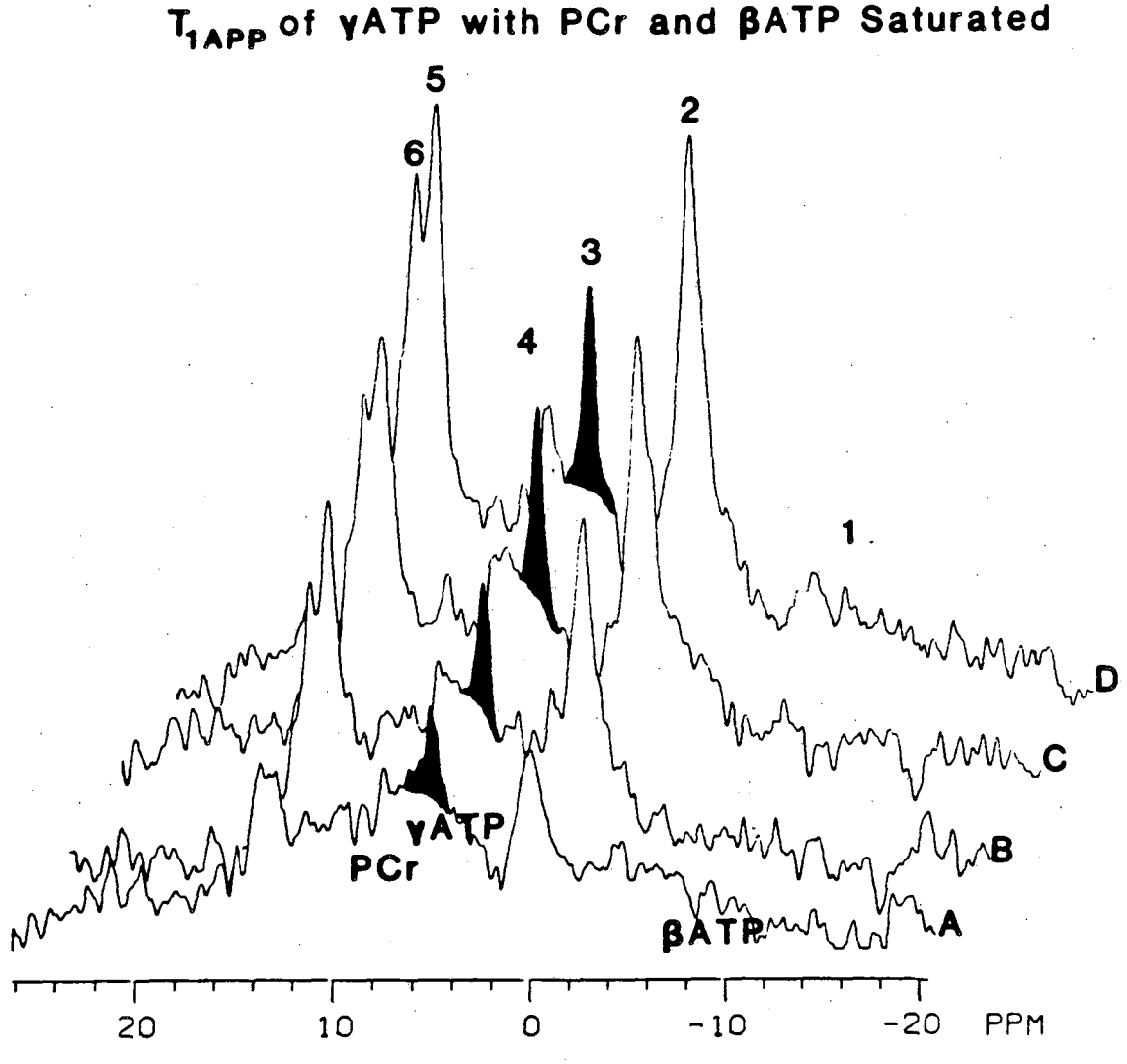

Figure 4-6. Spectra used to obtain T_{1APP} of γATP with both PCr and βATP (missing peaks 1 and 4) saturated. The area of the γATP resonance was measured at A) 100 msec, B) 450 msec, C) 900 msec, and D) 1.5 sec after saturation of the whole spectrum. The PCr and βATP peaks were kept continually saturated. Peaks are numbered as in Fig. 4-1.

Table 4-3. The effects of saturating PCr and/or ATP on the γ, β, and PCr peaks and the T_{1APP} of γATP.

Observed Peak	$\frac{M^{ss}}{M^{o}}$		T_{1APP}
	Saturating PCr	Saturating βATP	Saturating both PCr and βATP
γATP	0.73 (n=7)	0.80 (n=3)	0.63 sec (n=3)
βATP	1 (n=3)	--	--
PCr	--	0.92 (n=3)	--

results suggest that the effect of exchange between β and γATP is not sufficent to explain the discrepancy in the measured forward and reverse rates of the creatine kinase reaction in this system.

4.4 Discussion

KIDNEY. Recent results in the perfused kidney (13), interpreted the measured exchange between Pi and γATP to be due to the net synthesis of ATP via oxidative phosphorylation. If whole kidney ATP is assumed to be 1.7 μmol/gm wet weight (30), and the Pi/ATP ratio is 1.03 (present results), then a value of 1.8 μmol/gm wet weight for whole kidney Pi can be derived. Multiplying this Pi concentration by the measured rate constant (Table 4-1) gives a rate of 0.22 μmol/sec/gm wet weight or 13 μmol/min/gm wet weight, for the incorporation of Pi into ATP. Previously published rates of oxygen consumption and sodium reabsorption for the intact rat kidney range from 4-9 μmol of O_2/min/gm wet weight and 48-128 μmol of Na^+/min/gm wet weight (31). Using these values it is estimated that the J_{ATP}/J_O ratio is in the range of 0.8-1.7, and the J_{Na^+}/J_{ATP} ratio ranges from 4-10. These results are consistent with the hypothesis that saturation transfer measures net ATP synthesis in a physiologically relevant range. Experiments to measure NMR parameters, O_2 consumption, and Na^+ reabsorption simultaneously in the same animal are in progress. These studies have been aided by the recent acquisition of a horizontal bore superconducting magnet so that the rats do not have to hang vertically. Furthermore, the recent developement of a chronic renal venous catheter in our laboratory (31a) will allow these measurements to be performed on a rat which has not had surgery performed the day of experiments.

There are several problems concerning the general interpretation of saturation transfer experiments in vivo. Several of these problems complicate interpretation of the kidney results. First, as much as 30% of the Pi peak intensity could be due to to extracellular Pi plus the 2 phosphate of 2,3-diphosphoglycerate (2,3-DPG)(16). This may lead to an underestimate of $(M^o-M^{ss})/M^o$ for Pi. A significant non-exchanging pool would also lead to an overestimate of the exchanging Pi concentration, which would balance the error in $(M^o-M^{ss})/M^o$ in the calculation of the rate of Pi incorporation into ATP. However, the T_{1APP} of the Pi peak will also be affected by extracellular Pi and 2,3-DPG. The 2 phosphate of 2,3-DPG in arterial blood has a T_1 of approximately 2.2 sec at 97.2 MHz. Extracellular Pi would also be expected to have a longer T_1 than intracellular Pi. These influences tend to cause an overestimation of the T_{1APP} of intracellular Pi. If 2,3-DPG contributes 20% to the Pi peak, then from the measured T_{1APP} of 1.24 sec, a value of 1 sec can be derived for the T_1 of intracellular Pi. This implies that the rate constant and the rate were underestimated, possibly explaining the low J_{ATP}/J_O and high J_{Na^+}/J_{ATP} ratios obtained. The quality of the T_{1APP} data obtained was not suitable to separate out the various components of the Pi relaxation curve with a multi-exponential fit. This might be possible if more time were used to make the T_1 measurement. Another alternative would be to perform the experiment by varying the the time that the γATP resonance was saturated (6,19,Chapter 2). In this case, the time dependence of the decay of Pi magnetization would be due only to the exchanging component of the peak. To be reliable this technique requires greater signal-to-noise than we can presently obtain.

A second problem of interpretation is whether the rate of Pi ATP

exchange represents net ATP synthesis. In experiments with perfused heart (12) and kidney (13), an expected J_{ATP}/J_O of approximately 3 was obtained. However, in yeast the J_{ATP}/J_O was found to be 88 (33) suggesting that a rapid Pi⇌ATP exchange rather than net synthesis was being measured. The results presented here and the recent results of Yahaya et al. (13a) in intact kidney have indicated low values for J_{ATP}/J_O. It is possible that a component of the Pi⇌ATP exchange measured in kidney does not represent net ATP synthesis. Saturation transfer studies to measure ATP synthesis are based upon the assumption that all of the Pi participating in the exchange reaction is visible to NMR. Freeman et al. (13) reported that only 25% of total Pi was visible to NMR in the perfused kidney. It is possible that the rate of ATP synthesis is overestimated because of rapid Pi⇌ATP exchange and underestimated because of NMR invisible metabolites. An approach which is being pursued to shed some light on this problem is, that instead of measuring a single value of Pi⇌ATP exchange, the work function of the kidney can be changed (eg. partial ischemia, inhibitors of oxidative phosphorylation) and the resulting change in O_2 consumption can be compared to the change in ATP synthesis rate. If the NMR experiment is measuring net ATP synthesis, one would expect the rate of ATP synthesis to change in the same proportion as O_2 consumption. Furthermore, there are inhibitors of net ATP synthesis which do not effect the rapid Pi⇌ATP exchange catalyzed by mitochondria. If the saturation transfer experiment is measuring net synthesis, these inhibitors should decrease the measured rate. If, however, saturation transfer is measuring rapid Pi⇌ATP exchange, the inhibitors will have little effect on the rate. These experiments all

require a great deal of time and will probably only be successful in the kidney in situ.

Finally , it is appreciated that the kidney is a very heterogeneous organ in terms of its cell types. At this stage NMR can measure exchange rates only from the whole kidney. Therefore, any rate measured is an average over the different cell types in the kidney. There are inhibitors of transport which work selectively on some cells in the kidney but not others which would allow the estimate of the contribution of various cell types to the net rate measured by saturation transfer. Very recently, techniques have been described (34) which allow a ^{31}P metabolite image to be generated from the kidney. It would be very exciting if this technique could be combined with magnetization transfer techniques to measure rates at selected points in the kidney.

HEART. PCr is generally considered to be a reservoir of high energy phosphate for times when work demands on a tissue rapidly increase (26). To satisfy this role, the rate of the creatine kinase reaction must be significantly larger than the rate of ATP synthesis or utilization. To compare our measured rates of creatine kinase activity to ATP synthesis rates it is assumed that values for oxygen consumption and ATP concentrations in the perfused working heart approximate those found in vivo. Using an oxygen consumption rate of 1.4 μmol/sec/gm dry weight (27), an ATP synthesis rate of 9 μmol/sec/gm dry weight (3.5 mM/sec, making corrections as did Matthews et al. (7)) can be calculated assuming J_{ATP}/J_O equals 3. An assumed ATP concentration of 33 μmol/gm dry weight (29) with our NMR determined values of PCR/ATP, allows the forward and reverse rates of creatine kinase to be estimated

as 24 μmol/sec/gm dry weight (10 mM/sec) and 17 μmol/sec/gm dry weight (7 mM/sec), respectively. Thus, the forward rate through creatine kinase is approximately 3 times higher than the rate of ATP synthesis. This agrees with results obtained from the isolated perfused rat heart (7), where the forward rate through creatine kinase ranged from 13 to 3.3 times the ATP synthesis rate as workload increased towards that found *in situ*. The value of 24 μmol/sec/gm dry weight estimated for the forward rate of creatine kinase *in situ* is somewhat smaller than the value of 35 μmol/sec/gm dry weight reported for the pyruvate perfused working heart (24).

The present experiments measured a 33% difference in the forward and reverse rates of the creatine kinase reaction for the heart *in situ*. This discrepancy in rates has also been measured in the perfused heart (5-7,24), isolated muscle (8), and brain *in situ* (10). Experiments using a double saturation technique to account for the only significant competing reaction (*i.e.* exchange between β and γATP), demonstrate that the measured reverse rate of creatine kinase is not significantly effected. This is in contrast to the conclusions of other workers who estimated that exchange catalyzed by ATP synthesis and adenylate kinase could account for the measured discrepancy (7). However, these calculations only accounted for the effects of the competing reaction on $(M^o-M^{ss})/M^o$ of γATP and ignored the effects on T_{1APP}. The double saturation technique accounts for the effect of competing reactions on both T_{1APP} and $(M^o-M^{ss})/M^o$.

4.5 Conclusions

Using implanted rf coils, saturation transfer NMR experiments can

be used to measure metabolite interconversion rates in the rat heart and kidney in situ. In the kidney, the rate of ATP synthesis was estimated and compared to the the physiologic parameters of oxygen consumption and Na^+ reabsorption rates. A lower than expected J_{ATP}/J_O and a larger than expected J_{Na^+}/J_{ATP} were obtained. These results point to the problems associated with interpreting the measured ATP synthesis rate. In particular the heterogeniety of the Pi peak may be leading to erroneous results. The groundwork has been laid so that further experiments probing the problems of interpretation can be performed.

In the heart in situ, the rate of the forward reaction catalyzed by CK was estimated to be larger than the ATP synthesis rate. This is consistent with the postulated role of PCr as a high energy phosphate reservoir. In addition, the forward rate through CK was measured to be greater than the reverse rate in the heart. A double saturation technique accounted for the affects of the competing exchange between β and γATP. This exchange did not account for the measured discrepancy in forward and reverse rates.

Another explanation offered for the difference in forward and reverse rates of creatine kinase is intracellular compartmentation (6). It is interesting to note that the difference in creatine kinase rates measured in the heart in situ (7 μmol/sec/gm dry weight) is roughly equal to the estimate of the ATP synthesis rate (8 μmol/sec/gm dry weight). This observation suggests a model for compartmentation of ATP which may explain the discrepancy in measured rates. The advantages of comparing different magnetization transfer techniques with a discussion of the compartmentation model is the subject of the next chapter.

4.6 References

1) Hansford, R.G. in Current Topics in Bioenergetics, Vol 10, Sanadi, D.R. (ed) pp. 217-278 Academic Press, N.Y., 1980.

2) Mandel, L.J., and Balaban, R.S. (1981) Am. J. Physiol. 240, F357-F371.

3) Brown, T.R., Ugurbil, K., and Shulman, R.G. (1977) Proc. Natl. Acad. Sci. USA 74, 5551-5553.

4) Gupta, R.K. (1979) Biochim. Biophys. Acta. 586, 189-195.

5) Brown, T.R., Gadian, D.G., Garlick, P.B., Radda, G.K., Seeley, P.J., and Styles, P. in Frontiers of Biological Energetics Vol 2, Dutton, P.L., Leigh, J.S., and Scarpa, A. (eds.) pp. 1341-1349, Academic Press, N.Y., 1979

6) Nunnally, R.L., and Hollis, D.P. (1979) Biochemistry 18, 3642-3646.

7) Matthews, P.M., Bland, J.L., Gadian, D.G., and Radda, G.K. (1982) Biochim. Biophys. Acta. 721, 312-320.

8) Gadian, D.G., Radda, G.K., Brown, T.R., Chance, E.M., Dawson, J.S., and Wilkie, D.R. (1981) Biochem. J. 194, 215-228.

9) Balaban, R.S., Kantor, H.L., and Ferretti, J.A. (1983) J. Biol. Chem. 258, 12787-12789.

10) Shoubridge, E.A., Briggs, R.W., and Radda, G.K. (1982) FEBS Letts. 140, 288-292.

11) Wemmer, D., Wade-Jardetzky, N., Robin, E., and Jardetzky, O. (1982) Biochim. Biophys. Acta 720, 281-287.

12) Matthews, P.M., Bland, J.L., Gadian, D.G., and Radda, G.K. (1981) Biochem. Biophys. Res. Comm. 103, 1052-1059.

13) Freeman, D., Bartlett, S., Radda, G., and Ross, B. (1983) Biochim.

Biophys. Acta 762, 325-336.

13a) Yahaya, H., Chan, L., Freeman, D., Holloway, P., and Ross, B. (1984) Clin. Sci. 66, 35p.

14) Weiner, M.W., Greene, K., Vreman, H., Wemmer, D., Wade-Jardetzkky. N., and Jardetzky, O. (1980) ICRS Med. Sci. 8, 671.

15) Koretsky, A.P., Strauss, W., Basus, V., Murphy, J., Bendel, P., James, T.L., and Weiner, M.W. in Acute Renal Failure Eliahu, H.E. (ed) pp. 42-46 John Libbey, London, 1982.

16) Koretsky, A.P., Wang, S., Murphy-Boesch, J., Klein, M.P., James, T.L., and Weiner, M.W. (1983) Proc. Natl. Acad. Sci. USA 80, 7491-7495

17) Koretsky, A.P., Wang, S., Klein, M.P., James, T.L., and Weiner, M.W. (1984) Magn. Reson. Med. 2, 186-187.

18) Murphy-Boesch, J., and Koretsky, A.P. (1983) J. Magn. Reson. 54, 526-532.

19) Forsén, S.,and Hoffman, R.A. (1963) J. Chem. Phys. 39, 2892-2901.

20) McDonald, G.G., and Leigh, J.S. (1973) J. Magn. Reson. 9, 358-370.

21) Matson, G.B., Schleich, T., Serdahl, C., Acosta, G., and Willis, J.A. (1984) J. Magn. Reson. 56, 200-206.

22) Ackerman, J.J.H., Evelhoch, J.L., Berkowitz, B.A., Kichura, G.M., Deuel, R.K., and Lown, K.S. (1984) J. Magn. Reson. 56, 318-322.

23) Gonzalez-Mendez, R., Litt, L., Koretsky, A.P., von Colditz, J., Weiner, M.W., and James, T.L. (1984) J. Magn. Reson. 57, 526-533.

24) Kobayashi, K., Fossel, E., and Ingwall, J. (1982) Biophys. J. 37, 123a.

25) Perrin, C.L., and Johnston, E.R. (1979) 33, 619-626.

26) Lehninger, A.L. in Biochemistry 2nd Ed. p. 406 Worth, N.Y., 1975.

27) Taegtmeyer, H., Hems, R., and Krebs, H.A. (1980) Biochem. J. 186,

701-711.

28) Wikman-Coffelt, J., Sievers, R., Coffelt, R.S., and Parmley, W.W. (1983) Am. J. Physiol. 245, H354-H362.

29) Koretsky, A.P., Basus, V.J., James, T.L., Klein, M.P., and Weiner, M.W. (1984) Personal Communication.

30) Hems, P.A., and Brosnan, J.T. (1970) Biochem. J. 120, 105-111.

31) Weinstein, S.W., and Szyjewicz, J. (1971) Am. J. Physiol. 227, 171-177.

31a) Xian Ai (1984) Personal Communication

32) Saki, R., Ikura, K., Sugimoto, E., and Chiba, H. (1974) Anal. Biochem. 61, 43-47.

33) Alger, J.R., den Hollander, J.A., and Shulman, R.G. (1982) Biochemistry 21, 2957-2963.

34) Schleich, T., Matson, G.B., Garwood, M., and Acosta, G. (1984) Biophys. J. 45, 321a.

CHAPTER 5: DETECTION OF EXCHANGE REACTIONS INVOLVING SMALL METABOLITE POOLS USING NMR MAGNETIZATION TRANSFER TECHNIQUES: RELEVANCE TO SUBCELLULAR COMPARTMENTATION OF CREATINE KINASE.

5.1 Introduction

Nuclear magnetic resonance spectroscopy (NMR) has been used to monitor biochemical events in isolated cells (1), perfused organs (2), intact animals (3,4, Chapter 3), and human subjects (5). In addition ^{31}P NMR magnetization transfer techniques are capable of measuring enzymatically catalyzed reactions involving high energy phosphate compounds, in vivo (6-11, Chapter 4). In particular, the rate of phosphate exchange between phosphocreatine (PCr) and ATP, catalyzed by creatine kinase (CK) has been studied in muscle, heart, and brain using saturation transfer techniques (7-11, Chapter 4). In these studies it was found that under steady-state conditions, the rate of the forward reaction (PCr + ADP → ATP +Cr) was larger than the reverse rate (ATP +Cr → PCr + ADP). However, the net forward rate must have equaled the reverse rate, because metabolite levels were not changing and CK is the only enzyme known to utilize PCr. This discrepancy between the measured unidirectional rates of the CK reaction in vivo, has been attributed to the involvement of ATP in competing reactions (7,10); however, attempts to estimate the magnitudes of these reactions seems to indicate that they do not account for the measured discrepancy (10). Measurements performed in this laboratory (12, Chapter 4), using a double saturation technique to quantitate the involvement of competing reactions, indicate that these reactions do not account for the measured discrepancy in CK

catalyzed rates. Alternatively, Nunnally and Hollis (8) proposed that the difference in rates of CK is due to the the distribution of metabolites and enzymes in various compartments of the cell, leading to an ambiguous result.

Models for compartmentation may involve pools of metabolites whose concentrations are below the detection limits of NMR. As currently applied to living systems ^{31}P NMR can detect metabolite concentrations only at approximately 1 mM. Many important metabolic intermediates (e.g. ADP) are at μM levels or less and not detectable in ^{31}P NMR spectra of most living tissue (e.g. heart) (4, Chapter 2). Furthermore, it is probable that small, NMR invisible pools of metabolites, such as mitochondrial ATP, coexist with large pools which are detectable in the spectrum.

Most exchange measurements in vivo, have been performed using saturation transfer techniques. Recently, a few studies using inversion transfer (13) and two dimensional (2D) NMR techniques (14,15) have also been performed. While saturation transfer experiments have measured a greater forward than reverse rate for the CK reaction in muscle and brain (9,11), 2D exchange results have indicated equal rates in these tissues (15). The saturation transfer experiments also detected exchange between the γ and β phosphates of ATP (γATP, βATP) which was not seen in the 2D spectrum. Magnetization transfer techniques differ qualitatively. Saturation transfer continuously perturbs the labeled peak; thus a small exchanging pool is continously labeled. In contrast, 2D exchange and inversion transfer employ a pulse labeling technique. Therefore, in principle, the various exchange techniques should be very different in their ability to detect reactions between small, NMR

undetectable metabolites and larger, NMR visible metabolites. This difference may explain the discrepancies in results obtained with saturation transfer and 2D NMR.

The present experiments were performed to verify the idea that saturation transfer is able to detect the presence of exchange with small metabolite pools, while 2D NMR cannot. The results obtained lead to the conclusion that a quantitative comparison between saturation transfer and 2D or inversion transfer performed in vivo will reveal the involvement of small pools of metabolites (16). These observations suggest a model whereby low levels of compartmented ATP are in exchange with PCR; the PCR is also in exchange with cytoplasmic ATP. This model may provide an explanation for the discrepancy found in the measured forward and reverse rates of the CK reaction.

5.2 Theory

For the exchange process $A \rightleftharpoons B$, the expressions used to obtain rate information from saturation transfer, 2D NMR exchange, and inversion transfer experiments reveal the effect of a low concentration of one of the reactants (e.g. B). In a saturation transfer experiment, the change in the magnetization of the nucleus A (M_A) while in site after saturating the nucleus while in site B at time t = 0 and maintaining B saturated, is given by (17):

$$M_A(t) = \frac{M_A^0}{1+k_1 T_{1A}} \{1+k_1 T_{1A} \exp[-t(\frac{1+k_1 T_{1A}}{T_{1A}})]\} \qquad [5\text{-}1]$$

where M_A^o is the equilibrium magnetization of A, T_{1A} is the spin-lattice relaxation time at site A, and k_1 is the first order rate constant for the reaction A → B. The concentration of B does not affect the measurement of the rate A → B.

For the 2D exchange experiment, performed by using three successive 90° pulses separated, respectively, by an evolution time and a mixing time (τ_m), the intensity of the crosspeak (I_{AB}) between A and B, as a function of mixing time, is given by (18):

$$I_{AB}(\tau_m) = \frac{(M_A^o M_B^o)^{1/2}}{M_A^o + M_B^o} \sinh([k_1 k_2]^{1/2} \tau_m) \exp(-\frac{\tau_m}{T_1}) \qquad [5\text{-}2]$$

where the T_1 for spins A and B were assumed to be equal, M_B^o is the equilibrium magnetization of B and k_2 is the first order unidirectional rate constant for the reaction B → A. In this case the intensity of the crosspeak is proportional to the concentration of B. A very low concentration of B would make the crosspeak difficult to detect.

Finally, for an inversion transfer experiment where B is inverted at time t = 0, the variation in M_A with time after the inversion of B is given by (19):

$$M_A(t) = \frac{2M_A^o M_B^o}{M_A^o + M_B^o} \{\exp(\lambda_- t) - \exp(\lambda_+ t)\} + M_A^o \qquad [5\text{-}3]$$

with

$$\lambda_{\pm} = \frac{1}{2} \{-(\frac{2}{T_1} + k_1 + k_2) \pm (k_1 + k_2)\}$$

where the T_1 for A and B are assumed to be equal. In the inversion transfer experiment, the change in the magnetization of A is proportional to the amount of B present. If the concentration of B is vanishingly small, the effect of exchange on A would also be vanishingly small.

The above equations indicate that the magnitude of the effect of exchange on the magnetization of A in the inversion transfer experiment (eqn. 5-3) and the cross peak intensity in the 2D experiment (eqn.5-2) depends not only on the rate of exchange and on relaxation but on the amount of B present as well. In the saturation transfer experiment, as long as B is completely saturated (i.e., $M_B = 0$) and so maintained, the change in A depends only on k_1 and T_{1A}. If B is undetectable within reasonable averaging times in a normal one dimensional spectrum, only the saturation transfer experiment will detect the exchange. This does, however, presume a priori knowledge of where to place the saturating radiofrequency field. Therefore, saturation transfer provides information concerning small pools (not directly detectable) which are in exchange with larger pools (NMR detectable), whereas 2D or inversion transfer does not.

5.3 Results

Experiments were performed using solutions containing approximately 1900 units of creatine kinase (rabbit muscle, Sigma), PCr, Cr, ADP, and ATP buffered at pH 7.2 (30°C, 10 mM free Mg^{2+}). Solutions were prepared so that ADP concentrations ($\sim$ 100 μM) were approximately 100-fold less than those of ATP and Cr, or PCr ($\sim$ 10 mM). A ^{31}P NMR spectrum of the

solution obtained at 97.2 MHz showed no detectable ADP peaks. A 2D exchange experiment performed as described by Jeener et al. (18), with the addition of phase cycling (20) to allow proper phasing and quantitation of peaks in the spectrum, was performed on a similar solution. Fig. 5-1 shows the results for a mixing time of 600 msec. Peaks along the diagonal correspond to the resonances observed in the one dimensional spectrum. Cross peaks due to exchange are seen between the PCr and γATP peaks, as expected. The two crosspeak intensities were equal for all mixing times between 50 msec and 1.5 sec (Fig. 5-2). This indicates that, under these conditions, the measured forward rate was equal to the reverse rate for the isolated enzyme, as has been noted previously by other workers using saturation transfer (7,8) and inversion transfer (13). No crosspeaks were detected between the βATP signal and any other resonances, as can be more readily seen in one dimensional slices of the 2D spectrum taken through the maxima of the diagonal peaks (Fig. 5-3). This result was true for all mixing times ranging from 0.1 to 1.5 sec.

Saturation of the γATP peak (Fig. 5-4B) led to a reduction in the PCr magnetization due to the exchange of phosphate between PCr and γATP. Saturation of the PCr resonance caused a reduction in the γATP signal due to the reverse reaction, γATP $\rightarrow$ PCr. The ratio of forward to reverse rates was 0.98 ± 0.18 (Table 5-1), indicating that saturation transfer measured equal rates, in agreement with the 2D result and those of previous workers (7,8,13). In addition to the effect on the PCr intensity, there was a reduction in the βATP peak, as can be clearly seen in the difference spectrum (Fig. 5-4C). Saturation of the βATP

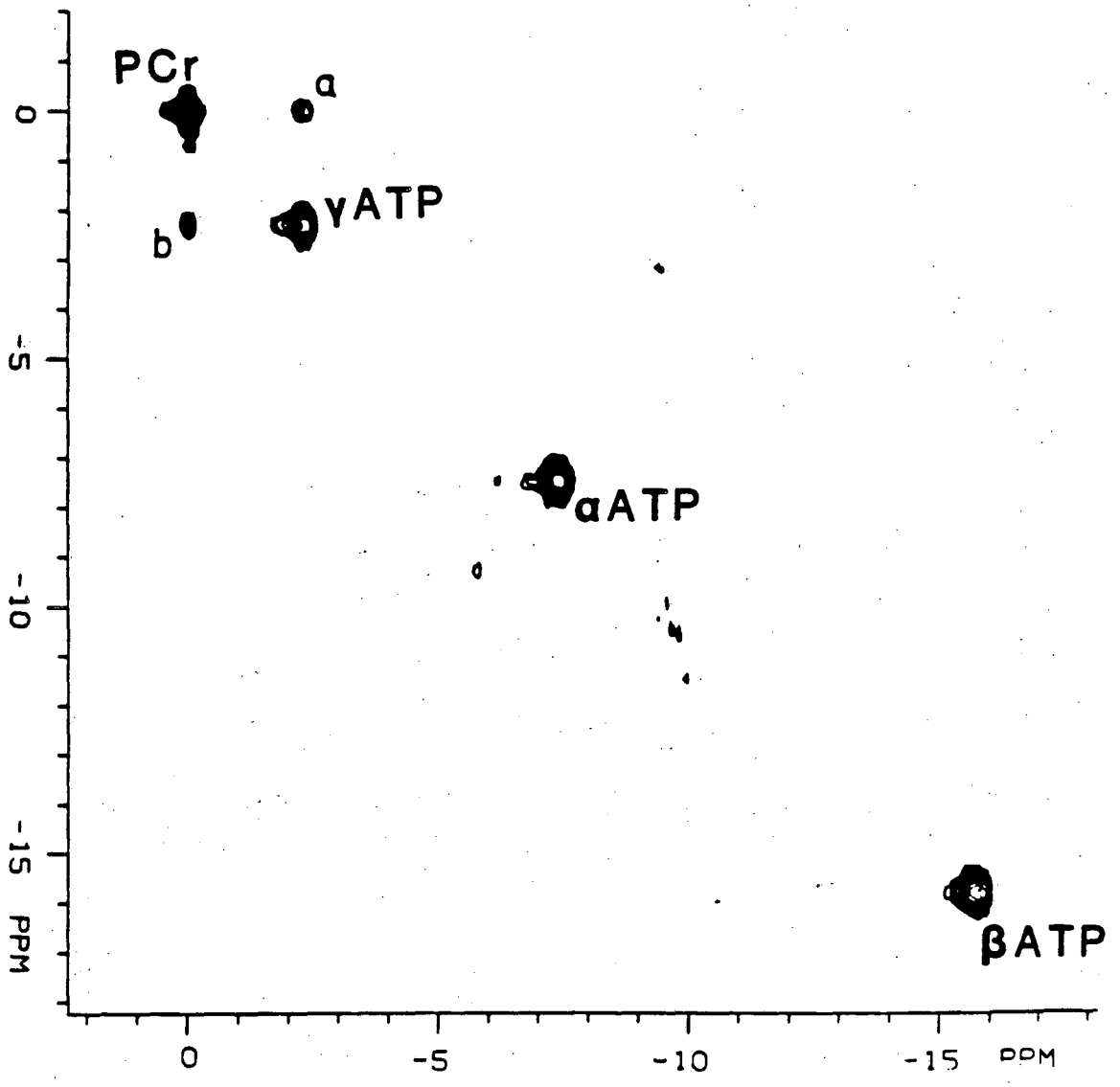

Figure 5-1. Contour plot of a pure absorption phase two-dimensional ^{31}P NMR spectrum of the creatine kinase reaction mixture. Data were collected at a phosphorus frequency of 97.2 MHz, using a mixing time of 600 msec. 64 different evolution times ranging from 0.5-32 msec were used with an overall cycle of 32 acquisitions per evolution time (21). A spectral width of 2000 Hz, exponential line broadening of 10 Hz in both dimensions, and zero filling from 256 to 1024 points in the second dimension were used. Peaks are as labeled with a and b representing the cross peaks due to exchange between PCr and γATP.

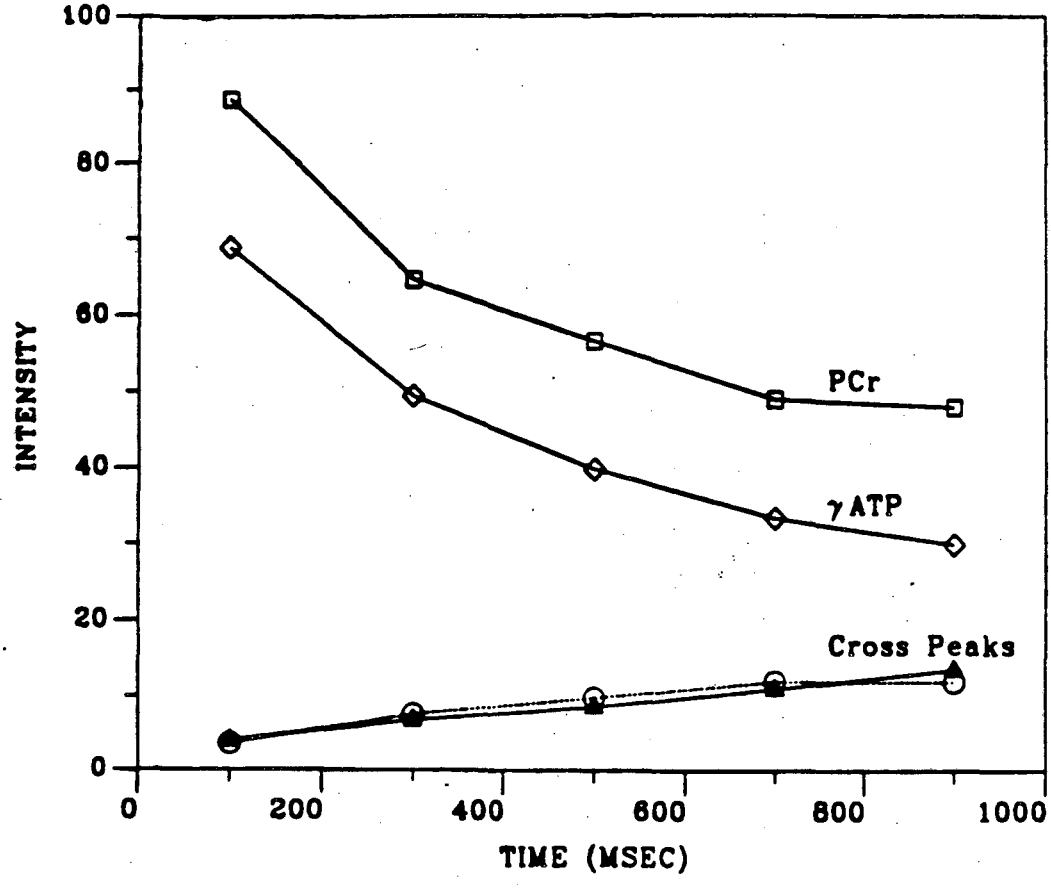

Figure 5-2. Change in intensities of peaks with increasing mixing time in 2D exchange spectra of the creatine kinase solution. Using the initial rate of buildup of the cross peaks a rate of 7 μmol/sec for the creatine kinase reaction was calculated. 2D spectra were acquired as described in Fig. 5-1 except for the varying mixing times.

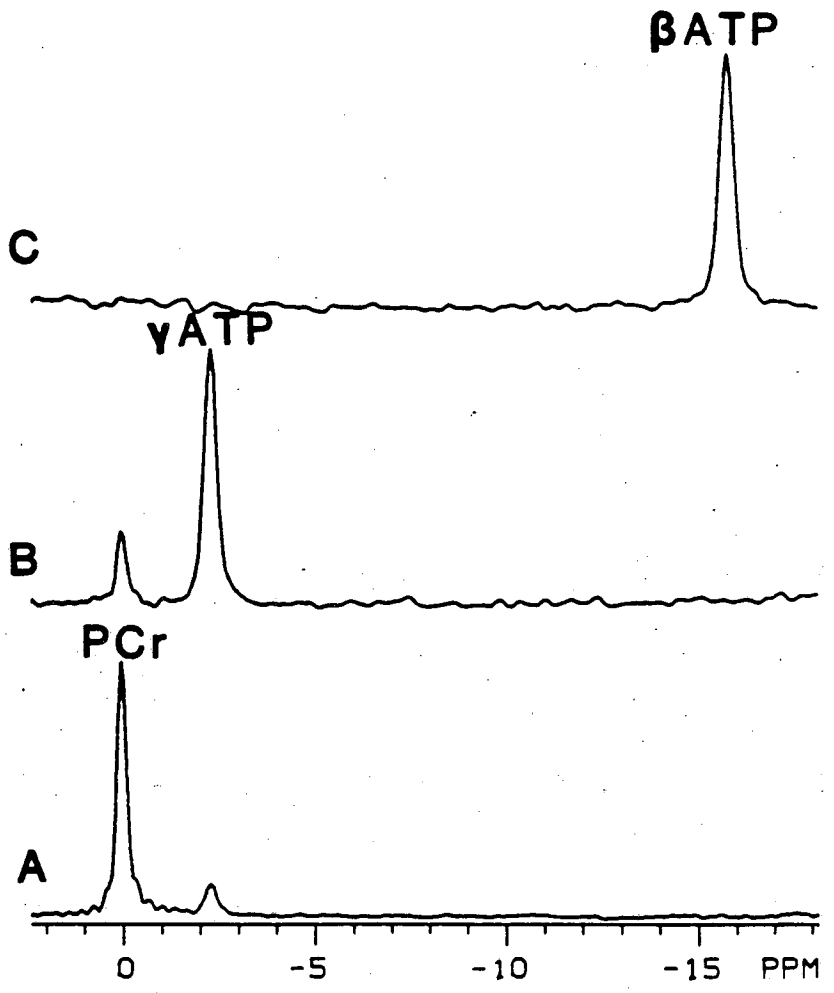

Figure 5-3. Vertical slices through the intensity maxima of the diagonal peaks of the 2D spectrum of Fig. 5-1. A represents the slice through the PCr peak; the smaller peak represents the cross peak due to exchange between PCr and γATP (peak b, Fig. 5-1). B represents the slice through the γATP peak; the smaller peak represents the cross peak due to exchange between γATP and PCr (peak a, Fig. 5-1). C represents the slice through the βATP peak. The ordinate for B and C equals 2x that of A.

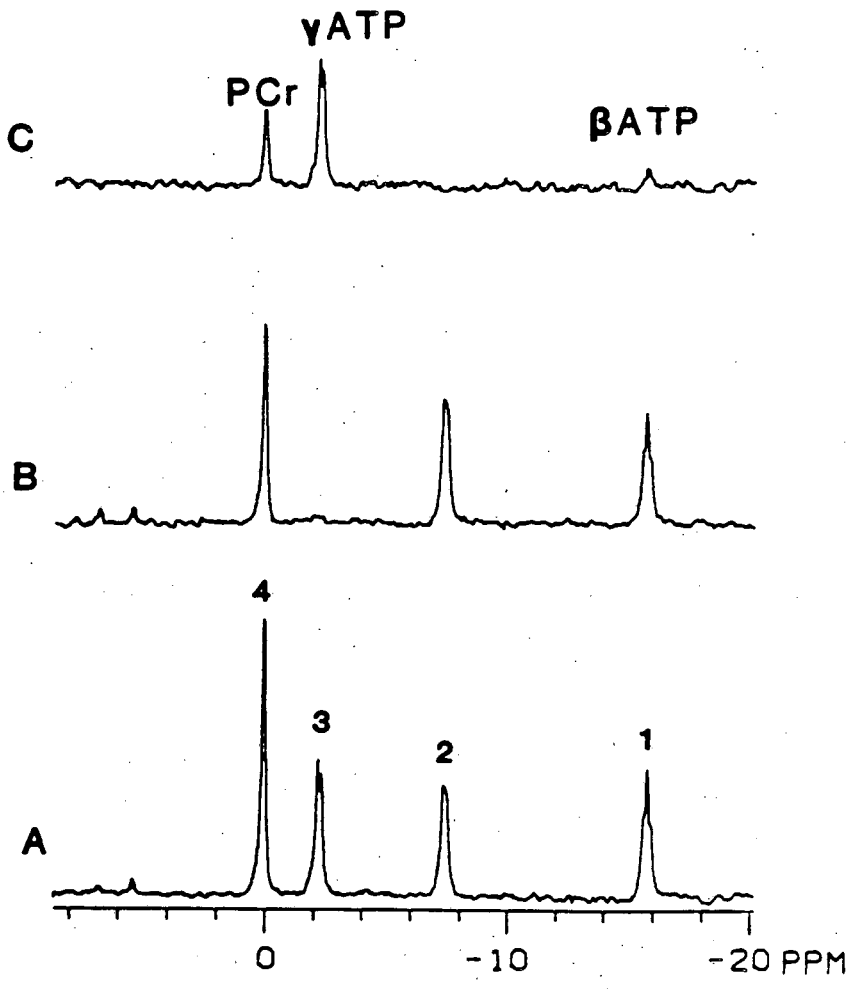

Figure 5-4. ^{31}P NMR saturation transfer experiment of the creatine kinase reaction. Spectra were obtained at 97.2 MHz and represent the sum of 16 acquisitons using a 90° pulse (22 μsec) and a 8 sec recycle time. During the delay between pulses the selective radiofrequency irradiation, generated using the decoupler channel, was left on. A represents a control spectrum with the selective irradiation at 2.5 PPM. B represents a spectrum with the γATP peak saturated. C is the difference of A- B. Peaks are: 1, βATP; 2, αATP; 3, γATP; 4, PCr.

Table 5-1. Results of saturation transfer experiments performed on solutions containing isolated CK, ATP, PCr, ADP, and Cr, buffered at pH 7.2. The results of five separate experiments performed on different solutions are presented.

	PCr $\longrightarrow$ ATP				ATP $\longrightarrow$ PCr				
Expt.	$\frac{M^o-M}{M^o}$	T_{1APP} (sec)	k (sec^{-1})	Rate ($\frac{\mu mol}{sec}$)	$\frac{M^o-M}{M^o}$	T_{1APP} (sec)	k (sec^{-1})	Rate ($\frac{\mu mol}{sec}$)	Ratio of Rates
1	0.42	1.38	0.30	5.9	0.49	1.08	0.49	7.1	0.83
2	0.38	1.64	0.23	4.6	0.25	1.53	0.25	4.1	1.13
3	0.30	1.11	0.27	5.3	0.37	0.63	0.37	6.2	0.85
4	0.27	0.81	0.33	7.0	0.37	0.77	0.48	8.2	0.85
5	0.32	1.17	0.27	5.6	0.33	1.03	0.32	4.6	1.22

Avg. = 0.98 ± 0.18

peak had no effect on the γ resonance. This finding, and the absence of a cross peak between the β and γ ATP resonances in the 2D spectrum, rules out a negative nuclear Overhauser effect. CK does not catalyze exchange between γ and βATP, but does catalyze exchange between the β phosphate of ADP (βADP) and βATP. To determine if the reduction in magnitude of the βATP peak was due to simultaneous saturation of a small pool of βADP when the γATP resonance was saturated, the frequency of the saturation pulse was varied and the effects on PCr and βATP peak intensities monitored. Fig. 5-5 shows that the PCr intensity reached a minimum when the saturation pulse was directly on the γATP resonance (0 Hz). The βATP intensity reached a minimum at a frequency which corresponded to the βADP chemical shift (arrow in Fig. 5-5), as determined from a solution with limiting amounts of PCr so ADP could be detected. To determine if the presence of enzyme bound intermediates, (e.g. ADP-E or PCr-E) could be detected, selective rf irradiation was moved across the entire spectral width. In all cases, the maximum effect of saturation occurred at the resonance frequencies of the free metabolites. It is concluded from these experiments that saturation transfer measurements may be used as an indirect detection experiment(20) to detect small pools participating in exchange reactions, whereas 2D cannot detect small exchanging pools. Furthermore, it is possible that an experiment of the type illustrated in Fig. 5-2 could lead to an estimate of the βADP linewidth which, in turn, may be related to the binding rate of the substrate to the enzyme.

5.4 Implications for Creatine Kinase Reaction Rate Measurements, in Vivo

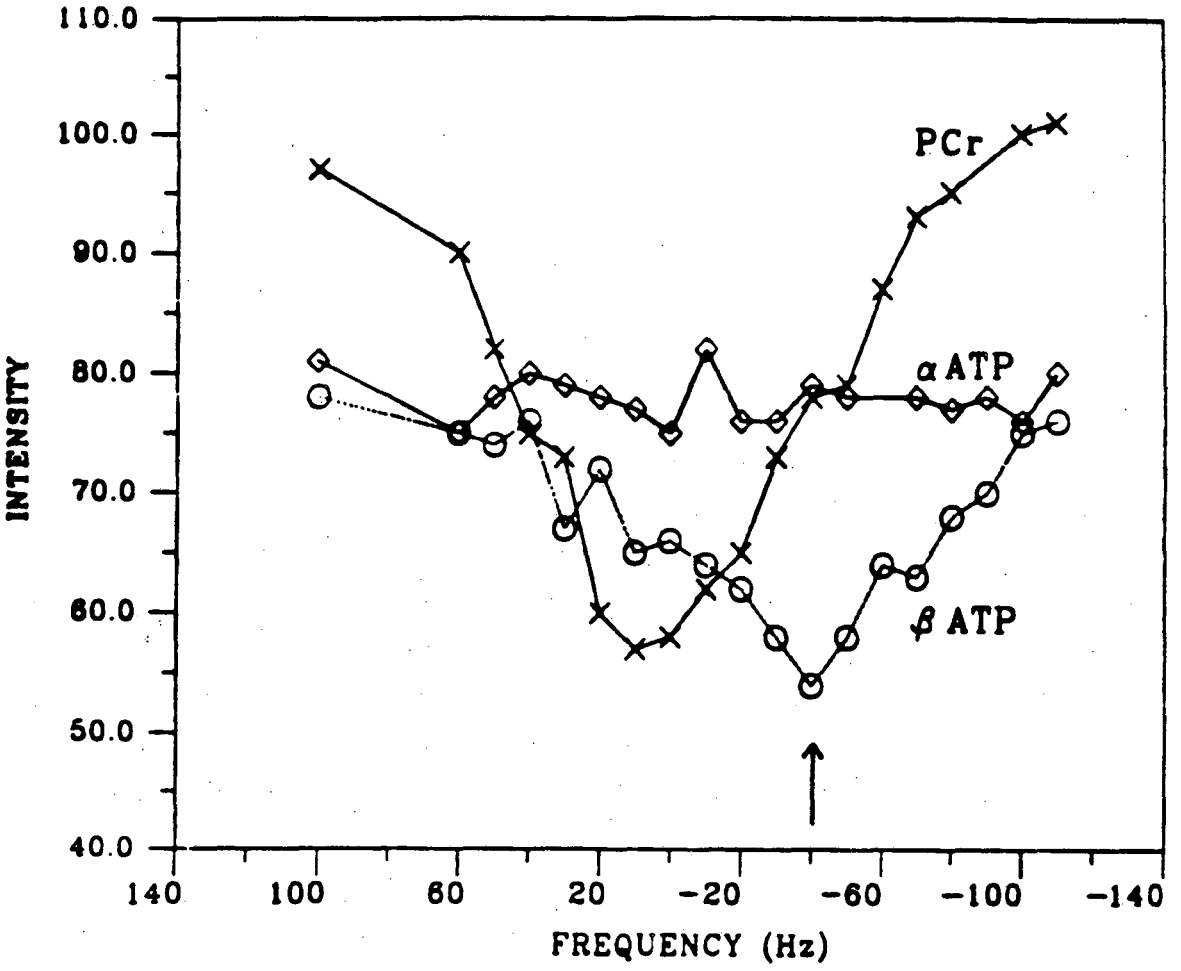

Figure 5-5. Effect of varying the frequency of the saturation pulse on the intensity of PCr (X), βATP (O), and γATP (◇) peaks. Zero Hz corresponds to the resonance position of γATP, and the arrow indicates the the resonance position of βADP. Variations in the αATP peak intensity give an indication of systematic errors. Spectra were obtained as in Fig. 5-4. Peak intensities were determined using the integration routine on the Nicolet 1180 computer.

The ability of saturation transfer to detect small pools of metabolites suggested a model to account for the difference between the forward and reverse rates of CK measured in vivo. In this model a large pool of PCr is assumed to be in exchange with both a large (NMR detectable) and a small pool of ATP (undetectable by NMR) (Fig. 5-6A). 2D or inversion transfer experiments are able to detect only the exchange between the large pools of PCr and ATP (rates 3 and 4, Fig. 5-6a). Irradiation of the γATP peak saturates both the small and large pools of ATP so rates 1 and 3 are measured. Saturation of the PCr resonance leads to the measurement of rate 4 because only the large pool of ATP is detected. Rate 2 is not measured because the fractional change of the small pool of γATP, produced by saturating the PCr peak, cannot be detected. Thus, the rate PCR → γATP (rates 1 + 3) appears larger than the rate γATP → PCr (rate 4).

A biologically relevant version of the model, based on the "PCr shuttle" (22,23), is depicted in Fig. 5-6b. A large PCr pool is in exchange with cytosolic ATP (rates 3 and 4, Fig. 5-6b), as well as with smaller pools of ATP which are produced at the mitochondrion (rate 2) and utilized by the muscle fiber (rate 1). In this case the discrepancy between the measured forward (rates 1+3) and reverse (rate 4) rate is related to the net rate of ATP utilization (rate 2). That is, as net ATP utilization and thus net synthesis increases, the flow through the small pools becomes more important, increasing the measured difference between forward and reverse rates. The model predicts that the difference in forward and reverse rates of the CK reaction should be directly proportional to the rate of ATP synthesis. To test this hypothesis, data previously reported from the perfused heart (10), in situ brain

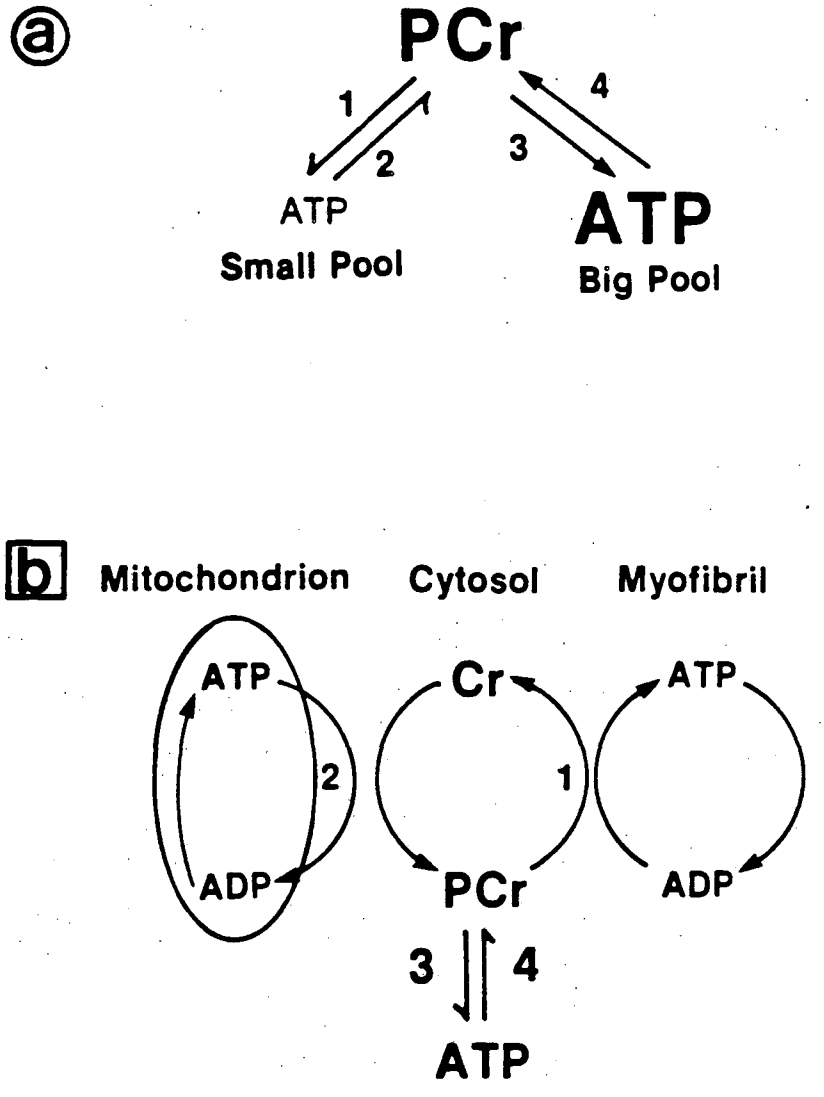

Figure 5-6. Compartmentation model to explain the discrepancy in the forward and reverse rates of creatine kinase measured in vivo. The basic features of the model are illustrated in a. Both a small and a large pool of ATP are in exchange with a PCr pool. A more specific biological version of a is illustrated in b. The small pool of ATP is located in the mitochondria and the myofibrils. The large ATP pool is cytoplasmic ATP and both ATP pools are in exchange with cytoplasmic PCr. Numbers represent rates for the specific reactions occuring in the direction indicated by the arrows.

(11), and in situ heart (12), were used to construct a plot of the difference in CK rates vs. the net rate of ATP synthesis covering a wide range of values (Fig. 5-7). The model implies a straight line with slope of 1 (dashed line Fig. 5-7). The line which best fits all the points gives a slope of 0.9, in agreement with the predicted slope of unity. Two variations of the model would give rise to a more complicated relation between net ATP synthesis and the difference in CK catalyzed rates. First, if a percentage of the ATP produced in the mitochondria diffuses into the large ATP pool before reacting to form PCr, i.e., there is some exchange between the two ATP pools, the measured difference in rates would be less than net ATP synthesis. Second, if instead of a undirectional reaction (small ATP pool → PCr) at the mitochondria, a rapid exchange occurred (small ATP pool $\rightleftharpoons$ PCr) the difference in rates would be larger than net ATP synthesis.

This model makes other predictions which can be tested experimentally. Measurement of CK exchange kinetics in vivo using 2D or inversion transfer should measure equal forward and reverse rates. This is supported by the results of Balaban et al. (15), who measured equal forward and reverse rates for the CK reaction in rat brain and muscle using 2D exchange techniques. If the 2D or the inversion transfer experiment and the saturation transfer experiment were performed concurrently on the same preparation, the 2D or inversion transfer measured rates should equal the reverse rate as measured by saturation transfer. Finally, exchange between inorganic phosphate and γATP and between β and γ ATP have been measured in rat brain using saturation transfer (11) but were not detected in the 2D spectrum (15). This suggests the possible involvement of small metabolite pools in these

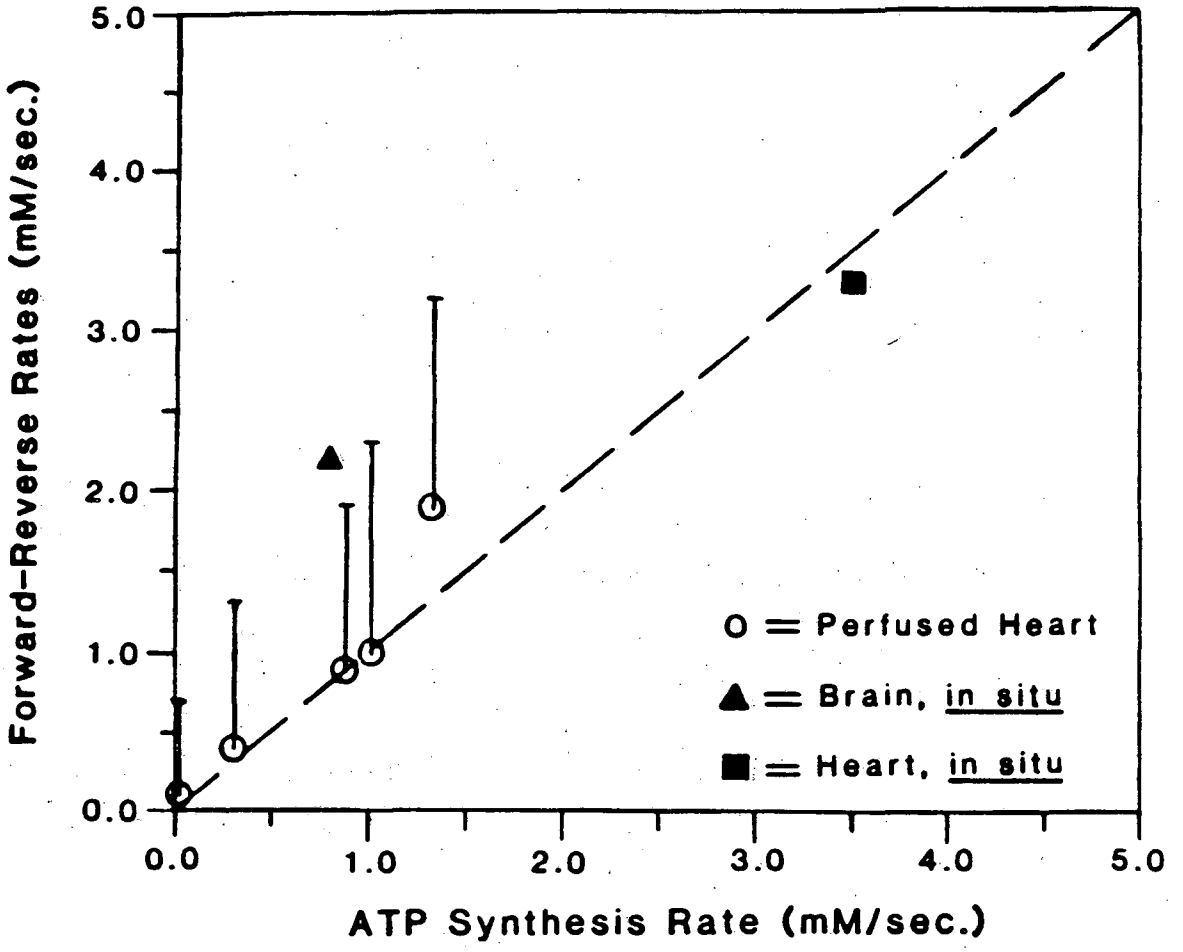

Figure 5-7. Plot of the forward minus reverse rates of the creatine kinase reaction measured in vivo vs. the net rate of ATP synthesis. Data were obtained from previously published results in perfused heart (O, reference 10), brain in situ (▲, reference 11) and heart in situ (■, Chapter 4). The dashed line of unit slope represents the theoretical prediction made assuming the model of Fig. 5-6b. Error bars are + one standard deviation.

reactions as well.

5.5 Conclusions

Metabolic reactions occurring in vivo are considerably more complex than the simple two site exchange system usually used to analyze magnetization transfer studies. Models for more complex multiple exchange systems may be used to analyze NMR data (12) but are dependent on knowing the exchange network. A comparison of 2D or inversion transfer results with saturation transfer should indicate the extent of involvement of small metabolic pools in exchange reactions.

Furthermore, the use of saturation transfer as an indirect detection procedure should prove useful in studying metabolic exchange reactions with other nuclei, including ^{1}H or ^{13}C. In these cases metabolites which are interconnected may not be both directly detectable. For example, glucose labeled with ^{13}C in the 1 position when metabolized by yeast anaerobically gives resonances for the C1 and C6 carbon of fructose-1,6-diphosphate; however, no resonances for dihydroxyacetone phosphate or 3-phosphoglycerate are detected (24). Saturation at the expected frequency for the proper carbon of dihydroxyacetone phosphate may cause an effect on the fructose-1,6-diphosphate carbon. A similar strategy may be useful in measuring kinetics of the lactate dehydrogenase reaction using ^{1}H spectroscopy.

5.6 References

1) Navon, G., Ogawa, S., Shulman, R.G. and Yamane T. (1977) Proc. Natl. Acad. Sci. USA 74, 87-91.

2) Gadian, D.G., Radda, G.K., Richards, R.E. and Seeley, P.J. (1979) in "Biological Applications of Magnetic Resonance" ed. Shulman, R.G. (Academic Press, NY) pp. 463-535.

3) Ackerman, J.J.H., Grove, T.H., Wong, G.G., Gadian, D.G. and Radda, G.K. (1980) Nature 283, 167-170.

4) Koretsky, A.P., Wang, S., Murphy-Boesch, J., Klein, M.P., James, T.L. and Weiner, M.W. (1983) Proc. Natl. Acad. Sci. USA 80, 7491-7495.

5) Chance, B., Eleff, S., and Leigh, J.S. (1980) Proc. Natl. Acad. Sci. USA 77, 7430-7434.

6) Brown, T.R., Ugurbil, K. and Shulman, R.G. (1977) Proc. Natl. Acad. Sci. USA 74, 5551-5553.

7) Brown, T.R., Gadian, D.G., Garlick, P.B., Radda, G.K., Seeley, P.J. and Styles, P. (1979) in "Frontiers of Biological Energetics", eds. P.L. Dutton, J.S. Leigh and A. Scarpa (Academic Press, NY) Vol. 2, pp. 1341-1349.

8) Nunnally R.L. and Hollis, D.P. (1979) Biochemistry 18, 3642-3646.

9) Gadian, D.G., Radda, G.K., Brown, T.R., Chance, E.M., Dawson, J.S., and Wilkie, D.R. (1981) Biochem. J. 194, 215-228.

10) Matthews, P.M., Bland, J.L., Gadian, D.G. and Radda, G.K. (1982) Biohim. Biophys Acta 721, 312-329.

11) Shoubridge, E.A., Briggs, R.W. and Radda, G.K. (!982) FEBS Letts. 140, 288-292.

12) Koretsky, A.P., Wang, S., James, T.L., Klein, M.P. and Weiner, M.W. (1984) Personal Communication

13) Meyer, R.A., Kushmerick, M.J. and Brown, T.R. (1982) Am. J. Physiol. 242, C1-C11.

14) Garlick, P.B. and Turner, C.J. (1983) J. Magn. Reson. 51, 536-539.

15) Balaban, R.S., Kantor, H.L. and Ferretti, J.A. (1983) J. Biol. Chem. 258, 787-789.

16) Koretsky, A.P., Basus, V.J., James, T.L., Klein, M.P. and Weiner, M.W. (1984) Biophys. J. 45, 32a.

17) Forsén, S. and Hoffman, R.A. (1963) J. Chem. Phys. 39, 2892-2901.

18) Jeener,J., Meier, B.H., Bachman, P. and Ernst, R.R. (1979) J. Chem. Phys. 71, 4546-4553.

19) Campbell, I.D., Dobson, C.M., Ratcliffe, R.G. and Williams, R.J.P. (1978) J. Magn. Reson. 29, 397-417.

20) Llinas, M., Horsley, W.J. and Klein, M.P. (1976) J. Am. Chem. Soc. 98, 7554-7558. Indirect detection experiments were first performed to determine the resonance position of insensitive nuclei (^{15}N) which were coupled to more sensitive nuclei (^{1}H). In the present case exchange couples an observble pool to a non-obsevable pool.

21) States, D.J., Haberkorn, R.A. and Ruben, D.J. (1982) J. Magn. Reson. 48, 286-292.

22) Bessman, S.P. and Geiger, P.J. (1981) Science 211, 448.

23) Jacobus, W.E. (1980) in "Heart Creatine Kinase, the Interaction of Isozymes for Energy Distribution", eds. Jacobus, W.E. and Ingwall, J.S. (Williams and Wilkens, Baltimore), p. 1.

24) den Hollander, J.A., Brown, T.R., Ugurbil, K. and Shulman, R.G. (1979) Proc. Natl. Acad. Sci. USA 76, 6096-6100.

APPENDIX 1: SATURATION OF A NMR SIGNAL

To describe the time course of the intensity of an NMR signal after application of a selective rf pulse to that signal, we need consider all the processes effecting that peak. Following Portis (1), the effect of the rf on the magnitization of the signal is given by:

$$\left(\frac{dM_1}{dt}\right)_{rf} = -\frac{1}{4}\gamma^2 H_1^2 T_2 M_1 \qquad [A1\text{-}1]$$

where M_1 is the magnetization of the signal at time t, γ is the nuclear gyromagnetic ratio, H_1 is the magnitude of the magnetic component of the applied rf field, and T_2 is the spin-spin relaxation time.

The signal will try to recover from the effects of the rf pulse at a rate defined by the spin-lattice relaxation time, T_1. This rate is given by:

$$\frac{dM_1}{dt} = \frac{M_1^0 - M_1}{T_1} \qquad [A1\text{-}2]$$

where M^0_1 is the equlibrium magnetization of spin 1.

The total effect is expressed by the sum of these two competing effects:

$$\frac{dM_1}{dt} = \frac{M_1^0 - M_1}{T_1} - \frac{1}{4}\gamma^2 H_1^2 T_2 M_1 \qquad [A1\text{-}3]$$

Thus it can be seen that if $\gamma^2 H_1{}^2 >> (T_1 T_2)^{-1}$, the effects of the rf pulse will dominate and the signal intensity will go to zero, exponentially with a time constant of $-(1/T_1 - (\gamma^2 H_1{}^2 T_2)/4)$.

If, in addition, peak 1 is in exchange with another peak, 2,

then equation A1-2 becomes:

$$\frac{dM_1}{dt} = \frac{M_1^o - M_1}{T_1} - k_1 M_1 + k_2 M_2 \qquad [A1\text{-}4]$$

where M_2 is the magnetization of the additional peak and k_1 and k_2 are the appropriate rate constants.

This suggests a way to determine the rate constants due to exchange. If signal 2 is first saturated (M_2=0) and maintained that way, then a selective rf field applied to signal 1 will cause the intensity of signal 1 to decay in the rf field according to:

$$\frac{dM_1}{dt} = \frac{M_1^{ss} - M_1}{T_1} - k_1 M_1 - \frac{1}{4}\gamma^2 H_1^2 T_2 M_1 \qquad [A1\text{-}5]$$

where M^{ss}_1 is the magnetization of peak 1 after peak 2 has been saturated to the stedy state. Thus signal 1 decays exponentially with a time constant equal to $-(1/T_1 + k_1 - (\gamma^2 H_1{}^2 T_2)/4)$. A plot of this time constant vs $H_1{}^2$ would yield a straight line with intercept, $1/T_1 + k_1$.

References

1) Portis, A.M. (1953) Phys. Rev. 91, 1071-1078.

APPENDIX 2: AN IN VIVO PROBE CIRCUIT FOR IMPROVED SENSITIVITY

A2.1 Introduction

Success in using NMR to study metabolic processes and to produce well resolved images of living tissues has led to a rapid increase in its application to problems in biology and medicine (1,2). A serious problem with all of these studies is the degrading effect that intact tissues have upon probe sensitivity. The desire to perform these kinds of experiments has therefore necessitated studies of loss mechanisms associated with conductive samples (3,4). A tuning scheme which greatly minimizes losses associated with biological NMR is described. The success of this scheme demonstrates the importance of coil-to-ground parasitic losses. A model for this loss mechanism is described, and it is shown how a simple modification of the normal tuning scheme can minimze its effects. The improvement in sensitvity afforded is illustrated using model circuits and ^{31}P NMR spectra obtained in vivo using implanted coils.

A2.2 Background

Biological tissues can produce large losses in the tuned circuit of an NMR probe because of their high conductivity. These losses are reflected in a reduction of the circuit quality factor (Q). Losses associated with the high conductivity of the sample are caused primarily by currents induced in the sample by the electric and magnetic fields produced by the coil. While little can be done to reduce currents generated by the magnetic field, shielding of the

sample from the electric field can reduce dielectric losses.

Previous workers have developed circuit models for dielectric losses assuming that the paths of the electric fields which penetrate the sample extend in a distributed manner from one side of the coil to the other (3,4). Their models of these coil-to-coil parasitics can be reduced to a capacitance, C_d, and a resistance, R_d, connected in parallel with the coil (Fig. A2-1). R_d and C_d have the effect of lowering both the resonance frequency and Q of the tuned circuit. This description gives good quantitative explanations for the behavior of the losses incurred when biological samples are placed in a glass tube within a standard probe of a high resolution spectrometer (4).

For the types of coils used to study animal organs in situ, additional paths for the electric fields exsist. In the probe used for the studies described in Chapter 3, the laboratory rat is supported by a metal cradle. For proper shielding of external rf noise, the cradle, the probe casing, and the tuning circuit must all be grounded. Hence, paths for electric fields exist not only across the coil but between the coil within the animal, and the probe ground. The influence of these coil-to-ground parasitics can be modeled with two lumped element branches between each side of the coil and ground (Fig. A2-2a). For simplicity, each branch consists of only a resistance in series with a capacitor, with the capacitance modeling both the insulation around the coil wire and the reactive influence of the sample. In this circuit, the second branch involving R_{d2} and C_{d2} can be neglected because it is shorted by the ground lead of the tuning circuit. As indicated in Fig. A2-2b, the remaining branch transforms to the equivalent parallel components R_α and C_α, given by:

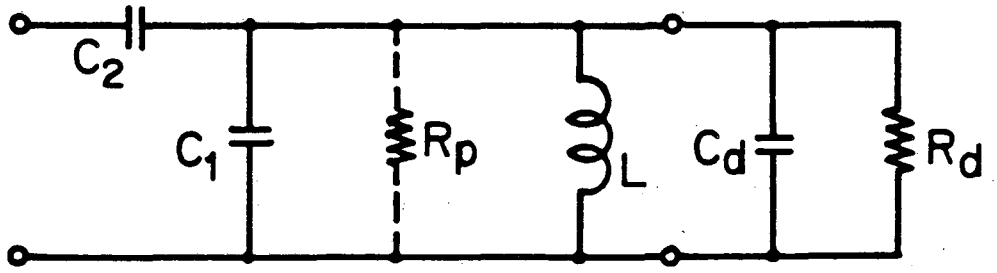

Figure A2-1. A probe circuit employing standard tuning and matching, which models coil-to-coil influences of the sample. L is the inductance of the sample coil, C_1 and C_2 are the tuning and matching capacitors, and R_p models the coil resistance. C_d and R_d model the coil-to-coil parasitics.

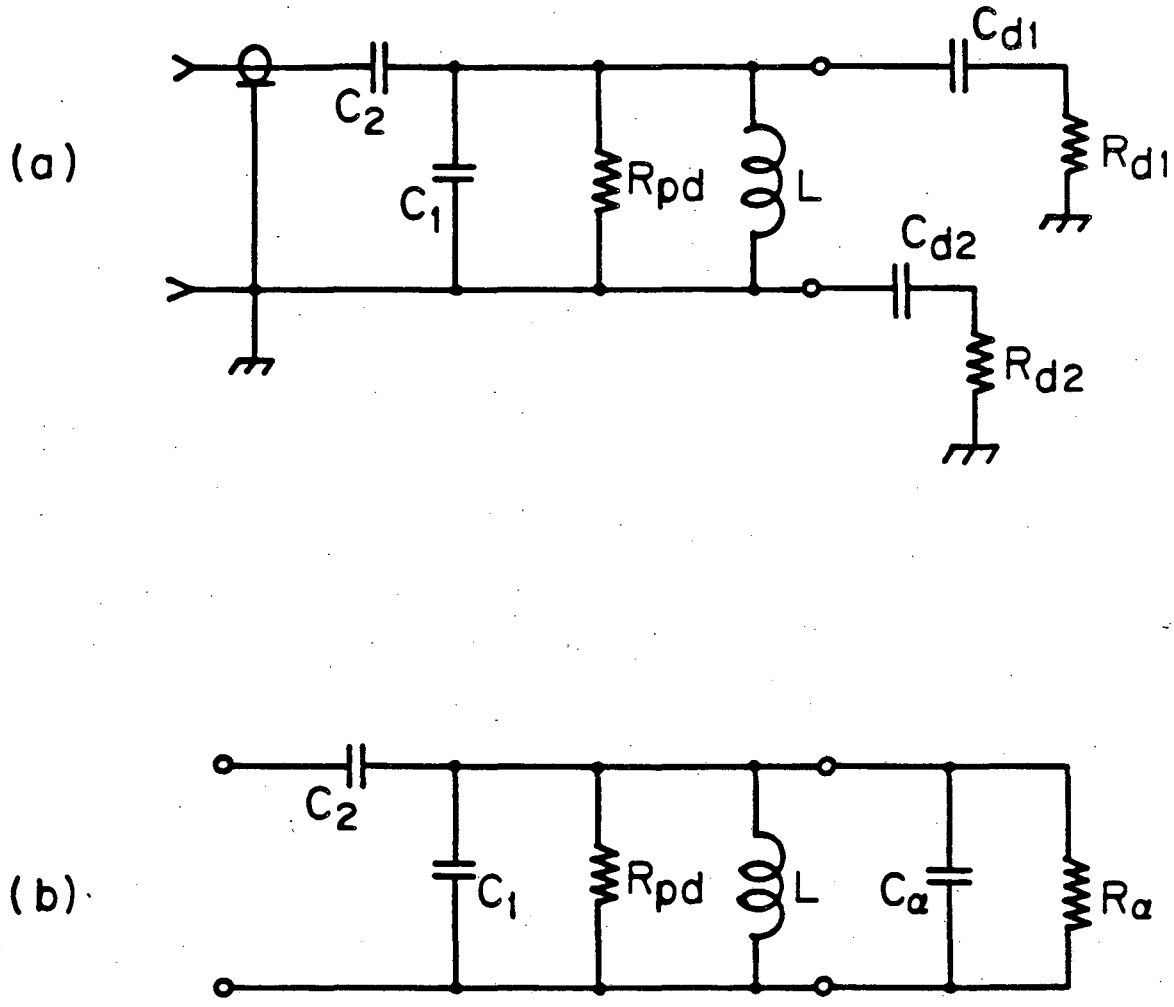

Figure A2-2. Probe circuits employing standard tuning and matching, which model (a) the additional influences of coil-to-ground parasitics, and (b) an equivalent parallel circuit. The tuned circuit elements are defined as in Fig. A2-1, except that R_{pd} represents the parallel combination of R_p and R_d, and C_1 incorporates C_d into the tuning. The branches R_{d1} and C_{d1}, and R_{d2} and C_{d2}, model the distributed influences of the coil-to-ground parasitics. R_α and C_α are given by Eqs. A2-1 and A2-2.

$$R_{\alpha}^{-1} = \frac{\omega_o^2 R_{d1} C_{d1}^2}{1+\omega_o^2 R_{d1}^2 C_{d1}^2} \qquad [A2\text{-}1]$$

$$C_{\alpha} = \frac{C_{d1}}{1+\omega_o^2 R_{d1}^2 C_{d1}^2} \qquad [A2\text{-}2]$$

where $\omega_o/2\Pi$ is the resonance frequency of the tuned circuit. The influence of these additional components on the tuned circuit is the same as that of the coil-to-coil parasitics. The total Q of the circuit can then be expressed as:

$$\frac{1}{Q_s} = \frac{1}{Q_{pd}} + \frac{1}{Q_{\alpha}} \qquad [A2\text{-}3]$$

where $Q_{pd} = R_{pd}/\omega_o L$, and $Q_{\alpha} = R_{\alpha}/\omega_o L$.

A2.3 The New Circit

Once recognized, the influence of coil-to-ground parasitics can be minimized with a balanced tuning circuit containing matching capacitors of equal size on both sides of the coil (Fig. A2-3a). Because the matching capacitors are essentially in series, their values must be approximately twice as large as the single matching capacitor of the standard circuit.

To illustrate why the balanced scheme is effective in reducing the losses associated with coil-to-ground parasitics, two simplifying assumptions are made. First, it is assumed that the circuit Q is high enough to make the impedance of the matching capacitors small compared with the 50 ohm input impedance. Thus, the parasitic elements link in series through ground, reducing the circuit to that shown in Fig. A2-

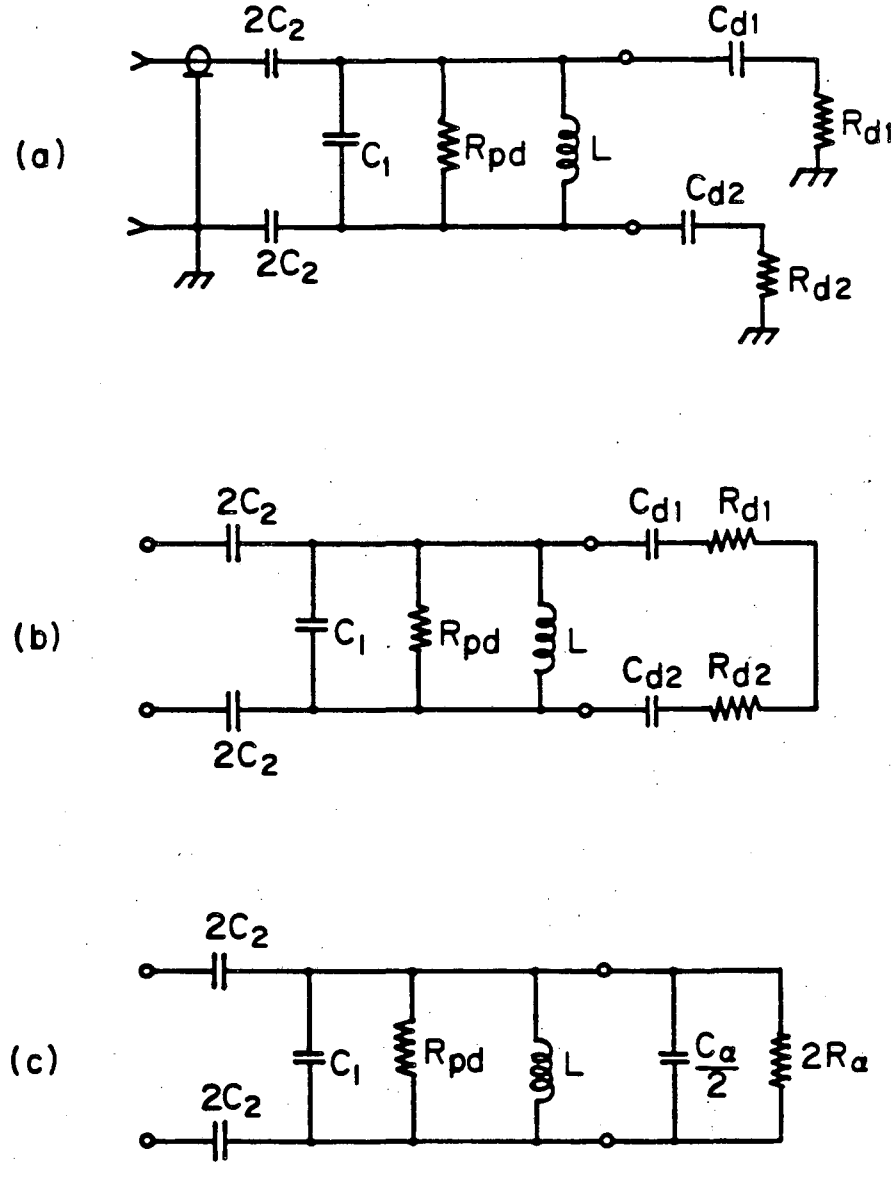

Figure A2-3. Circuit models showing (a) the influence of coil-to-ground parasitics on the balanced matching and tuning scheme, (b) the reduced circuit assuming a high circuit Q, and (c) the equivalent parallel circuit. Circuit elemnts are as defined in Fig. A2-2.

3b. Second, it is assumed that the two branches are identical, that is, $C_{d1} = C_{d2}$ and $R_{d1} = R_{d2}$. The coil is thereby balanced with respect to ground. Using transformation equations similar to Eqs. A2-1 and A2-2, the circuit reduces to that of Fig. A2-3c. The total Q for the balanced circuit can be expressed as:

$$\frac{1}{Q_b} = \frac{1}{Q_{pd}} + \frac{1}{2Q_\alpha} \qquad [A2\text{-}4]$$

Comparing Eqs. A2-3 and A2-4, it is apparent that the new circuit configuration has reduced the influence of the coil-to-ground parasitics by approximately one-half. The balanced matching circuit yields a higher Q and, because sensitivity of the NMR spectrum varies as the $Q^{1/2}$ for a fixed frequency (5), an improved signal-to-noise ratio.

A2.4 Experimental Verification of the New Tuning Scheme

MODEL CIRCUITS. To demonstrate the advantage of using the balanced tuning scheme in the presence of strong coil-to-ground parasitics, a series of model circuits was constructed. All the circuits employed a two-turn, half-inch diameter coil, tuned and matched with variable ceramic capacitors (3-20 pf). All parasitic elements consisted of a 22 ohm carbon resistor placed in series with a 5 pf silver mica capacitor. These particular component values were chosen to simulate the variations in tuning and Q typically observed for the in vivo experiments. Q measurements were performed near 100 MHz with a Wavetek Model 1062 sweep generator and a 20 db directional coupler used to measure the reflected power from the tuned circuit.

The Qs were calculated by dividing the resonance frequency of the circuit by the width of the resonance curve at the half-power points. The oscilloscope used for these measurements was calibrated with 1 MHz frequency markers from the sweep generator.

The variation in Q for different loss mechanisms and tuning schemes are shown in Table A2-1. The first column shows that the Q of the unloaded coil is insensitive to the matching scheme used. The second column shows that the balanced matching configuration does not reduce the effects of coil-coil parasitics. Only when the loading is placed from each side of the coil to ground does the balanced matching scheme significantly improve the circuit Q. The improvement is greater than predicted by the simple model presented above, indicating that some other factors may be at play. Because the balanced matching improves only losses associated with coil-to-ground parasitics, tuning the circuit in the balanced configuration is a method of determining if such losses are important.

IMPLANTED COIL CIRCUIT. As described in Chapter 3, ^{31}P NMR spectroscopy can be performed on rat organs by implanting the coil around the organ of interest. This necessitates that there be some transmission line from the coil, in the rat, to the tuning circuit, outside the rat. Because of this transmission line the circuit which has been used (Fig. A2-4) is a modification of the balanced matching circuit just described. The circuit differs from that of Fig. A2-3 in several respects. First, the tuning capacitor C_1 is no longer placed directly across the coil leads, but instead has one of its leads connected directly to ground. C_s and C_t are small chip capacitors (American Technical Ceramics) placed as close to the coil as possible

Table A2-1. Measurements of circuit Q for the standard and balanced configurations.

Tuning Scheme	Lossless Circuit[1]	Coil-to-Coil Loading[2]	Coil-to-Ground Loading[3]
Standard	59	29	26
Balanced	59	29	45

[1]Tuned circuit with no loading elements.

[2]Simulated with a single parasitic element across the coil.

[3]Simulated with two parasitic elements between each side of the coil and ground.

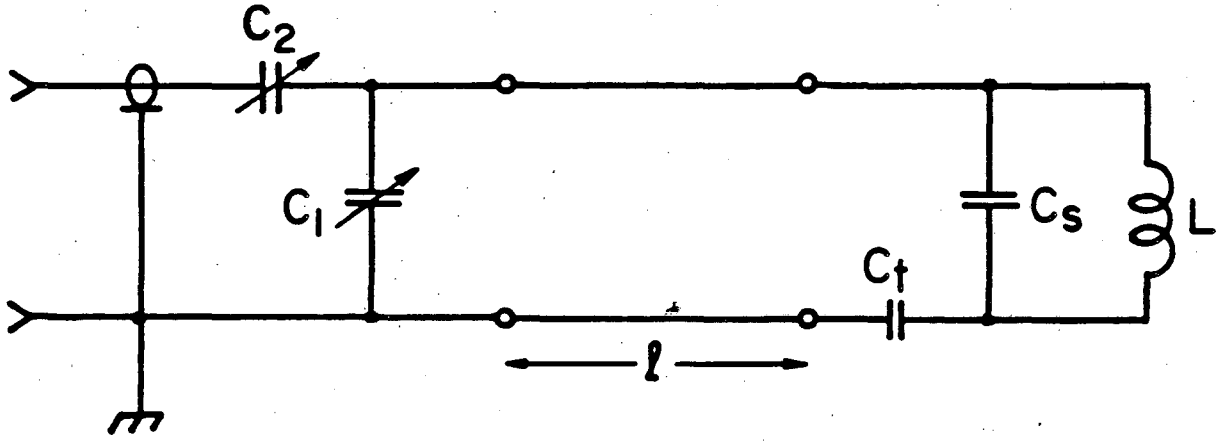

Figure A2-4. A modified, balanced tuning circuit for in vivo experiments where a length of transmission line is required between the coil and the tuning and matching capacitors, C_1 and C_2 respectively. C_s and C_t are mounted near the coil and perform partial tuning, partial matching, and balancing.

and insulated from the tissue with silicone sealant (Dow Corning). C_s helps to confine the large circulating current of the tuned circuit to the coil, thus improving the filling factor. C_t performs a partial transformation to a lower impedance, reducing the rf voltage and, therefore, the conductive losses across the transmission line. C_t also plays the role of the balancing capacitor and is chosen to be somewhat larger than C_2 to offset the imbalancing effect of C_1 and to assure that C_2 will always be in range, regardless of variations in sample coil inductance. The net results of these modifications are that: 1) the sample coil remains relatively balanced with respect to ground, 2) the transmission line does not have undue influence upon the filling factor or the circuit Q, and 3) the entire circuit can be tuned and matched outside the animal.

To demonstrate that the improvement in Q obtainable with the balanced matching scheme is applicable to implanted coils, spectra were obtained from rat kidneys. The coils used consisted of two 1/2" diameter loops separated by approximately 1/4" (Fig. 3-3). The coil was wound from 22 gauge copper wire insulated with polyethylene tubing (Clay Adams. PE-100). The transmission line consisted of approximately 7 cm of this wire in twisted pair. The capacitors C_s and C_t were 13 and 27 pf, respectively. The Q of this coil-capacitor arrangement was typically 60 prior to implantation. This arrangement was surgically implanted around the kidney following the procedure described in Chapter 3. Two days after surgery the animals were anesthesized, positioned in the probe, and the transmission line leads were soldered to the capacitors C_1 and C_2 (Fig. A2-4). The values for these capacitors were in the range of 5-15 pf. The measured Q of the

tuned circuit was 38. The transmission line leads outside the animal were then reversed so that the capacitor configuration resembled that of the standard tuning circuit of Fig. A2-1. In this configuration the capacitor C_t performs only a partial impedance match. The Q for this arrangement was foung to be 13, indicating that coil-to-ground parasitics are an important loss mechanism for these implanted coils.

To compare the two circuits it would have been ideal to obtain NMR spectra using the two configurations. However, because of (predicted) excess capacitance on the coil, the low Q scheme resembling the standard circuit (Fig. A2-1) could not be tuned to the ^{31}P operating frequency of 97.3 MHz. Therefore, a spectrum was obtained from a second rat kidney using a coil with only a single, 10 pf tuning capacitor placed close to the coil. The Q of this coil was also 13 when implanted in a rat. The spectrum obtained with the single capacitor is shown in Fig. A2-5a, while the spectrum obtained using the balanced configuration is shown in Fig. A2-5b. The signal-to-noise ratio of the βATP was 16 for the former and 41 for the latter. This is a greater improvement in sensitivity than is predicted from the change in circuit Q (13 to 38) and probably results from the increased filling factor obtained with the partial matching capacitor in the balanced scheme.

A2.5 Conclusions

While employing a Faraday shield to completely eliminate electric fields from the sample is certainly the most desired approach for eliminating dielectric losses (3), it is not always a practical solution. This is true for implanted coils as well as large imaging

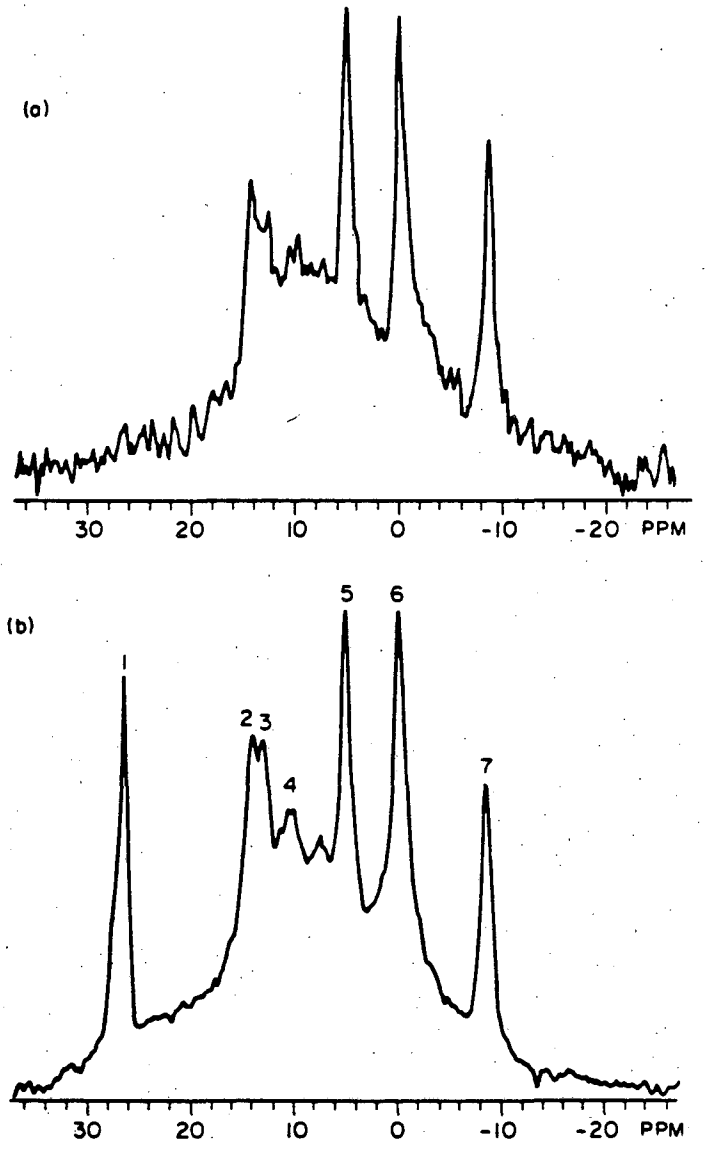

Figure A2-5. ^{31}P NMR spectra of two rat kidneys at 97.3 MHz using (a) an implanted coil with only a single tuning capacitor mounted near the coil and (b) an implanted coil employing the modified, balanced tuning scheme. Spectra were obtained in 2600 scans using 45^{o} pusles and a 130 msec recycle time. A 30 Hz exponential filter was applied to the free inducton decay prior to Fourier transformation. Peaks are: (1) MDPA, (2) phosphomonoesters, (3) Pi, (4) urine Pi and phosphodiesters, (5) γATP, (6) αATP, NAD(H), and (7) βATP.

coils, where the size of the Faraday shield approaches the wavelength of the operating frequency and thus may act as an antenna for external rf. The balanced matching scheme is an easily implemented alternative to reduce the coil losses associated with living tissue. Because the balanced matching circuit actually performs better than the proposed model predicts, the notion of coil-to-ground parasitics serves only as a starting point for a more complete description. In particular, it was assumed that having the animal close to ground was important for the electric fields to get from the coil to ground. However, preliminary experiments on an insulated rat have shown that in this case the balanced matching circuit is effective. This is probably due to the fact that at these frequencies a rat is an excellent antenna allowing the electric fields to radiate from the coil through the rat. This situation is formally equivalent to coil-to-ground parasitics.

Finally, because the coils used in the model circuits are similar to those used as surface coils (6), it is expected that an improvement in sensitivity will occur if the balanced matching circuit is employed. Similar tuning and loss considerations hold for imaging coils, so the balanced matching circuit should yield improvements for human, whole body imaging and spectroscopy. It is hoped that this last mentioned application of balanced matching makes this author financially comfortable in his old age.

A2.6 References

1) Gadian, D.G. NMR and its Applications to Living Systems Clarendon, Oxford, 1982.

2) Bottomley, P. (1982) Rev. Sci. Instrum. 53, 1319-1337.

3) Hoult, D.I., and Lauterbur, P.C. (1979) J. Magn. Reson. 34, 425-433.

4) Gadian, D.G., and Robinson, F.N.H. (1979) J. Magn. Reson. 34, 449-455.

5) Hoult, D.I., and Richards, R.E. (1976) J. Magn. Reson. 24, 71-85.

6) Ackerman, J.J.H., Grove, T.H., Wong, G.C., Gadian, D.G., and Radda, G.K. (1980) Nature(London) 283, 167-170.

This report was done with support from the Department of Energy. Any conclusions or opinions expressed in this report represent solely those of the author(s) and not necessarily those of The Regents of the University of California, the Lawrence Berkeley Laboratory or the Department of Energy.

Reference to a company or product name does not imply approval or recommendation of the product by the University of California or the U.S. Department of Energy to the exclusion of others that may be suitable.

TECHNICAL INFORMATION DEPARTMENT
LAWRENCE BERKELEY LABORATORY
UNIVERSITY OF CALIFORNIA
BERKELEY, CALIFORNIA 94720